

Aspects of the PP wave/CFT Correspondence

by

Umut Gürsoy

Submitted to the Department of Physics
in partial fulfillment of the requirements for the degree of

Doctor of Philosophy in Physics

at the

MASSACHUSETTS INSTITUTE OF TECHNOLOGY

May 2005 [June 2005]

© Massachusetts Institute of Technology 2005. All rights reserved.

Author 

Department of Physics

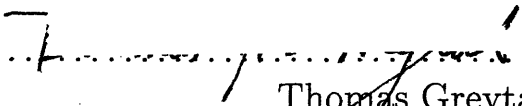
May 2, 2005

Certified by 

Daniel Z. Freedman

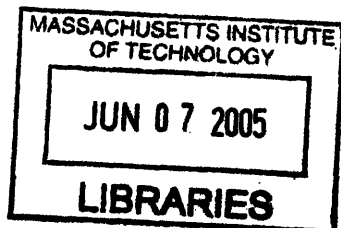
Professor

Thesis Supervisor

Accepted by 

Thomas Greytak

Professor and Associate Department Head for Education



ARCHIVES

Aspects of the PP wave/CFT Correspondence

by

Umut Gürsoy

Submitted to the Department of Physics
on May 2, 2005, in partial fulfillment of the
requirements for the degree of
Doctor of Philosophy in Physics

Abstract

In this thesis, I discuss various aspects of the PP wave/CFT duality as a concrete example of the gauge-gravity correspondence.

Thesis Supervisor: Daniel Z. Freedman

Title: Professor

Acknowledgments

I am greatly indebted to my supervisor, Dan Freedman, for his constant advice and help during my studies at MIT. It is a great privilege to learn the precise ways of investigating theoretical physics problems and learn the need to make ones understanding “crystal clear” from him. I am also grateful to Carlos Nuñez and Hong Liu for sharing with me their enthusiasm and knowledge while working on various problems during the first and final years of my PhD study. It was a great pleasure to enjoy the collaboration with my friends Sean Hartnoll, Ruben Portugues and Martin Schvellinger. Finally, it is pleasure to thank all of my friends, post-docs, professors, students and staff in the Center for Theoretical Physics at MIT.

Finally, I thank my parents for their constant support throughout my studies and my love, Arzu Aysu, for sharing with me the five years of her life in Cambridge with the joy, the pain and the enigma.

Contents

1	Introduction	17
1.1	Early ideas	18
1.2	The Maldacena Conjecture	19
1.3	D-Branes as Gravitational Objects	19
1.4	Gauge Theory on the D-Branes	21
1.5	Weak and Strong Forms of the Conjecture	22
1.6	Some Aspects of the Duality	24
1.7	Limitations of the Original Conjecture	26
1.8	The BMN Conjecture	26
2	The BMN Correspondence	31
2.1	The Geometry and Symmetries of AdS_5	32
2.2	Energies of States vs. Conformal Dimensions of Operators	33
2.3	The PP-wave Limit	35
2.4	SYM_4 theory in Components	39
2.5	BMN sector of the SYM_4 Hilbert Space	40
2.6	Map of the parameters	42
2.7	Construction of BMN operators	44
2.8	Operator Mixing	46
2.9	Anomalous dimensions of BMN operators	48
2.10	Identification of String Hamiltonian with the Dilatation Operator	49

3	The Analysis of Vector Operators	51
3.1	Vector BMN Operators and Conformal Symmetry	51
3.2	Free Two-point Function at Torus Level	54
3.3	Planar interactions of the two-point function	57
3.3.1	Non-renormalization of chiral primary correlator	59
3.3.2	D-term and self-energies	61
3.3.3	External gluons	64
3.4	Anomalous dimension on the torus	68
3.4.1	Contractible diagrams	69
3.4.2	Semi-contractible diagrams	71
3.4.3	Non-contractible diagrams	73
3.4.4	Special diagrams	76
3.5	A SUSY argument	81
3.6	Discussion and outlook	86
4	Analysis of Multi-Trace Operators	89
4.1	Operator mixing at g_2^2 level	92
4.2	Dependence on g_2 and J of an arbitrary gauge theory correlator . . .	101
4.3	Anomalous dimension of a general multi-trace BMN operator at $\mathcal{O}(g_2^2)$	103
4.4	Matrix elements of pp-wave Hamiltonian in 2-2 and 1-3 sectors	113
4.5	Discussion and outlook	116
5	Instability and String Decay in BMN Correspondence	119
5.1	Introduction	119
5.2	The Effective Gauge Theory Hamiltonian	123
5.3	Quantum Mechanical Models	126
5.4	Basis Independence	133
5.5	Computation of the decay rate	136
5.6	Discussion	137
A	D-term and external gluon contributions at $\mathcal{O}(\lambda')$	141

B	Trace identities and F-term contribution at $\mathcal{O}(\lambda')$	149
C	Disconnectedness of GT correlators	155
D	Field theory basis change at finite g_2	163
E	Sum formulas	169
F	Computation of G^{13}, G^{23}, Γ^{13} and Γ^{23}	177

List of Figures

1-1	Two asymptotic regions of the D-brane.	21
2-1	Five dimensional Anti-de-Sitter times 5 dimensional sphere. The geodesic that the PP-wave limit blows up is obtained by identifying the the thick solid lines.	38
3-1	A typical torus digram. Dashed line represents ϕ and arrow on a solid line is $\partial_\mu Z$. The derivative ∂_ν can be placed on any line.	54
3-2	Combination of g_{YM}^2 corrections under a total vertex.	60
3-3	Planar interactions of chiral primaries can be obtained by placing the total vertex between all adjacent pairs. To find the vector correlator one simply dresses this figure by ∂_μ^q and $\partial_\nu^{\bar{r}}$	61
3-4	Two-loop diagrams of vacuum polarization in scalar QCD. Treatment of other four diagrams obtained by replacing the scalar lines with gluons can be separately and do not affect our argument.	64
3-5	First class of $\mathcal{O}(g_{YM}^2)$ diagrams involving external gluons. These do not yield anomalous dimension as there are no internal vertices.	65
3-6	Second class of diagrams which involve one external gluon. Derivative of the \bar{O}_ν^J can be placed at any position. Integration over the internal vertex yields a contribution to anomalous dimension.	66
3-7	A generic $\mathcal{O}(g_{YM}^2)$ interaction on a torus diagram. The internal vertex generates two interaction loops in space-time graphs.	69
3-8	A generic contractible diagram. Total vertex includes, D-term quartic vertex, gluon exchange and self-energy corrections.	70

3-9	Same diagram as Fig.8, but represented on a periodic square.	71
3-10	A semi-contractible diagram shown on the cylinder.	72
3-11	Same diagram as Fig. 3-10, but represented on a periodic square. . .	73
3-12	External gluon interactions with semi-contractible topology.	73
3-13	Non-contractible diagrams on the cylinder.	74
3-14	A Non-contractible diagram on the periodic square. Note that 3rd block of Z -lines is missing.	75
3-15	External gluon interactions with non-contractible topology.	76
3-16	Orientations of F-term and D-term quartic vertices.	77
3-17	Special diagrams shown on a cylinder.	78
3-18	Periodic square representation of Special diagrams.	79
3-19	External gluons with special diagram topology.	80
3-20	Torus level non-contractible contribution to $\langle O_\mu^n \bar{O}_f^m \rangle$ transition ampli- tude. Derivative in O_μ^n can be placed on any line connected to O_μ^n , although it is not shown explicitly. There is a similar graph obtained by interchanging internal vertices.	85
4-1	Left figure shows that connected contribution to $2 \rightarrow 3 \rightarrow 2$ process is suppressed by $1/J$. Right figure shows similar suppression of mixing of double trace operators with single-traces.	104
4-2	A representation of planar contributions to $\langle : \bar{O}_n^{J_1} \bar{O}^{J_2} :: O_m^{J_3} O^{J_4} : \rangle$ at $\mathcal{O}(g_2^2 \lambda')$. Dashed lines represent scalar impurities. We do not show Z lines explicitly. Vertices are of order $g_2 \sqrt{\lambda'/J}$. a Connected contribu- tion. b, c, d Various disconnected contributions.	111
4-3	Connected contribution to double-triple correlator, $\langle \bar{O}_{ny} O_{myz} \rangle$, does give non-zero contribution in $1 \rightarrow 1$ process. For example this diagram will show up in the computation of $\mathcal{O}(g^6)$ scale dimension of single- trace operators.	113

A-1	Feynman rules for vertices. Same rules hold when Z is replaced by ϕ . In the θ - Z - $\bar{\theta}$ vertex, exchanging chiral fermion flavor 2 with 3 gives a minus sign and replacing Z with \bar{Z} changes the chirality projector from L to R . The analogous \bar{Z} - $\bar{\lambda}$ - θ vertex is obtained by replacing R with $-L$	142
A-2	Chiral fermion loop contributions to self-energy of Z	144
B-1	A torus level diagram with “special” topology.	150
B-2	A planar diagram with same interaction vertex as fig. B-1.	151
C-1	A typical planar contribution to $C^{1,i}$. Circles represent single-trace operators. Dashed lines denote impurity fields. Z lines are not shown explicitly and represented by “...”.	156
C-2	All distinct topologies of planar Feynman diagrams that contribute to $\langle: \bar{O}_n^{J_1} \bar{O}^{J_2} :: O_m^{J_3} O^{J_4} O^{J_5} : \rangle$. Nodes represent the operators while solid lines represent a bunch of Z propagators. Line between the nodes 1 and 3 also include two scalar impurities ϕ and ψ . All other topologies are obtained from these two classes by permutations among 3,4,5 and 1,2 separately. Other planar graphs are obtained from these by moving the nodes within the solid lines without disconnecting the diagram. For example 4 in the first diagram can be moved within the solid line 1-3.	157
C-3	Simplest connected tree diagram for the loop counting purposes. The solid line between 1 and $i + 1$ includes ϕ and ψ	158
C-4	A quartic interaction in a typical diagram introduce two interaction loops. Here, loop 1 is contractible while loop 2 is non-contractible, therefore this diagram represents a semi-contractible interaction.	159
C-5	Orientations of F-term and D-term quartic vertices.	161
C-6	In a both of the interactions loops are non-contractible due to case 1: incoming and outgoing line pairs of the quartic vertex connect to different operators. In b one interaction loop is non-contractible due to case 1 the other due to case 2.	162

F-1	Two different classes of free diagrams. Dashed lines denote propagators of impurity fields.	178
F-2	Two different types of semi-contractible diagrams. One should also consider the cases when two incoming and outgoing lines are interchanged. Also analogous contributions come from exchanging operator 2 with operator 3.	181
F-3	Contributions form non-contractible planar interactions. There are four more diagrams which are obtained by exchanging operator 2 with operator 3.	183

List of Tables

Chapter 1

Introduction

The Physics phenomena that we observe in the domain of elementary particles and their interactions through vector particles are described by the gauge theory of quantum fields. The quantum gauge theory lies at the core of our current understanding of the strong, weak and electromagnetic interactions that is described by the standard model of particle physics, to excellent accuracy.

String theory, on the other hand, is generally accepted as the strongest candidate for a quantum theory that includes gravitational interactions. There are various interesting phenomena in string theory that has the possibility of being realized in nature. Among them is the realization of a long suspected correspondence between the gauge and gravity theories. This correspondence renders string theory also as a theoretical laboratory that allows one to study various aspects of gauge theories from an alternative point of view. For example, it becomes possible to explore the strong coupling dynamics of various gauge theories by mapping specific phenomena in the gauge theory to its counterpart in the string theory side. In most cases the treatment in the string theory side is much easier to tackle with, or it at least provides an alternative description of the phenomena in terms of a completely different language. This new window into the non-perturbative physics of QCD-like gauge theories, for instance, may provide the key for an elegant solution of the long-standing problem of understanding confinement.

1.1 Early ideas

Since the seminal paper of 't Hooft [1] in 1974 people long suspected a correspondence between string theory and gauge theories. 't Hooft considered a gauge theory with or without matter in the large color limit, $N \rightarrow \infty$. In this limit he showed that the effective coupling constant of the theory that governs the perturbative expansion of the correlators becomes

$$\lambda = g^2 N = \text{fixed}, \quad (1.1)$$

where g is the original bare coupling constant of the gauge interactions. In addition, the correlation functions admit a well defined “genus expansion” in powers of $1/N^2$ in this limit. The reason for the term “genus expansion” is that the contributions to the correlation function from various Feynman diagrams can neatly be classified according to their topology, *i.e.* number of genera, and the power of $1/N^2$ corresponds to this number: If one can draw a Feynman graph only on a genus- g surface so as to avoid intersections of the propagator lines (apart from the interaction vertices), then the Feynman diagram is called a *non-planar* graph with genus g .

On the other hand, closed string theory – in striking similarity with the aforementioned genus expansion in t' Hooft limit – is perturbatively defined again by a similar topological expansion, but this time various topologies in question is that of the two-dimensional string world-sheets embedded in the space-time. [2]. For example, comparison of the aforementioned perturbative expansions, leads to the identification of the inverse color parameter in gauge theory with the closed string coupling constant:

$$g_s \sim \frac{1}{N}.$$

Indeed 't hooft [1] argued that the gauge theory in this regime of parameters is described by some kind of string theory. However, these general considerations do not allow one to specify the candidate string theory that is conjectured to govern the gauge theory dynamics. In particular, more detailed questions, *e.g.* the spectrum of the candidate string theory, the geometry of background space-time that the strings

propagate in, etc., goes unanswered in this framework.

1.2 The Maldacena Conjecture

A big step toward the realization of this idea came with the conjecture of Maldacena in 1997 [3] where a concrete duality between the supersymmetric $\mathcal{N} = 4$ gauge theory in four dimensional Minkowski space-time with gauge group $U(N)$ and type IIB closed string theory on a particular 10D manifold, namely the $AdS_5 \times S^5$ space-time was conjectured. This is called the AdS/CFT correspondence. Here, Anti-de Sitter space is a maximally symmetric solution to Einstein's equations with a negative cosmological constant. We describe the geometry of this space in section 2.1. S^5 is a 5D sphere. There is a well-defined and detailed prescription that matches the parameters, operators and the interactions on the two sides of the correspondence.

At first sight, it may seem rather surprising that these theories that are completely different in nature (one a very specific gauge theory, other a gravitational theory on a very particular background) possess exactly the same physics content. However, there is a slick argument (that was in fact the original motivation behind the conjecture) that relates the two theories through the use of the D-brane physics. In what follows, we will review this argument [4] without getting into much detail. This will also serve to introduce various definitions that shall appear frequently in the next chapters.

1.3 D-Branes as Gravitational Objects

Just as an electron in the presence of an electromagnetic field can be viewed as a source particle whose world-line couples to the electromagnetic field through the following particle action,

$$S = \int dx_\mu A^\mu,$$

there exist in the superstring theory, some p -dimensional space-time defects, Dp -branes, whose $p + 1$ dimensional world-volume couple to various generalized $p + 1$ form fields that appear at the massless level of the string spectrum. Let us specify to

the case of N $D3$ branes in IIB string theory that are located at the same point in 10 dimensional Minkovski space-time. These space-time defects viewed as a background solution to Einstein's equations, have the following properties:

- They carry N units of charge under the 4-form gauge field $A_{\mu\nu\rho\sigma}$ of IIB closed string theory.
- They preserve $SO(1, 3)$ Lorentz symmetry along their world-volume and $SO(6)$ rotational symmetry in the six dimensional transverse space.
- They preserve half of the supersymmetries, namely 16 supercharges of the IIB string theory.
- The solution becomes asymptotically flat as one approaches infinity in the radial direction.

Space-time backgrounds with these properties resemble charged black-holes. Solutions to Einstein's equations with these properties were discovered in 1991 [5] where they were called "Black 3-branes". The curvature scale that measures how much this massive object curves the space-time around it is given by

$$R = (g_s N)^{\frac{1}{4}} \alpha'^{\frac{1}{2}}, \quad (1.2)$$

where $\alpha' = l_s^2$ is the string length scale square. As shown in fig. 1-1, the solution has two asymptotic regions, the "throat" and the "flat space" that are separated by the curvature scale.

Maldacena observed the following [3]: in a *double scaling limit* where $l_s \rightarrow 0$ (so that the total energy of the solution is much smaller than the string energy scale) together with the limit where the radial coordinate, $r \rightarrow 0$ (so that one scales the coordinate system to focus on the throat region), in such a way that the wave excitations in the throat region has constant energy, *i.e.* $E \sim r/l_s^2 = const.$, the geometry of the throat region becomes $AdS_5 \times S^5$ and the dynamics of closed strings in the flat space completely decouples from the dynamics of closed strings in the throat

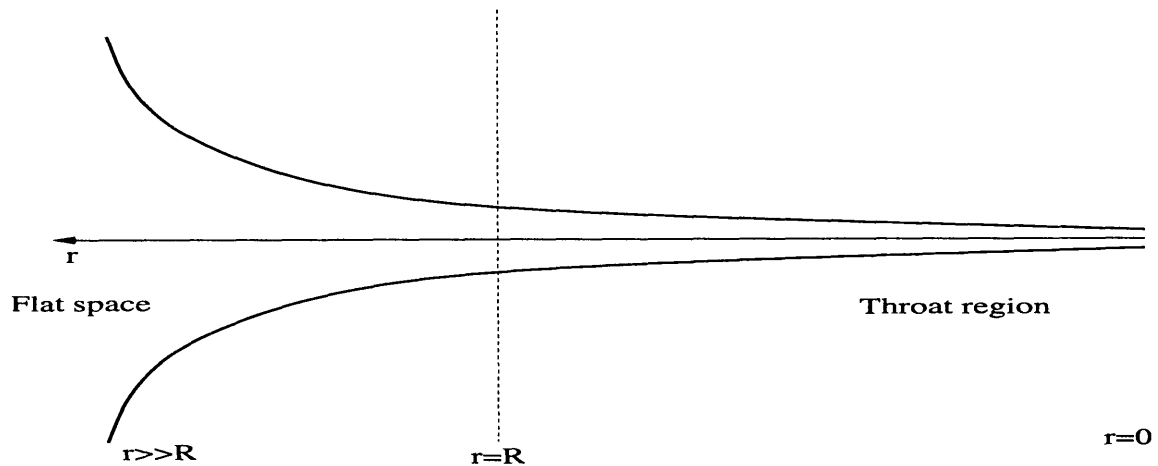


Figure 1-1: Two asymptotic regions of the D-brane.

region.¹ It is also well-known that in this low energy limit, IIB closed string theory effectively reduces to IIB Supergravity theory (SG). Therefore, in this limit, the entire theory reduces to two decoupled systems: IIB supergravity in 10D Minkowski space (flat region) plus IIB supergravity on the geometry $\text{AdS}_5 \times S^5$ (throat region).

1.4 Gauge Theory on the D-Branes

On the other hand, as shown by Polchinski in 1995 [7], D-branes in string theory admit an alternative description as space-time defects that open strings can end on. One can carry out the above decoupling limit analysis in this “open string picture” as follows. Consider separating one of the D3-branes from the stack of $N - 1$ D3 branes by a distance r . Now, one takes the double scaling limit, $l_s \rightarrow 0$, $r \rightarrow 0$. As $l_s \rightarrow 0$, only the massless string excitations survive in the string spectrum. In the open string sector these massless fields are the massless excitations confined to the world-volume of the branes. They consist of $U(N)$ gauge fields, 6 scalar fields in the adjoint representation of $U(N)$ (we denote them as X^k) and their fermionic superpartners. Together, they form an $\mathcal{N} = 4$ supersymmetric $U(N)$ gauge theory living on the D3 brane. We shall refer to this quantum gauge theory as (Super Yang-

¹For example the absorption cross section of an S-wave that is sent from infinity vanishes at the throat region in this limit [6].

Mills) “SYM₄ ” for short. Details of this theory shall be described in section 2.4. In the closed string sector, that lives on the flat Minkowski space that is transverse to the branes, the massless excitations consist of the massless IIB supergravity (SG) fields (the graviton, two gravitinos, 4-form gauge field etc). Furthermore, the zero modes of the open string that stretches between the stack of $N - 1$ D-branes and the one that is separated from the rest provide an energy scale for the SYM theory, $E \sim r/l_s^2$ that is kept constant in this limit. Maldacena further showed that the dynamics of the closed string sector completely decouples from the open string sector in this limit. Therefore, the total system is again described by two completely decoupled systems: a supersymmetric gauge theory ($\mathcal{N} = 4$ supersymmetric $U(N)$ gauge theory in 4D Minkowski space) and IIB SG on 10 dimensional Minkowski space. Comparison of this result with that of the gravitational description given in the previous paragraph yields the conclusion that IIB SG on $AdS_5 \times S^5$ is the same theory as SYM theory in 4D Minkowski space.

1.5 Weak and Strong Forms of the Conjecture

Comparison of two different descriptions that we described above, yields important relations between various parameters that appear in the field theory (SYM) side and the supergravity side: By studying the effective field theory action on the D-branes and by comparing it with the action of SYM theory one learns that the string coupling constant and the SYM coupling constant is related in the following way:

$$4\pi g_s = g^2. \tag{1.3}$$

The only other parameter in SYM, namely the number of colors, N , is related to the curvature of the SG solution in the gravitational description by the formula, (1.2). By using the definition of the 't Hooft coupling in eq. (1.1), it is very useful to summarize

these relations in the following way:

$$\lambda = \frac{R^4}{l_s^4}, \quad \frac{1}{N} = \frac{g_s}{\lambda}. \quad (1.4)$$

It is instructive to write the relation in the above form because it points out different regimes of validity of the conjecture. The D-brane argument that we presented above strongly relies on two facts: that the curvature scale of the solution is much larger than the string scale (hence low energy) $R \gg l_s$, namely, λ very large but constant, and that one can ignore string interactions, i.e. $g_s \rightarrow 0$ which, by (1.4), is equivalent to the large color limit: $N \rightarrow \infty$. Therefore, one can view above argument as a “proof” of the Maldacena conjecture, only in the classical SG limit. It is clear from (1.4) that, in this regime of parameters, one has a SYM theory with infinite number of colors and with large 't Hooft coupling constant, $\lambda \gg 1$. In short one has a SYM theory with infinite colors and in the strong coupling. On the gravity side this limit yields classical (tree level) SG theory on $AdS_5 \times S^5$. In fact, only in this regime of parameters, most of the tests of the AdS/CFT duality has been performed and succeeded. We shall refer to this regime of validity as the *weak form of the AdS/CFT correspondence*.

However, Maldacena conjecture goes beyond the low energy limit that we described above and further states that IIB *closed string theory* on $AdS_5 \times S^5$ is dual to $\mathcal{N} = 4$ Super Yang-Mills (SYM) theory for all values of N and g_s . It states that the relations between the parameters of two theories, eq, (1.4) is always valid. This is why it is termed a “conjecture”:

Type IIB String theory on $AdS_5 \times S^5$ with N units of flux of the 4-form field is dual to $\mathcal{N} = 4$ super Yang-Mills theory with gauge group $U(N)$ on 4D Minkowski space-time.

Since 1997, many checks has been performed and the correspondence has been extended to other geometries, different number of supersymmetries and different matter contents. A crucial development by the authors of [8] and [9] put the weak form of the AdS/CFT correspondence in a very firm footing. In particular, the correspond-

ing observables on the two sides is made clear and methods of computation of the correlation functions in SYM theory using the SG quantities on the gravity side has been outlined. It shall be useful to briefly discuss these aspects of the duality.

1.6 Some Aspects of the Duality

A necessary ingredient for duality to hold is the matching of various symmetries on both sides. Let us consider the gravity side first. As we briefly mentioned, in the decoupling limit, the gravity side of the correspondence is described by SG theory on $AdS_5 \times S^5$. The isometries of AdS_5 (space-time transformations that leave the background invariant) form the group $SO(2, 4)$. Similarly the five dimensional sphere is left invariant under $SO(6)$ rotations. In addition to these symmetries there are supersymmetric transformations that are preserved by the background. It turns out that the maximally symmetric $AdS_5 \times S^5$ background preserve 32 supercharges.

Let us now consider the symmetries on the gauge theory side of the correspondence, namely SYM_4 in four dimensional Minkowski space. An ordinary quantum field theory on 4D Minkowski space has Poincare symmetry that includes 4 translations and 6 Lorentz rotations. However, there is an extremely important property of the special $\mathcal{N} = 4$ SYM theory: there is no mass scale in the theory even at the quantum level. This is because of the fact that the β -function of the theory vanishes as there is no UV divergences from the loop diagrams that enter into the computation of the correlation functions of the canonical fields. As a result:

$\mathcal{N} = 4$ SYM theory in 4D is conformal invariant at the quantum level.

Therefore the group of space-time symmetries in this theory is enhanced to that of conformal group in 4D, which in addition to the 10 usual Poincare symmetries includes the scale transformation $x^\mu \rightarrow \rho x^\mu$ and 4 special conformal transformations. All in all, they form a 15 dimensional algebra of $SO(2, 4)$. The theory is also maximally supersymmetric, namely, there are 32 real supercharges that form 4 different types of Majorana spinors: $Q^i, \bar{Q}^i, S^i, \bar{S}^i$. The first two supercharges are Poincare supercharges and the latter two are called conformal supercharges. They all carry the index $i =$

1, 2, 3, 4 that indexes 4 different types. They are Lorentz spinors of definite chirality, hence each has two real d.o.f. Thus, in total there are 32 real supercharges. There is also the so-called *R-symmetry* which is a global symmetry that rotates the index i above. This gives rise to the R-symmetry group of $SU(4) \approx SO(6)$. We therefore conclude that, the total amount of bosonic and fermionic symmetries on the gauge theory side is exactly the same as the amount of symmetry on the gravity side. The entire symmetry group on both sides that contain both the bosonic and fermionic symmetry generators form a supergroup that is denoted as $SU(2, 2|4)$.

This observation is not only a necessary condition for the duality but also a practical guide in the classification of corresponding observables on two sides of the duality. The Hilbert space of the composite gauge invariant operators that are formed by the canonical fields of the $N=4$ SYM theory carry representations of the symmetry group $SU(2, 2|4)$. Similarly the string states of IIB string theory on $AdS_5 \times S^5$, when Kaluza-Klein reduced on S^5 , can be classified according to their representations under the same symmetry group. For example, the so called simplest *chiral primary multiplet* of $N=4$ operators are obtained from the scalar operators of the following form

$$\mathcal{O} = \text{tr} X^2, \tag{1.5}$$

by acting on them with various supercharges in the theory.² These class of operators play an extremely important role in the correspondence. Their counterparts in the gravity side turns out to be the *supergravity multiplet* that is obtained by acting with the supercharges on the scalar excitations $h_\alpha^\alpha + A_{\alpha\beta\gamma\delta}$. Here, the first field is the trace of metric excitation on S^5 and the second is the components of the 4-form field on S^5 . One concludes:

The operators of the form, $\text{tr} X^2$, and their supersymmetric descendants are dual to the supergravity multiplet that contain various massless supergravity fields.

²Here, we write the operator schematically. More precisely it is given as, $\text{str}[X^{i_1} X^{i_2}]$, where X^{i_k} are 6 scalar fields that are in the adjoint representation of the $U(N)$ gauge group and transform as vectors under the internal symmetry group $SO(6)$. “str” denotes the symmetrized trace over the $U(N)$ matrices with the condition that the trace part over the $SO(6)$ representations is subtracted away.

However, the correspondence goes beyond mere kinematic identification of various operators of $N=4$ SYM theory and dual fields on the gravity side. It further asserts that the *dynamics* of these dual partners also match! In particular, there is a by now well-established method [8][9], to compute the correlation functions of the composite operators on the SYM side from the propagators of their dual fields on the gravity side. Very non-trivial checks by using this idea has been performed and the conjecture was confirmed. See *e.g.* [10] for one of the first non-trivial checks where three and four point functions in SYM_4 theory is computed by means of the SG dual.

1.7 Limitations of the Original Conjecture

Despite the enormous success of the original formulation of the AdS/CFT correspondence, most of the progress has been made in the weak form of the duality that we described above. Beyond the supergravity regime, one faces serious obstacles. Among them, there are the following:

- The gravity method for computing the correlation functions is established only for the massless supergravity excitations. In fact, the operators in the SYM that are dual to *string excitations* have anomalous dimensions that diverge as $\lambda^{\frac{1}{4}}$ in the strong coupling limit.
- We do not know how to quantize and study the interactions of IIB string theory on the $AdS_5 \times S^5$ background. Therefore, use of gravitational theory on this background to study the corresponding gauge theory is amenable only in the supergravity limit, namely the weak form of the conjecture, at the moment.

1.8 The BMN Conjecture

Both of these obstacles have been circumvented to some extent by the discovery of the BMN correspondence [11] by Berenstein, Maldacena and Nastase. The idea behind this new duality is as follows. One begins with the AdS/CFT duality as explained

above in the *strong form*. Namely that, IIB closed string theory on $\text{AdS}_5 \times S^5$ with N units of flux being the same theory as $N=4$ SYM of gauge group $U(N)$. Then, one performs a special limit of this duality so as to decouple the supergravity and the massive string excitations from each other and focus on the latter. On the gravity side, this is accomplished by the so called *Penrose limit* of $\text{AdS}_5 \times S^5$: One blows up the neighborhood of a null trajectory along the equator of S^5 . This is established by focusing on the geometry that is seen by a particle rotating along the equator with infinite angular momentum, J . The technical aspects of this limit will be discussed in section 2.3. At the same time N is taken to infinity such that J^2/N is fixed. The resulting geometry is known as a ten dimensional *PP-wave*.

Of course, the Penrose limit has a dual on the gauge theory side: The corresponding limit in the gauge theory sweeps out all of the operators in the Hilbert space of $N=4$ SYM, except the ones which carry infinite R-charge J , and $(\Delta - J)/J \rightarrow 0$ where Δ is the anomalous dimension of the operator. These operators are called BMN operators and are conjectured to be dual to the string excitations in the PP-wave geometry. Details of this identification will be discussed in the next chapter. The rationale of defining a modified 't Hooft limit in this way, is to focus on the operators dual to the string excitations. Note that the operators dual to the massless supergravity excitations ($\text{tr}X^2$ operators of eq. (1.5)) satisfy $\Delta = J$ hence their scale dimension is protected. On the other hand, the operators dual to the string excitations had divergent scale dimensions in the original theory. Having introduced the Penrose limit, hence a new divergent parameter J , the dimensions of these operators become $\Delta = J + \text{finite}$. In this controlled way of taking the limit, one can compute the finite part in the desired order in the gauge coupling constant and the in the genus expansion parameter.

A crucial fact which makes this limit attractive is that we know how to quantize and study interactions of string theory on the PP-wave. Further research in the field showed that the effective gauge coupling constant, λ of eq. (1.1) is modified to

$$\lambda' \equiv \frac{\lambda}{J^2} \tag{1.6}$$

and the genus expansion parameter - which was λ/N in the original theory - now becomes,

$$g_2 \equiv \frac{J^2}{N}. \quad (1.7)$$

Both parameters are finite and tunable. In order to compute the mass of a string excitation in the dual prescription, one considers the two-point function of the BMN operator that corresponds to this excitation and computes the anomalous dimension Δ to a desired order in λ' and g_2 . Higher order corrections in g_2 are dual to higher string loop corrections. Corrections to the anomalous dimensions beyond the planar limit (*i.e.* $g_2 \neq 0$) are dual to corrections to the mass of string excitations from string interactions. This quantity can also be computed directly in the string theory side, thanks to the solvability of IIB string theory on the PP-wave background. Comparison yields exact match. It should be stressed that the new feature that this new limit of the AdS/CFT correspondence achieves is the possibility to study string excitations and their interactions in the gauge theory side.

Therefore one can think of the PP-wave/CFT correspondence as the first example of the strong form of the AdS/CFT correspondence.

In the next chapter we describe the details of the BMN correspondence. The Penrose limit is explained and the resulting geometry of the PP-wave is studied. We briefly discuss the string spectrum on the PP-wave and basic results concerning their interactions. The emphasis however is on the gauge theory side. We describe the BMN operators as duals of string excitations and outline the computation of their anomalous dimensions. Some subtle features as operator mixing beyond the planar limit is also described.

The third chapter is devoted to a detailed study of our first example of the BMN correspondence, namely the computations of the anomalous dimensions of a particular class of BMN operators: the *vector operators* [12]. They transform as vectors under the Lorentz symmetry of the 4D Minkowski space and they are dual to string excitations along $i = 5, 6, 7, 8$ transverse directions of the PP-wave. String theory tells us that these operators should carry the same anomalous dimensions as the scalar

BMN operators to first order in λ' . We confirm this expectation and extend this result to first order in non-planar corrections in g_2 . The equality of anomalous dimensions of the scalar and vector BMN operators are also shown by the use of supersymmetry that relates the two.

Chapter four investigates the role of the multi-trace BMN operators in the duality [13]. These operators are conjectured to be dual to multi-string states. In particular we extend the recent progress in this direction to the triple-trace operators. A careful study of the multi-trace anomalous dimensions led to [14] a precise identification between the matrix of anomalous dimensions Δ in the multi-trace BMN Hilbert space with the matrix of light-cone energy operator P^- in the space of multi-string states. We compute the anomalous dimension of a scalar BMN operator to order g_2 and λ' with arbitrary number of traces and related it to the dimension of the single-trace operator. Based on the gauge-theory computations we also make a prediction for the single-string/three-string and double-string/double-string matrix elements of P^- .

The eigenvalues of Δ are in fact degenerate among single and triple-trace BMN operators. In order to study this degeneracy appropriately [15] we use an effective time-dependent QM perturbation theory and compute the real and imaginary parts of Δ in this sector. Imaginary part is conjectured to be dual to the decay rate of single-string states into triple string states hence it provides a prediction for the string perturbation theory. This computation is the subject of chapter 5. Each chapter contains a separate discussion section. Finally, six appendices detail our computations.

Chapter 2

The BMN Correspondence

As discussed in the Introduction, the AdS/CFT correspondence, as an explicit realization of string/gauge duality, passed many tests performed in the supergravity approximation over the last eight years. Yet, this correspondence suffers, at least quantitatively, from the obstacles in extending it into a full string theory/gauge theory duality. This is mainly due to the lack of a clear dictionary between massive string modes of IIB on $AdS_5 \times S^5$ and gauge invariant operators in the dual $\mathcal{N} = 4$ SYM at strong coupling. Specifically, the massive modes are dual to operators in long supersymmetry multiplets of SYM and have divergent anomalous dimensions as $\lambda = g_{YM}^2 N \rightarrow \infty$. This fact, among others, hinders our understanding of strongly coupled gauge theory as a string theory.

However, Berenstein, Maldacena and Nastase has taken an important step in this direction [11]. BMN focused on a particular sector of the Hilbert space of gauge theory in which the observables themselves also scale with λ , such that they remain nearly BPS, namely their anomalous conformal dimension acquire only finite corrections. They identified a class of operators in the Hilbert space of SYM₄ the operators which carry large R-charge, J , under a $U(1)$ subgroup of $SU(4)$ — the full R-symmetry of SYM₄ —and this R-charge is subject to a scaling law as, $J \approx \sqrt{N}$. As described in section 2.7 in detail, these are essentially single trace operators that involve a chain of J fields which are +1 charged under $U(1)$ with a few $U(1)$ -neutral *impurity* fields inserted in the chain and the number of these *impurities* corresponds to the number

of string excitations on the world-sheet.

The conjecture is that, BMN operators of SYM are in one-to-one correspondence with the string states which carry large angular momentum, J , along the equator of S^5 . Below, we shall demonstrate the well-known relation between the states in the bulk of AdS and the operators on the boundary. This requires a discussion of the geometry of AdS. Then we discuss the so-called Penrose limit of the geometry $AdS_5 \times S^5$ geometry and investigate the related scaling in the Hilbert space of the dual SYM₄. The analysis of the scaling in SYM₄ provides us with conditions that are satisfied by the operators dual to the string excitations on the pp-wave. Then we discuss the precise dictionary between the parameters of the gauge theory and the string theory on the pp-wave. Finally we shall move on to discuss various new features that arise in this duality.

2.1 The Geometry and Symmetries of AdS_5

Lorentzian Anti-de-Sitter space is a maximally symmetric solution to Einstein's equations with negative cosmological constant Λ . In five dimensions, the space is a 5D hyperboloid with radius R that is embedded in flat 6D space with $(-, -, +, +, +, +)$ signature:

$$-y_0^2 - y_5^2 + \sum_{i=1}^4 y_i^2 = -R^2. \quad (2.1)$$

The radius of the hyperboloid is related to the cosmological constant by,

$$\Lambda = -\frac{12}{R^2}. \quad (2.2)$$

It is easy to see from (2.1) that the topology of this space is $R \times S^1 \times S^3$ where S^1 corresponds to a compact “time” direction. In order to define particle dynamics on this space in a meaningful way, one works with the “universal cover” of AdS where one simply decompactifies S^1 . We shall refer to the universal cover also as AdS for simplicity. Then, the topology becomes, $R \times R \times S^3$. This space can best be parametrized by globally well-defined coordinates as a solid cylinder in the following

way:

$$ds^2 = \frac{R^2}{\cos^2 \rho} \left(-dt^2 + d\rho^2 + \sin^2 \rho d\Omega_3^2 \right) \quad (2.3)$$

The geometry is depicted in fig. 2-1. One imagines that, at every point on this figure there sits a three dimensional sphere, S^3 . Ranges of the coordinates are,

$$-\infty < t < \infty, \quad 0 \leq \rho \leq \frac{\pi}{2} \quad (2.4)$$

The boundary of AdS_5 , as seen from fig. 2-1 is located at $\rho = \pi/2$ and has the geometry of $R \times S^3$.

The symmetries of AdS_5 is most easily seen from the defining equation (2.1): The geometry is invariant under rotations of the non-compact group of $SO(2, 4)$. In particular, the rotations in the $y_0 - y_5$ plane corresponds (after decompactification) to time translations. This isometry can also directly be seen from (2.3) as the metric is invariant under shifts of t . The corresponding generator defines the energy of the particle states that propagate on AdS:

$$E = i\partial_t. \quad (2.5)$$

2.2 Energies of States vs. Conformal Dimensions of Operators

As we mentioned in the Introduction, there is a very clean definition of the AdS/CFT correspondence — in the weak form — that is given by the map of states in the bulk of AdS and the operators of the QFT that are inserted in the boundary of AdS [8, 9]. For every state of the bulk theory one associates an operator in the boundary QFT. This matching is possible essentially because one can define the quantization of the QFT on the boundary of AdS through the so-called “radial quantization”. Here, we describe this procedure without getting in much detail.

The QFT that lives on the boundary in the AdS/CFT correspondence is SYM_4 , which is conformally invariant, hence it can couple to a background metric in a Weyl

invariant manner. Therefore the quantization of SYM_4 on $R \times S^3$ is equivalent to quantization in a different geometry if the two are related by a Weyl transformation:

$$g_{\mu\nu} \rightarrow \Omega(x)g_{\mu\nu}. \quad (2.6)$$

Of course, the corresponding physical quantities will have different interpretations. Specifically, one can map $R \times S^3$ onto flat four dimensional space, R^4 by the following Weyl transformation:

$$ds^2 = dr^2 + r^2 d\Omega_3^2 = e^{2\tau}(d\tau^2 + d\Omega_3^2). \quad (2.7)$$

Here, LHS is R^4 and RHS is a Weyl scaling of $R \times S^3$ where the scaling factor is given by, $\tau = \log(r)$. In a conformal field theory, all of the observables carry eigenvalues of the scaling operator. This is an operation that scales all of the coordinates on R^4 as,

$$x^i \rightarrow \lambda x^i.$$

This operation is also referred to as the *Dilatation* and the eigenvalues of the operators under this symmetry is denoted as Δ . From (2.7) we clearly see that, dilatations ($r \rightarrow \lambda r$ in the parametrization of (2.7)) correspond to time translations in $R \times S^3$:

$$r \rightarrow \lambda r \quad \leftrightarrow \quad \tau \rightarrow \tau + \log \lambda. \quad (2.8)$$

(In order to define Lorentzian time, one needs to Wick rotate as $t = i\tau$.) Since the time translations in the boundary is equivalent to time translations in the bulk (as clearly seen from fig. 2-1) we have just demonstrated the crucial fact that, *the time translations in AdS is equal to dilatations on the boundary QFT.*

Now, the idea of radial quantization is (see [16] for details) to use the relationship in (2.7) to introduce the Hamiltonian quantization on R^4 (or 4D Minkowski) by defining the Hilbert space of the theory at constant radius slices. They correspond to the constant time slices in $R \times S^3$. A crucial property is that for every state $|\psi\rangle$ that

is defined on $R \times S^3$ there is a one-to-one correspondence with an operator, \mathcal{O} , that is inserted at the origin of R^4 . By the argument that we gave above—see eq. (2.8)—the dilatation eigenvalue of \mathcal{O} is equal to the energy of the corresponding state:

$$E_{R \times S^3} = \Delta_{R^4}. \quad (2.9)$$

This relation is at the core of our investigation of the relation between the states in the gravitational theory and the corresponding operators in the gauge theory on R^4 : For every state in the bulk of AdS_5 one can associate a state at the boundary by,

$$\phi_{0E}(\vec{x}) = \lim_{\rho \rightarrow \frac{\pi}{2}} \phi_E(\rho, \vec{x}). \quad (2.10)$$

This state corresponds in a one-to-one manner with a gauge-invariant operator of SYM_4 on R^4 (or Minkowski space after the Wick rotation) where the energy of the bulk state E and the conformal dimension of the operator, \mathcal{O} are related as in (2.9).

The real problem is, of course, to find the explicit form of a gauge invariant operator in SYM_4 that is dual to a given specific state in the gravitational theory in AdS_5 . As we discussed in the Introduction, the high degree of supersymmetry allows one to associate particular BPS operators — that are protected from quantum corrections by supersymmetry, hence have the same form at the weak and strong coupling — to excitations of the fields in the supergravity multiplet of the IIB SG theory. However, the real challenge is to find the operators that are dual to string excitations. The only known way of accomplishing this is in a particular limit of the original correspondence that is called the PP-wave (or Penrose) limit.

2.3 The PP-wave Limit

The systematic way of taking this particular limit in the gravity side is to consider a null geodesic along the equator and blow up the neighborhood of the geodesic through constant scaling of the metric [17][18]. The homogeneity property of Einstein-Hilbert action guarantees that end-product is also a solution of the Einstein equations, and in

fact it is a plane-wave geometry supported by the RR 5-form. To discuss the pp-wave limit, it is convenient to make the following coordinate transformation in (2.7):

$$\tan \rho = \sinh r.$$

Then the metric of $AdS_5 \times S^5$ can be written as,

$$ds^2 = R^2 \left(-dt^2 \cosh^2 r + dr^2 + \sinh^2 r d\Omega_3^2 + d\theta^2 + \cos^2 \theta d\psi^2 + \sin^2 \theta d\Omega_3'^2 \right). \quad (2.11)$$

Consider an excitation, *e.g.* a beat wave propagating on the geodesic that is shown in fig. 2-1 with the speed of light. This geodesic is parametrized by,

$$r = 0, \theta = 0, \psi = t.$$

The pp-wave limit is obtained by scaling the coordinates of (2.11) in such a way to focus on the geometry that is seen by this particle:

$$x^- = \mu \frac{R^2}{2} (t - \psi), \quad x^+ = \frac{t + \psi}{2\mu}, \quad r = \frac{\bar{r}}{R}, \quad \theta = \frac{\bar{\theta}}{R}, \quad R \rightarrow \infty. \quad (2.12)$$

Here we introduced a parameter μ with the dimension of mass in order to make the units right. When one affects this coordinate transformation in (2.11) and takes the limit $R \rightarrow \infty$ it is easy to see that the following PP-wave geometry follows:

$$ds^2 = -4dx^+ dx^- - \mu^2 z^2 dx^{+2} + dz^2, \quad (2.13)$$

Here, dz^2 is the 8 dimensional flat space that is transverse to the pp-wave. It follows from the original coordinates as follows:

$$dz^2 = d\bar{\theta}^2 + \bar{\theta}^2 d\Omega_3'^2 + d\bar{r}^2 + \bar{r}^2 d\Omega_3^2.$$

The original geometry also had constant RR field flux on S^5 :

$$F_5 = 16\pi N(\text{vol}(S^5) + \text{vol}(AdS_5))$$

where vol is the 5-dimensional volume element on the denoted space. N is the number of flux that is related to the common radius, R , of AdS_5 and S^5 by the Einstein's equations in IIB SG as in (1.2). The method of taking the pp-wave limit of this quantity is explained in [19] and one obtains the following result:

$$F_{+1234} = F_{+5678} = \frac{\mu}{4\pi^3 g_s \alpha'^2}, \quad (2.14)$$

Let us briefly discuss the isometries of the pp-wave solution (2.13),(2.14). Both the metric and the RR form are obviously invariant under the two translations along x^+ and x^- :

$$\frac{2}{\mu}P^- = -p_+ = i\partial_+ = i(\partial_t + \partial_\psi), \quad (2.15)$$

$$2\mu P^+ = -p_- = \frac{i}{R^2}\partial_- = \frac{i}{R^2}(\partial_t - \partial_\psi). \quad (2.16)$$

There are also the obvious rotational symmetries as separate $SO(4)$ rotations along the 1234 and 5678 transverse directions:

$$J_{ij}, \quad J_{ab} \quad (2.17)$$

where i, j take values in the 1234 and a, b in 5678 directions. For completeness let us also mention the less obvious boost symmetries, under which one shifts one of the transverse coordinates simultaneously with either x^+ or x^- :

$$J_{I+}, \quad J_{I-}, \quad (2.18)$$

where I stands for a combined transverse index, $I = i, a$. In addition there is the obvious discrete \mathbf{Z}_2 symmetry under the exchange of 1234 and 5678 indices. We shall say more about the implications of this symmetry in the dual gauge theory in the

next chapter. In addition to these bosonic symmetries, 32 supercharges are preserved by this geometry, just as in the case of $AdS_5 \times S^5$. This is the maximum amount of supersymmetry that one can have in 10 dimensions.

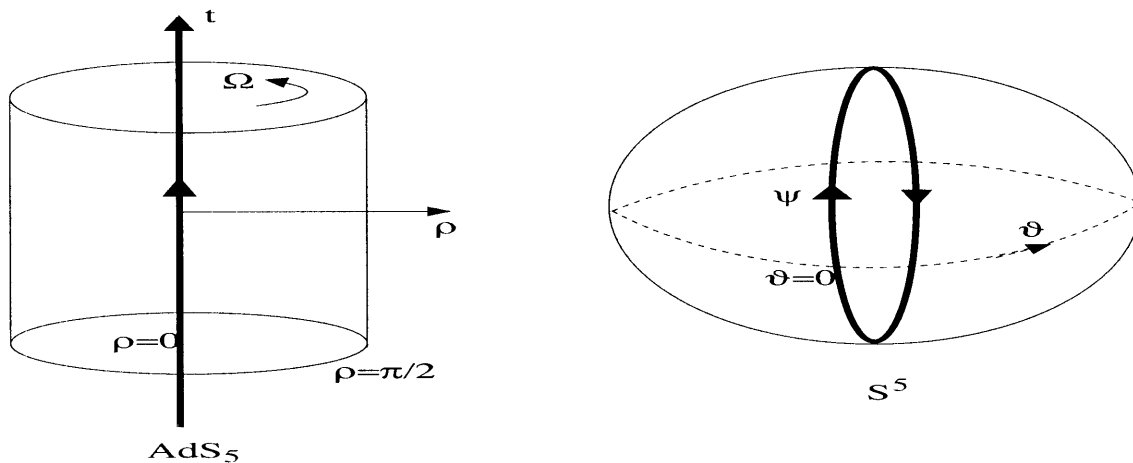


Figure 2-1: Five dimensional Anti-de-Sitter times 5 dimensional sphere. The geodesic that the PP-wave limit blows up is obtained by identifying the the thick solid lines.

One can easily work out the algebra that is satisfied by these bosonic and fermionic generators, see for example [20]. However, it will suffice for us to mention one important fact: P^+ in (2.16) *commutes* with all of the other generators, hence is a central charge. In other words its eigenvalue, the light-cone momentum p^+ , is just a parameter of the theory. It is called a *kinematical* generator. On the other hand, the light-cone energy, P^- , satisfies non-trivial commutation relations with other generators: it is called a *dynamical* generator.

What makes the background (2.13)(2.14) very attractive for string theory is that quantization of strings on the pp-wave background is known [21]. RR 5-form field strength curves the space-time in such a way that oscillator modes of the 8 transverse world sheet fields (and their fermionic partners) in the light-cone gauge acquire a mass proportional to F . In turn, light-cone energy of string modes read,

$$p^- = \mu \sum_{n=-\infty}^{\infty} N_n \sqrt{1 + \frac{n^2}{(\mu p^+ \alpha')^2}} \quad (2.19)$$

where N_n is the occupation number of n -th oscillator mode. The detailed derivation

of (2.19) can be found elsewhere, see for example [20].

2.4 SYM₄ theory in Components

The Lagrangian of SYM₄ in the $\mathcal{N} = 1$ component notation is given as follows:

$$\begin{aligned}
\mathcal{L} = & \frac{1}{4}F_{\mu\nu}^2 + \frac{1}{2}\bar{\lambda}\not{D}\lambda + \overline{D_\mu Z^i}D_\mu Z^i + \frac{1}{2}\bar{\theta}^i\not{D}\theta^i \\
& + i\sqrt{2}gf^{abc}(\bar{\lambda}_a\bar{Z}_b^iL\theta_c^i - \bar{\theta}_a^iRZ_b^i\lambda_c) - \frac{g}{\sqrt{2}}f^{abc}(\epsilon_{ijk}\bar{\theta}_a^iLZ_b^j\theta_c^k + \epsilon_{ijk}\bar{\theta}_a^iR\bar{Z}_b^j\theta_c^k) \\
& - \frac{1}{2}g^2(f^{abc}\bar{Z}_b^iZ_c^i)^2 + \frac{g^2}{2}f^{abc}f^{ade}\epsilon_{ijk}\epsilon_{ilm}Z_b^jZ_c^k\bar{Z}_d^l\bar{Z}_e^m
\end{aligned} \tag{2.20}$$

where $D_\mu Z = \partial_\mu + ig[A_\mu, Z]$ and L, R are the chirality operators. The component fields that appear in this Lagrangian are as follows:

- The vector potential of $U(N)$ gauge theory, A_μ^a . Here a is the adjoint index of the gauge group running from 1 to N^2 .
- Six real scalar fields, X_i^a . These six fields transform as a vector (the vector index being i) under the internal R -*symmetry* group of $SO(6)$. They also transform in the adjoint representation of the gauge group, $U(N)$. For convenience we define three complex combinations of them as,

$$Z_1 \equiv Z \equiv \frac{X_5 + iX_6}{\sqrt{2}}, \quad Z_2 \equiv \phi \equiv \frac{X_1 + iX_2}{\sqrt{2}}, \quad Z_3 \equiv \psi \equiv \frac{X_3 + iX_4}{\sqrt{2}}. \tag{2.21}$$

- The fermions in the theory consist of the gluino field, λ^a , and four fermions θ_i^a both in the adjoint of $U(N)$. In addition the θ 's transform under the four dimensional spinor representation of internal $SO(6)$.

Let us briefly describe the nature of interactions that appear in (2.20). First of all there are the gauge interactions between the ‘‘matter’’ scalar and fermion fields, with the gauge potential. These are contained in the kinetic terms of the fields. They are represented by gluon exchange diagrams (see appendix A). Then there are the Yukawa type cubic interactions between the scalar fields and the fermions, λ and

θ 's. They are given by the second line in (2.20). Finally there is the scalar potential energy that is given in the last line of (2.20). The interactions that follow from this potential are quartic and of two different type: The first term in the last line of (2.20) is called *D-term interactions* and the last one is called *F-term interactions*. We shall mostly be concerned with the Feynman graph calculations that involve these scalar quartic vertices. The Feynman rules that follow from (2.20) are derived in Appendix A.

2.5 BMN sector of the SYM₄ Hilbert Space

The Hilbert space of SYM₄ consists of all gauge invariant operators in the theory that can be made out of the component fields that we listed above.¹

The most important class of operators are the BPS operators that are annihilated by one of the supercharges in the theory and as a consequence protected from radiative corrections. In other words, their conformal dimension Δ does not receive anomalous corrections and it is equal to the engineering dimension. As mentioned in the Introduction, these operators are dual to the fields in the supergravity multiplet of the dual gravitational theory. The simplest example is the following BPS operator that is composed of k scalar fields in a gauge invariant way:

$$\mathcal{O}_k = \frac{1}{\sqrt{kN^k}} \text{tr} (Z^k) \quad (2.22)$$

The normalization is chosen in such a way that the two point function $\langle \mathcal{O}_k \bar{\mathcal{O}}_k \rangle$ is finite as one takes $N \rightarrow \infty$ or $k \rightarrow \infty$. The reason for this requirement will be clear below. One can obtain other scalar, fermionic or vector BPS operators by acting on (2.22) with $SO(6)$, conformal or supersymmetry lowering operators. This procedure is detailed in the section 2.7.

Here, we would like to discuss how the PP-wave limit that we discussed above is realized in the dual gauge theory Hilbert space. Let us single out a particular $U(1)$

¹The term ‘‘Hilbert space’’ is not loosely used here. One can make the notion of Hilbert space precise by using the one-to-one correspondence of operators on R^4 with the states on $R \times S^3$.

subgroup of the internal R-symmetry group $SO(6)$. Take this as the rotations in the $i, j = 5, 6$ plane. According to (2.21), the complex scalar Z carries charge $+1$ under this $U(1)$. For example, the BPS operator in (2.22) has $U(1)$ charge $+k$. Berenstein, Maldacena and Nastase [11] identified this $U(1)$ symmetry with the rotations along the ψ direction of the S^5 . Denoting the $U(1)$ R-charge as J , the precise identification between these operators is:

$$J = -i\partial_\psi.$$

The idea of [11] is that, the pp-wave limit in the Hilbert space of the gauge theory is realized by sweeping out all of the operators from the Hilbert space, retaining only the ones that satisfy,

$$\frac{\Delta - J}{J} \rightarrow 0. \quad (2.23)$$

This is the exact analog of “focusing on the geodesic” $\psi - t \rightarrow 0$ in the geometry side, that was achieved by the redefinition of the coordinates and the infinite radius limit as in eq. (2.12). Then, the precise identification of the energy and R-charge operators, in the language of light-cone momentum of the pp-wave, (2.15)(2.16) becomes,

$$\frac{2}{\mu}P^- = i(\partial_t + \partial_\psi) = (\Delta - J), \quad (2.24)$$

$$2\alpha'\mu P^+ = \frac{i\alpha'}{R^2}\partial_- = \frac{i\alpha'}{R^2}(\partial_t - \partial_\psi) = \frac{\Delta + J}{\sqrt{4\pi\lambda^{\frac{1}{2}}}}. \quad (2.25)$$

In the last step of the bottom equation, we used the $AdS_5 \times S^5$ relation, (1.2). For fixed J , the only operators in the spectrum that retains finite conformal dimension as $N \rightarrow \infty$, are the BPS operators that we discussed above. However in this modified version of taking the 't Hooft limit where one also scales J (hence changing the form of the operators themselves!) one obtains additional operators that receive only finite radiative corrections to their anomalous dimensions, that also satisfy (2.23). In order to keep the light-cone momentum, p^+ in (2.25) finite, we see that from (1.1) that J should scale as $N^{\frac{1}{2}}$ as $N \rightarrow \infty$. BMN constructed these operators and conjectured that they are dual to string excitations in the pp-wave geometry. Their construction is discussed in section 2.7.

We shall refer to the subspace of the original Hilbert space of SYM_4 that is composed of the only operators that satisfy (2.23) as the *BMN sector of the Hilbert space*. This sector only consists of the BPS operators and the BMN operators of section 2.7. These are single trace operators that are composed of J Z fields and a small number of other component fields. In the limit $J \rightarrow \infty$ the engineering dimension of these operators is given by adding up the classic dimensions of these component fields which gives J .

2.6 Map of the parameters

Here we summarize the identification of the parameters in both sides of the correspondence. We begin with what we already discussed above. As mentioned in section 2.3, P^+ is a parameter of the string theory that is fixed. It is the light-cone momentum that is carried by the string vacuum state. This is dual to the $U(1)$ R-charge of SYM_4 in the BMN sector of the Hilbert space: In this sector, by (2.23), $\Delta \rightarrow J$ as $J \rightarrow \infty$ and from (2.16) we learn that P^+ is J . In summary,

$$\mu p^+ \alpha' = \frac{J}{\sqrt{\lambda}}, \quad \frac{2p^-}{\mu} = \Delta - J, \quad g_{YM}^2 = 4\pi g_s. \quad (2.26)$$

Utilizing the AdS/CFT correspondence BMN found a relation between the anomalous dimensions of the BMN operators and the oscillation number of the corresponding string states. From eq. (2.19) and using (2.26) we learn that the anomalous dimensions of the string operators are²:

$$(\Delta - J)_{n, N_n} = N_n \sqrt{1 + \frac{g_{YM}^2 N n^2}{J^2}}. \quad (2.27)$$

We see that in the large N limit, only the operators whose R-charge scale as $J \approx \sqrt{N}$ stays in the spectrum (along with chiral primaries) as the other observables decouple.

²The term “anomalous dimension” refers to the difference of the total quantum corrected conformal dimension, Δ , and the engineering dimension of the classical operator, which equals J in the BMN sector.

Therefore the BMN limit in detail is,

$$N \rightarrow \infty, \text{ with } \frac{J}{\sqrt{N}} \text{ and } g_{YM} \text{ fixed.} \quad (2.28)$$

This limit differs from the usual large N limit of gauge theory in that the observables are also scaled as J is not fixed. Therefore neither $\lambda \rightarrow \infty$ implies infinite coupling in SYM nor $1/N \rightarrow 0$ implies planarity. In fact, a detailed study of free and coupled correlation functions in the BMN sector of SYM revealed that [22][23][24] theory develops a different effective coupling constant,

$$\lambda' = \frac{g_{YM}^2 N}{J^2} = \frac{1}{(\mu p^+ \alpha')^2}, \quad (2.29)$$

and a different genus expansion parameter,

$$g_2^2 = \left(\frac{J^2}{N} \right)^2 = 16\pi^2 g_s^2 (\mu p^+ \alpha')^4. \quad (2.30)$$

As a result, in the modified large N limit, (2.28), one has an interacting gauge theory with a tunable coupling constant λ' . However non-planar diagrams are not ignorable necessarily. A direct consequence of this non-planarity in SYM interactions can be observed as mass renormalization of string states[24]. In [24], $\mathcal{O}(\lambda')$ contribution to the string state mass was related to torus level contribution to $\Delta - J$ and this value was computed. They observed that the effective string coupling (which appears in the physical quantities like $\Delta - J$ is not identical to the genus counting parameter g_2 but modified with $\mathcal{O}(\lambda')$ SYM interactions as³

$$g'_s = g_2 \sqrt{\lambda'}. \quad (2.31)$$

Now, we observe a very significant fact about the BMN limit. Since λ' and g'_s are independent and both can be made arbitrarily small, in that regime one has *a duality between weakly coupled gauge theory and interacting perturbative string theory*. This

³In [25], a generalization of g'_s to arbitrary values of λ' was proposed.

provides not only a duality between observables in SYM and string states on pp-wave background but also an explicit map between gauge and string interactions.

2.7 Construction of BMN operators

In this section we shall first review the BMN state/operator map between first few bosonic excitations of IIB string on the pp-wave background and corresponding operators in SYM on $\mathbf{R} \times S^3$. First of all, string vacuum corresponds to the BPS operator (with appropriate normalization) ⁴,

$$O^J = \frac{1}{\sqrt{J(N/2)^J}} \text{Tr}(Z^J) \longleftrightarrow |0, p^+\rangle. \quad (2.32)$$

To discuss the excitations it is convenient to form complex combinations of the 6 scalars of SYM as,

$$Z^1 = Z = \frac{X^5 + iX^6}{\sqrt{2}}, \quad Z^2 = \phi = \frac{X^1 + iX^2}{\sqrt{2}}, \quad Z^3 = \psi = \frac{X^3 + iX^4}{\sqrt{2}}. \quad (2.33)$$

Operators corresponding to the supergravity modes, $n = 0$, are obtained from O^{J+1} by the action of $SO(6)$, conformal or SUSY lowering operations. For example, the particular $SO(6)$ operation $\delta_\phi Z = \phi$ acting on O^{J+1} yields (by the cyclicity of trace),

$$O_\phi^J = \frac{1}{\sqrt{J}} \delta_\phi O^{J+1} = \frac{1}{\sqrt{(N/2)^{J+1}}} \text{Tr}(\phi Z^J). \quad (2.34)$$

This is in correspondence with the supergravity mode $\alpha_0^{\phi^\dagger} |0, p^+\rangle$ where $\alpha_0^{\phi^\dagger} = \frac{1}{\sqrt{2}}(\alpha^1 - i\alpha^2)$. Similarly $\delta_\psi Z = \psi$ and the translation D_μ yields other bosonic supergravity modes,

$$O_\psi^J = \frac{1}{\sqrt{(N/2)^{J+1}}} \text{Tr}(\psi Z^J) \longleftrightarrow \alpha_0^{\psi^\dagger} |0, p^+\rangle$$

⁴We use the common convention $\text{Tr}(T^a T^b) = \frac{1}{2} \delta^{ab}$.

$$O_\mu^J = \frac{1}{\sqrt{(N/2)^{J+1}}} \text{Tr}(D_\mu Z Z^J) \longleftrightarrow \alpha_0^{\mu\dagger} |0, p^+\rangle \quad (2.35)$$

where $\mu = 5, 6, 7, 8$ and $\alpha_0^\psi = \frac{1}{\sqrt{2}}(\alpha^3 - i\alpha^4)$. To find the operator dual to a supergravity state with N_0 excitations one simply acts on O^{J+N_0} with N_0 lowering operators.

Turning now to the string excitations $n \neq 0$, we see that momentum conservation on the world-sheet prohibits creation of a single-excitation state with nonzero n . Therefore the next non-trivial string state involves two creation operators. Corresponding nearly BPS operators are introduced in [11] and discussed in detail in the later literature but we would like to present here a slightly different approach with a more compact notation. This will prove very useful when we discuss interactions of BMN operators. To generalize from supergravity to string modes let us introduce a ‘‘quantized’’ version of the derivation rule and define a q -variation by

$$\begin{aligned} \delta^q(f_1(x)f_2(x)\dots f_k(x)) &= \delta^q f_1(x)f_2(x)\dots f_k(x) + qf_1(x)\delta^q f_2(x)\dots f_k(x) \\ &+ \dots + q^{k-1}f_1(x)\dots f_{k-1}(x)\delta^q f_k(x) \end{aligned} \quad (2.36)$$

where f_i are arbitrary operators and q is an arbitrary complex number to be determined below. With this notation, the operator dual to single-excitation state, say $\alpha_n^{\phi\dagger} |0, p^+\rangle$, can be obtained by acting on O^{J+1} with q -variation δ_ϕ^q with q depending on n . By cyclicity of trace one gets,

$$\frac{1}{\sqrt{J}} \delta_\phi^q O^{J+1} = \frac{1}{J\sqrt{(N/2)^J}} \left(\sum_{l=0}^J q^l \right) \text{Tr}(\phi Z^J).$$

As mentioned above, this should vanish by momentum conservation for $n \neq 0$ and should reduce to (2.34) for $n = 0$. This determines q at once,

$$q = e^{2\pi i n / (J+1)}.$$

Let us now determine the operator dual to the two-excitation state, $\alpha_m^\psi \alpha_n^{\phi\dagger} |0, p^+\rangle$. This is obtained by action of $\delta_\psi^{q_2} \delta_\phi^{q_1}$ on O^{J+2} with q_1 and q_2 depending on n, m re-

spectively. A single q -variation should vanish as above, hence fixing $q_1 = e^{2\pi i n/(J+2)}$, $q_2 = e^{2\pi i m/(J+2)}$. Double q -variation does not vanish in general because q -variation do not commute with cyclicity of trace. Trivial algebra gives,

$$\frac{1}{J+2} \delta_\psi^{q_2} \delta_\phi^{q_1} O^{J+2} = q_2 \frac{1}{(J+2)^{3/2} (N/2)^{J+2}} \left(\sum_{l=0}^J (q_1 q_2)^l \right) \sum_{p=0}^J q_2^p \text{Tr}(\phi Z^p \psi Z^{J-p}).$$

The first sum vanishes unless $q_1 q_2 = 1$. Thus we reach at momentum conservation on the world-sheet, $m = -n$. Also, one can simply omit the phase factor q_2 in front since the corresponding state is defined only up to a phase. Therefore one gets the BMN operator with two scalar impurities,

$$O_{\phi\psi}^n \equiv \frac{1}{J+2} \delta_\psi^{q_2} \delta_\phi^{q_1} O^{J+2} = \frac{1}{\sqrt{J(N/2)^{J+2}}} \sum_{p=0}^J e^{\frac{2\pi i n p}{J}} \text{Tr}(\phi Z^p \psi Z^{J-p}) \quad (2.37)$$

where we omitted $1/J$ corrections in large J approximation. In what follows, we will refer to the specific scalar impurity operator, (2.37) as the ‘‘BMN operator’’.

Generalization to N string states in any transverse direction is obvious: Take corresponding N q_i -variations (which might be $SO(6)$ transformation, translation or SUSY variation) of O^{J+N} where q_i are fixed as $q_i = e^{\frac{2\pi i n_i}{J+N}}$, and momentum conservation $\sum n_i N_n = 0$ will be automatic.

2.8 Operator Mixing

As emphasized above, a striking aspect of PP-wave/SYM correspondence is that, in a regime where both the effective GT coupling λ' and string coupling g_s are small, one has a duality between effectively weakly coupled gauge theory and perturbative string theory. This goes beyond the aforementioned duality between observables in SYM and string states on pp-wave background in the free string theory and provides an explicit map between gauge and string interactions. However, a clear understanding of the correspondence at the level of interactions still remains as an interesting challenge. One essential reason which hinders a complete understanding is the fact that, while

states with different number of strings are orthogonal in SFT Hilbert space at all orders in g_s , one gets a non-trivial mixing between BMN operators of different number of traces when one turns on the genus-counting parameter of SYM,

$$g_2 = \frac{J^2}{N},$$

which correspond to g_s on the string side. Namely,

$$\langle \bar{O}_i^J O_j^J \rangle_{g_2} \sim g_2^{|i-j|}, \quad i \neq j.$$

This is true even in the free theory, *i.e.* for $\lambda' = 0$.

Therefore, although it is true that when g_2 is set to zero, a single-trace BMN operator corresponds to a single string state, the identification of multi-string states with multi-trace BMN operators is plagued by this mixing between BMN operators of different trace number. To overcome this problem, a basis transformation was found [26, 27] that takes the multi-trace BMN operators (this is called the BMN basis) to a different basis (that is called the string basis) in which the operators are disentangled.

The idea of [27] is simple: To find the transformation U which diagonalizes the matrix of inner products between BMN operators, order by order in g_2 . In the *free* theory, we define the following matrix,

$$G_{ij} = \langle \bar{O}_j O_i \rangle.$$

Here n is a collective index for a generic n -trace BMN operator. One identifies the basis transformation, U by requiring that G is diagonal in the new, “string basis”:

$$U_{ik} G_{kl} U_{lj}^\dagger = d_{ij}, \quad \tilde{O}_i \equiv U_{ij} O_j.$$

The basis change U is specified only up to an arbitrary unitary transformation. One can fix this freedom by requiring that U is real and symmetric. Call this transforma-

tion, U_G . Then the solution of the above equation up to $\mathcal{O}(g_2^2)$ reads,

$$U_G = \mathbf{1} + g_2 \left(\frac{1}{2} G^{(1)} \right) + g_2^2 \left(-\frac{1}{2} G^{(2)} + \frac{3}{8} (G^{(1)})^2 \right) + \dots \quad (2.38)$$

where $G^{(i)}$ denotes $\mathcal{O}(g_2^i)$ piece of the metric.

The requirement of reality and symmetry completely fixes the freedom in the choice of the transformation. It was independently shown in [26] and [27] that this simple choice leads to an agreement with string theory calculations. In particular the inner product of a single and double trace operator in the *interacting* theory in this basis, agrees with the cubic string vertex. Recently, [28] also gives evidence for an agreement between the $\mathcal{O}(g_2^2 \lambda')$ eigenvalue of $\Delta - J$ and the matrix element of light cone Hamiltonian in single string sector. However, despite the agreement at this order, there is no reason to believe that this simple choice should hold at higher orders in g_2 or for higher trace multi-trace operators.

2.9 Anomalous dimensions of BMN operators

Viewed purely as a field theory problem, our task is to obtain the anomalous dimensions, $\Delta - J$ of the BMN operators. As discussed in the previous section, when the mixing parameter g_2 is turned on, one faces a harder problem of first identifying the true eigenstates of the operator $\Delta - J$ and then to find its eigenvalue.

For the simplest case of single-trace operators, the mixing is between single and double-trace BMN operators. In order to compute the anomalous dimension of the single-trace BMN operator (2.37), at the torus level, we need the following data: The two-point function of the single trace operator at order $\mathcal{O}(g_2^2)$, the two point function of the single-and double trace operator that it mixes with at $\mathcal{O}(g_2)$ and the two-point function of the double-trace operator only at $\mathcal{O}(g_2)$. The combined result of these computations for the case of (2.37) is as follows [29][30]:

$$\Delta - J = 2 + \lambda' \left[n^2 + \frac{g_2^2}{4\pi^2} \left(\frac{1}{12} + \frac{35}{32\pi^2 n^2} \right) \right]. \quad (2.39)$$

In the next chapter we compute the same quantity (more precisely the two-point function of the single-trace operator) for the case of the more complicated vector operator, eq. (3.3) and show that it gives rise to the same result as (2.39).

Finally, we would like to show here the result for the anomalous dimension of a general i -trace BMN operator that is formed out of one single-trace BMN operator and $i-1$ BPS type operators of section 2.7. This computation also requires entangling the mixing with lower and higher trace operators. This analysis is the subject of chapter 4 and the result for the anomalous dimension turns out to be surprisingly simple:

$$\Delta - J = 2 + \lambda' \left[\frac{n^2}{s_0^2} + \frac{g_2^2 s_0^2}{4\pi^2} \left(\frac{1}{12} + \frac{35}{32\pi^2 n^2} \right) \right] \quad (2.40)$$

where $s_0 = J_0/J$ is the ratio of the length of the single trace BMN to the total length of the multi-trace operator.

2.10 Identification of String Hamiltonian with the Dilatation Operator

Several important steps were taken in relation to the aforementioned mixing problem. In order to understand the implications of the mixing for the correspondence between field theory and string theory quantities, one needs a precise identification of the corresponding quantities at the interacting level. A natural route to take is to identify the *dynamical* generators P^- and $\Delta - J$ as,

$$\frac{2P^-}{\mu} = \Delta - J$$

also for non-zero values of g_2 and g_s [14]. Since these operators act on completely different Hilbert spaces, an unambiguous identification is achieved only by equating the eigenvalues of P^- and $\Delta - J$ in the corresponding sectors of the Hilbert spaces. In case of one-string states this problem was considered in a number of papers. On the gauge theory (GT) side, $\mathcal{O}(g_2^2)$ eigenvalue of BMN operators that correspond

to single-string states was obtained in [14][30][29]. On the string theory side, one-string eigenvalue of P^- at $\mathcal{O}(g_s^2)$ was first addressed in [26] where a computation that partially uses the language of String Bit Formalism (SBF) [31] was performed and exact agreement with the GT result was reported. As noted in that paper however, an ultimate check of the correspondence requires a purely string field theory (SFT) computation [32]. This calculation was carried out in [28] and also perfect agreement with GT eigenvalue was established.⁵

Apart from the correspondence of eigenvalues, it is also desirable to have an identification of the *matrix elements* of P^- and $\Delta - J$. This, of course requires, first to establish an isomorphism between the complete bases that these elements are evaluated in. We shall discuss this and related problems in chapter 4.

⁵Up to an ambiguity which arise from a particular truncation of the intermediate string-states.

Chapter 3

The Analysis of Vector Operators

3.1 Vector BMN Operators and Conformal Symmetry

In this chapter, we will mainly be concerned with the vector operator which involves two impurity fields and constructed in analogy with the BMN operator (2.37) but with ψ impurity replaced with $D_\mu Z = \partial_\mu Z + ig[A_\mu, Z]$. It should be defined such that it reduces to a *descendant of the chiral primary operator*, $\partial_\mu \text{Tr}[Z^{J+2}]$, when the phases are set to zero and it should be a *conformal primary* when the phases are present. Below, we will show that our general prescription for constructing BMN operators will do the job.

Before that, let us recall that two-point function of *conformal primary* vector operators $O_\mu(x)$ and $O_\nu(y)$ should have a specific transformation law under conformal transformations—particularly under inversion $x_\mu \rightarrow \frac{x_\mu}{x^2}$. The only possible tensorial dependence on x and y can be through the determinant of inversion,

$$J_{\mu\nu}(x-y) = \delta_{\mu\nu} - 2 \frac{(x-y)_\mu (x-y)_\nu}{(x-y)^2}. \quad (3.1)$$

Therefore the two-point function is restricted to the form,

$$\langle O_\mu(x)O_\nu(y) \rangle \sim \frac{J_{\mu\nu}(x, y)}{(x - y)^{2\Delta}}$$

where Δ is the scale dimension. On the other hand, translation descendants of scalar conformal primaries $O_\mu(x) = \partial_\mu O(x)$, will have the following correlator,

$$\begin{aligned} \langle O_\mu(x)O_\nu(y) \rangle &\sim \partial_\mu \partial_\nu \frac{1}{(x - y)^{2(\Delta-1)}} \\ &= \frac{2(\Delta - 1)}{(x - y)^{2\Delta}} \left(\delta_{\mu\nu} - 2\Delta \frac{(x - y)_\mu (x - y)_\nu}{(x - y)^2} \right). \end{aligned}$$

We would like to see whether the vector operator constructed with our prescription obeys these restrictions. We will not assume large J until we discuss correlators at the torus level and our construction will hold for *any* J . Therefore our prescription gives an analog of (2.37),

$$O_\mu^n \equiv \frac{1}{J + 2} D_\mu^{q_2} \delta_\phi^{q_1} O^{J+2} = \frac{1}{\sqrt{(J + 2)(N/2)^{J+2}}} \left\{ \sum_{l=0}^J q_2^l \text{Tr} \left(\phi Z^l D_\mu Z Z^{J-l} \right) + q_2^{J+1} \text{Tr} \left(D_\mu \phi Z^{J+1} \right) \right\}$$

where D_μ^q is the gauge covariant “ q -derivative” obeying the quantized derivation rule, (2.36). For $q = 1$, q -derivation coincides with ordinary derivation. We will use the following two forms of vector operator interchangeably,

$$O_\mu^n = \frac{1}{\sqrt{(J + 2)(N/2)^{J+2}}} D_\mu^q \text{Tr} \left(\phi Z^{J+1} \right) \quad (3.2)$$

$$= \frac{1}{\sqrt{(J + 2)(N/2)^{J+2}}} \left\{ \sum_{l=0}^J q^l \text{Tr} \left(\phi Z^l D_\mu Z Z^{J-l} \right) + q^{J+1} \text{Tr} \left(D_\mu \phi Z^{J+1} \right) \right\} \quad (3.3)$$

where,

$$q = e^{2\pi i n / (J+2)} \quad (3.4)$$

Note that in (3.2) the position of ϕ would matter generally since the trace loses its cyclicity property under q -derivation. However one can easily check that only for the particular value (3.4), the cyclicity is regained: under an arbitrary shift, say by m

units, in the position of ϕ , O_μ^n changes only by an overall phase q^m which is irrelevant to physics.

Having fixed the definition, it is now a straightforward exercise to compute the planar, tree level contribution to the two-point function $\langle O_\mu^n(x)\bar{O}_\nu^m(y)\rangle$ directly from (3.3) (or the one with ϕ shifted arbitrarily). Note that one can drop the commutator term in D_μ since it gives a g_{YM}^2 correction to tree level. Denoting the scalar propagator by $G(x, y) = \frac{1}{4\pi^2(x-y)^2}$, the result is

$$\langle O_\mu^n(x)\bar{O}_\nu^m(y)\rangle = 2\delta_{nm}\frac{J_{\mu\nu}(x-y)}{(x-y)^2}G(x, y)^{J+2} \quad (3.5)$$

for arbitrary nonzero m, n . The appearance of inversion determinant $J_{\mu\nu}$, (3.1) clearly shows that vector operator is a conformal primary for arbitrary J , not necessarily large (at the tree level). In fact, a slight change in the definition of q (for example $q^J = 1$) would generate terms like $\mathcal{O}(1/J)\delta_{\mu\nu}$ which spoils conformal covariance for small J . Conformal covariance will be a helpful guide in the following calculations, therefore we shall stick to the definition, (3.4).

We also note that momentum on the world sheet is conserved at the planar level, but we will see an explicit violation at the torus-level just like in the case of BMN operators. At this point we want to point out an alternative way to obtain above result directly by using (3.2) with $r = e^{2\pi im/(J+2)}$:

$$\begin{aligned} \langle O_\mu^n(x)\bar{O}_\nu^m(y)\rangle &= \frac{1}{\sqrt{(N/2)^{J+2}(J+2)}}\partial_\mu^q\partial_\nu^{\bar{r}}\langle\text{Tr}(Z^{J+1}\phi)\text{Tr}(\bar{Z}^{J+1}\bar{\phi})\rangle \\ &= \frac{1}{J+2}\partial_\mu^q\partial_\nu^{\bar{r}}\left(\frac{1}{(x-y)^{2(J+2)}}\right)\frac{1}{(4\pi^2)^{J+2}} \\ &= 2\delta_{nm}\frac{J_{\mu\nu}(x-y)}{(x-y)^2}G(x, y)^{J+2} \end{aligned}$$

using the planar tree level two-point function of chiral primaries and the definition of q -derivation, (2.36). This curious alternative way is a consequence of the fact that q -derivation and contraction operations commute with each other. We will use this fact to greatly simplify the calculations in the following sections. We also note that

when the phases are absent above result trivially reduces to two-point function of translation descendants since q -derivation reduces to ordinary derivation for $q = 1$.

3.2 Free Two-point Function at Torus Level

Torus contribution to free two-point function of BMN operators was calculated in [24]. Analogous calculation for vector operators is achieved simply by replacing one of the scalar impurities, say ψ field with the vector impurity $D_\mu Z$. Since our aim in this section is to obtain the free contribution, we can drop the commutator term in the covariant derivative which is $\mathcal{O}(g)$ and take the impurity as $\partial_\mu Z$. Consider the generic torus diagram in fig. 3-1 where we show the ϕ -line together with $\partial_\mu Z$ impurity of the upper operator, O_μ^J , inserted at an arbitrary position and denoted by an arrow on a Z -line. This arbitrary position is to be supplied with the phase q^l and summed from $l = 0$ to $l = J + 1$. To obtain $\langle O_\mu^J O_\nu^J \rangle_{\text{torus}}$ one simply takes \bar{r} -derivative of this diagram. One should consider the following two cases separately.

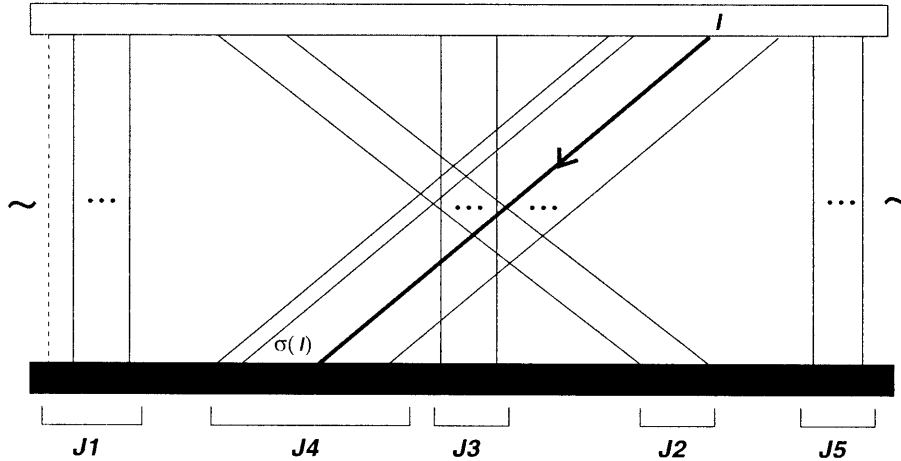


Figure 3-1: A typical torus digram. Dashed line represents ϕ and arrow on a solid line is $\partial_\mu Z$. The derivative ∂_ν can be placed on any line.

First consider the case when \bar{r} -derivative hits the same Z -line as with ∂_μ . Then the phase summation will be identical to the phase sum for BMN operators, which was outlined in section 3.3 of [24] with a $\mathcal{O}(1/J)$ modification coming from the fact that double derivative line can also coincide with the ϕ -line for vector operators. Here

we will summarize the calculation of [24] for completeness. For simplicity let us first consider operators of same momentum, *i.e.* $q = r$. The double derivative line may be in any of the five groups containing $J_1 + \dots + J_5 = J + 2$ lines. If it is in the first or the last group of $J_1 + J_5$ possibilities, then there is no net phase associated with the diagram. If it is in any of the other three groups there will be a non-trivial phase, *e.g.* $q^{J_2+J_3}$ for the case shown in fig. 3-1. Combining all possibilities the associated phase becomes $J_1 + J_2q^{J_3+J_4} + J_3q^{J_4-J_2} + J_4q^{-J_2-J_3} + J_5$. One should sum this phase over all possible ways of dividing $J + 2$ lines in five groups,

$$\begin{aligned}
& \frac{1}{(J+2)^5} \sum_{J_1+\dots+J_5=J+2} \left(J_1 + J_2q^{J_3+J_4} + J_3q^{-J_4+J_2} + J_4q^{J_2+J_3} + J_5 \right) \\
& \rightarrow_{N \rightarrow \infty} \int_0^1 dj_1 \cdots dj_5 \delta(j_1 + \dots + j_5 - 1) \\
& \quad \times \left(j_1 + j_2e^{-2\pi in(j_3+j_4)} + j_3e^{2\pi in(-j_4+j_2)} + j_4e^{2\pi in(j_2+j_3)} + j_5 \right) \\
& = \begin{cases} \frac{1}{24}, & n = 0, \\ \frac{1}{60} - \frac{1}{6(2\pi n)^2} + \frac{7}{(2\pi n)^4} & n \neq 0. \end{cases} \tag{3.6}
\end{aligned}$$

In taking the limit $N \rightarrow \infty$ the fractions $j_i = J_i/(J + 2)$ go over to continuous variables. Apart from this phase factor there is the obvious space-time dependence

$$\frac{1}{(x-y)^{2(J+1)}} \times f_{\mu\nu}$$

where $f_{\mu\nu} \equiv \partial_\mu \partial_\nu \frac{1}{(x-y)^2}$.

Now consider the second case when \bar{q} -derivative hits on a different Z -line than ∂_μ . For a fixed position of ∂_μ , say l , \bar{r} -derivative generates the phase sum

$$\sum_{l'=0; l' \neq \sigma(l)}^{J+1} \bar{q}^{l'} = -\bar{q}^{\sigma(l)},$$

where we defined $\sigma(l)$ as the position at which $\partial_\mu Z$ connects the bottom operator, *e.g.* $\sigma(l) = l - (J_3 + J_4)$ for the case shown in fig. 3-1, and used the definition $\bar{q}^{J+2} = 1$ to evaluate the sum over l' . Including the summation over l the total associated phase

factor becomes,

$$-\sum_{l=0}^{J+1} q^l \bar{q}^{\sigma(l)} \quad (3.7)$$

which is obviously the same as (3.6) up to a minus sign. The associated space-time dependence is different however,

$$\frac{1}{(x-y)^{2J}} \times f_\mu f_\nu$$

where $f_\mu \equiv \partial_\mu \frac{1}{(x-y)^2}$. It is now easy to see that the torus phase factor of the vector and BMN operators will exactly be the same also for generic momenta m, n , not necessarily equal. This general phase factor was computed in [24] and we merely quote the final result,

$$A_{m,n} = \begin{cases} \frac{1}{24}, & m = n = 0; \\ 0, & m = 0, n \neq 0 \text{ or, } n = 0, m \neq 0; \\ \frac{1}{60} - \frac{1}{6u^2} + \frac{7}{u^4}, & m = n \neq 0; \\ \frac{1}{4u^2} \left(\frac{1}{3} + \frac{35}{2u^2} \right), & m = -n \neq 0; \\ \frac{1}{(u-v)^2} \left(\frac{1}{3} + \frac{4}{v^2} + \frac{4}{u^2} - \frac{6}{uv} - \frac{2}{(u-v)^2} \right), & \text{all other cases} \end{cases} \quad (3.8)$$

where $u = 2\pi m, v = 2\pi n$. Note also that space-time dependences of two separate cases that were considered above nicely combine into the conformal factor, (3.1), as

$$\frac{f_{\mu\nu}}{(x-y)^2} - f_\mu f_\nu = 2 \frac{J_{\mu\nu}(x,y)}{(x-y)^6}. \quad (3.9)$$

Combining above results, free two-point function of the vector operators including genus one corrections can now be summarized as

$$\langle \bar{O}_\nu^m(y) O_\mu^n(x) \rangle_{\text{free torus}} = (\delta_{nm} + g_2^2 A_{nm}) \frac{2J_{\mu\nu}(x,y)}{(x-y)^2} G(x,y)^{J+2}. \quad (3.10)$$

This result clearly shows the mixing of O_μ^n operators at the torus level since the correlator is non-zero for $n \neq m$ (unless either n or m is zero). This operator mixing is described by the $\mathcal{O}(g_2^2)$ matrix $g_2^2 A_{nm}$. This particular momenta mixing issue of

the BMN operators was first addressed in [22]. The eigenoperators corresponding to the true string eigenstates can be obtained diagonalizing the light cone Hamiltonian at g_2^2 order. We will not need this diagonalization explicitly for our purposes. There is another type of mixing of the BMN operators at the torus level: single trace operators mix with the multitrace operators at $\mathcal{O}(g_2)$ [29]. Roughly, this corresponds to the fact that single string states are no longer the true eigenstates of the light-cone Hamiltonian when one considers string interactions but mixing with multi-string states should be taken into account. As in [24] we shall ignore these mixing issues in this paper.

3.3 Planar interactions of the two-point function

One of the main results of this manuscript is that vector operators possess the same anomalous dimension with the BMN operators. In this section we prove this result at the planar level and develop the techniques necessary to handle the interactions of vector operators which will also be used in the next section when we consider $\mathcal{O}(\lambda')$ interactions at genus one. These techniques can easily be used for $\mathcal{O}(\lambda')$ interactions at higher genera as well. However higher loop corrections would require non-trivial modifications.

Interactions of the vector operators are far more complicated than BMN operators because there are three new type of interactions that has to be taken into account. Recall $\mathcal{N} = 4$ SYM Lagrangian (with Euclidean signature) written in $\mathcal{N} = 1$ component notation [33],

$$\begin{aligned}
\mathcal{L} = & \frac{1}{4} F_{\mu\nu}^2 + \frac{1}{2} \bar{\lambda} \not{D} \lambda + \overline{D_\mu Z^i} D_\mu Z^i + \frac{1}{2} \bar{\theta}^i \not{D} \theta^i \\
& + i\sqrt{2} g f^{abc} (\bar{\lambda}_a \bar{Z}_b^i L \theta_c^i - \bar{\theta}_a^i R Z_b^i \lambda_c) - \frac{g}{\sqrt{2}} f^{abc} (\epsilon_{ijk} \bar{\theta}_a^i L Z_b^j \theta_c^k + \epsilon_{ijk} \bar{\theta}_a^i R \bar{Z}_b^j \theta_c^k) \\
& - \frac{1}{2} g^2 (f^{abc} \bar{Z}_b^i Z_c^i)^2 + \frac{g_{YM}^2}{2} f^{abc} f^{ade} \epsilon_{ijk} \epsilon_{ilm} Z_b^j Z_c^k \bar{Z}_d^l \bar{Z}_e^m
\end{aligned} \tag{3.11}$$

where $D_\mu Z = \partial_\mu + ig[A_\mu, Z]$ and L, R are the chirality operators. For convenience we use complex combinations of the six scalar and fermionic fields in adjoint representa-

tion,

$$Z^1 = Z = \frac{X^5 + iX^6}{\sqrt{2}}, \quad Z^2 = \phi = \frac{X^1 + iX^2}{\sqrt{2}}, \quad Z^3 = \psi = \frac{X^3 + iX^4}{\sqrt{2}}$$

with analogous definitions for fermions, θ^i .

Recall the result of [24], (also see [33]) that, the only interactions involved in correlators of BMN operators were coming from F-terms since D-term and self-energy contributions exactly cancels each other out. That was due to a non-renormalization theorem for two-point functions of chiral primary operators and unfortunately, this simplification will no longer hold for the correlators involving vector operators because of the covariant derivatives. It will be convenient to group interactions in three main classes because the calculation techniques that we use will differ for each separate class:

1. D-term and self energies
2. Interactions of external gluons in O_μ^n
3. F-terms

In the following subsection we will show that interactions in the first class can be rewritten as a correlator of the non-conserved current, $\langle \text{Tr}(J_\mu \bar{J}_\nu) \rangle$ where

$$J_\mu = Z \overset{\leftrightarrow}{\partial}_\mu Z. \tag{3.12}$$

This will be a consequence of the non-renormalization theorem mentioned above. Second class of interactions which are coming from the commutator term in the covariant derivative will then promote the ordinary derivative in J_μ to a covariant derivative, hence total contribution of the interactions in first and second class will be represented as the correlator of a gauge-covariant (but non-conserved) current $U_\mu = Z \overset{\leftrightarrow}{D}_\mu Z$. Computation of this correlator by differential renormalization method [34] is given in Appendix A. Last class of interactions originating from F-term in (3.11) are easiest to compute. This quartic vertex is only possible between a scalar impurity,

ϕ and an adjacent Z -field (at planar level), and its contribution to the anomalous dimension of BMN operators was already computed in [24]. We can confidently conclude that F-term contribution to vector anomalous dimension is half the BMN anomalous dimension because the BMN operator involves two scalar impurities which contribute equally whereas the vector operator involves only one scalar impurity. However, a rigorous calculation for vector operators is provided in Appendix B for completeness.

3.3.1 Non-renormalization of chiral primary correlator

Let us begin with recalling the non-renormalization theorem of the chiral primary correlator,

$$\langle \text{Tr}(\phi Z^{J+1}) \text{Tr}(\bar{\phi} \bar{Z}^{J+1}) \rangle. \quad (3.13)$$

For our purposes it will suffice to confine ourselves to planar graphs. D-term part of (3.11) includes the quartic interaction $\text{Tr}([Z, \bar{Z}]^2)$ (or $\text{Tr}([\phi, \bar{\phi}][Z, \bar{Z}])$) and the gluon exchange between two adjacent Z -lines,

$$\begin{array}{c} a \quad b \\ \text{---} \quad \text{---} \\ \text{---} \quad \text{---} \\ a' \quad b' \end{array} + \begin{array}{c} \text{---} \quad \text{---} \\ \text{---} \quad \text{---} \end{array} = (f^{pab} f^{pa'b'} + f^{pab'} f^{pa'b}) B(x, y) G(x, y)^2 \quad (3.14)$$

where a, a', b, b' indicate adjoint color indices, $G(x, y) = 1/(4\pi^2(x - y)^2)$ is the free scalar propagator and $B(x, y)$ is a function which arise from the integration over vertex positions and contains information about the anomalous dimension. self-energy corrections to Z and ϕ propagators arise from a gluon exchange, chiral-chiral and chiral-gaugino fermion loops. We represent this total self-energy contribution as,

$$\begin{array}{c} a \\ \text{---} \bullet \text{---} \\ a' \end{array} = \delta^{aa'} N A(x, y) G(x, y) \quad (3.15)$$

where $A(x, y)$ again contains $\mathcal{O}(g_{YM}^2)$ contribution to anomalous dimension.

Planar contributions to (3.13) are obtained by inserting (3.14) in between all adjacent Z - Z and ϕ - Z pairs and summing over self energies on all J lines including ϕ . Since every term in (3.11) is flavor blind except than the F-term, eqs. (3.14) and

(3.15) also hold for ϕ . Therefore, from now on we do not distinguish interactions of ϕ and Z fields and in all of the following figures a solid line represents either ϕ or Z (unless ϕ is explicitly shown by a dashed line).

A convenient way to represent sum of all these interactions is to define a total vertex as shown in fig. 3-2 and sum over $J + 2$ possible insertions of this vertex in between all adjacent lines. Note that in Fig. 3-2 the self-energy contributions on each

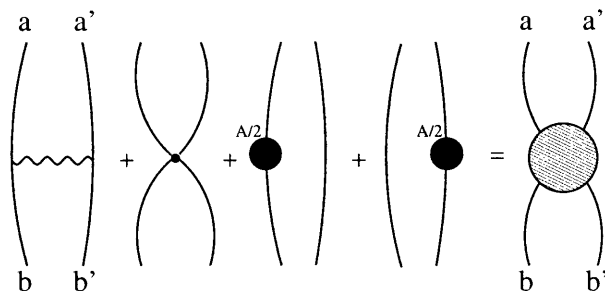


Figure 3-2: Combination of g_{YM}^2 corrections under a total vertex.

line are taken as half the original value, $A(x, y)/2$, to compensate the double-counting of self energies by this method. One of the $J + 2$ possible contributions is shown in Fig. 3-3. Using the trace identities given in Appendix B. it is straightforward to compute the amplitude represented by Fig. 3-3. One obtains,

$$\begin{aligned}
 \text{Fig.3-3} &= G(x, y)^J \left\{ \frac{1}{2} (N/2)^{J-3} \text{Tr}(T^a T^{a'} T^b T^{b'}) (f^{pab} f^{pa'b'} + f^{pab'} f^{pa'b}) B(x, y) + (N/2)^{J+1} A(x, y) \right\} \\
 &= G(x, y)^J (N/2)^{J+1} \left\{ B(x, y) \left(1 + \frac{2}{N^2} \right) + A(x, y) \right\} \\
 &\rightarrow G(x, y)^J (N/2)^{J+1} \{ B(x, y) + A(x, y) \}.
 \end{aligned}$$

$\mathcal{O}(1/N^2)$ term in second line is coming from the second permutation in (3.14) and is at torus order hence negligible in the BMN limit taken in the last line. Clearly, insertions in all other spots give equal contributions and the final answer becomes,

$$\langle \text{Tr}(\phi Z^{J-1}) \text{Tr}(\overline{\phi} \overline{Z}^{J-1}) \rangle = G(x, y)^J (J + 2) (N/2)^{J+1} \{ B(x, y) + A(x, y) \}. \quad (3.16)$$

Then, the non-renormalization theorem of this correlator [35][33] tells that,

$$4.33 \propto \text{Tr} \left(\text{two circles} \right) \propto (B + A) = 0 . \quad (3.17)$$

This identity greatly simplifies the following calculations.

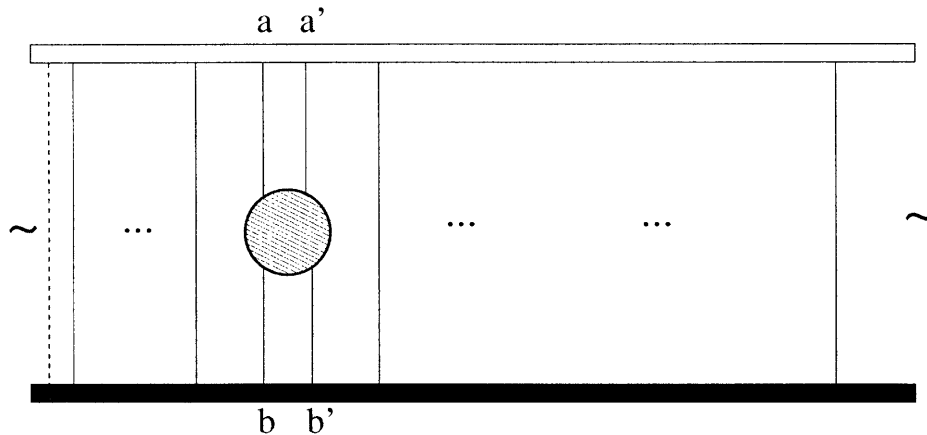


Figure 3-3: Planar interactions of chiral primaries can be obtained by placing the total vertex between all adjacent pairs. To find the vector correlator one simply dresses this figure by ∂_μ^q and $\partial_\nu^{\bar{r}}$.

3.3.2 D-term and self-energies

Now, consider the D-term and self-energy contributions to planar two-point function of vector operators,

$$\langle O_\mu^n(x) \bar{O}_\nu^m(y) \rangle_1 = \partial_\mu^q \partial_\nu^{\bar{r}} \langle \text{Tr}(\phi Z^{J+1}) \text{Tr}(\bar{\phi} \bar{Z}^{J+1}) \rangle \quad (3.18)$$

where we used the fact that q -derivation and commutation operations commute with each other to take q -derivatives out of the correlator. Once again, we note that minimal coupling in the covariant derivative can be dropped as its contribution will be of order $\mathcal{O}(g^3)$. Now it is clear that calculation is reduced to taking $\partial_\mu^q \partial_\nu^{\bar{r}}$ of Fig. 3-3 and summing over all possible locations of the total vertex in Fig. 3-3. In taking $\partial_\mu^q \partial_\nu^{\bar{r}}$ of Fig. 3-3, one encounters three possibilities.

If both of the derivatives hit lines other than the four legs coming into the total

vertex, than graph is proportional to $(B + A)\partial_\mu G(x, y)\partial_\nu G(x, y)$ hence vanishes by (3.17). Second possibility is when one of the q -derivatives hit the vertex and other outside. Supposing ∂_μ^q hits the vertex, trivial algebraic manipulations show that the graph will be proportional to,

$$\begin{aligned} \partial_\nu G(x, y)\partial_\mu^q \text{Tr} \left\{ \text{Diagram} \right\} &= \frac{1}{2}\partial_\nu G(x, y) \left[(1 - q)\text{Tr} \left\{ \text{Diagram} - \text{Diagram} \right\} \right. \\ &\quad \left. + (1 + q)\partial_\mu \text{Tr} \left\{ \text{Diagram} \right\} \right] \\ &= \frac{1}{2}\partial_\nu G(x, y) \left[(1 - q)\langle \text{Tr}(J_\mu \bar{Z} \bar{Z}) \rangle + (1 + q)\partial_\mu \left\{ (B + A)G(x, y)^2 \right\} \right]. \end{aligned}$$

where J_μ was defined in (3.12). The second term in the last line again vanishes by (3.17) whereas the first term is the self energy and D-term corrected two point function of a vector operator J_μ with a scalar operator \bar{Z}^2 . Now, it is immediate to see that by the antisymmetry of derivative in J_μ , both D-term quartic vertex and self ebergy corrections to $\langle J_\mu \bar{Z}^2 \rangle$ vanishes. With a little more afford one can also see that the gluon exchange contribution is identically zero as well and the second possibility givevs no contribution.

Therefore we are only left with the third possibility where both ∂_μ^q and $\partial_\nu^{\bar{r}}$ are acting on the vertex in Fig. 3-3. With similar algebraic manipulations of this graph and the use of (3.17) one obtains,

$$\partial_\mu^q \partial_\nu^{\bar{r}} \text{Tr} \left\{ \text{Diagram} \right\} = \frac{1}{4}(1 - q)(1 - \bar{r})\langle \text{Tr}(J_\mu(x)\bar{J}_\nu(y)) \rangle. \quad (3.19)$$

Recall that there is a phase factor depending on the position of the vertex in Fig.3-3. If this position is l then this factor equals $(q\bar{r})^l$ and one should sum over the vertex position from $l = 0$ to $l = J + 1$ to obtain the total contribution. Using our definition of the vector phase, (3.4), this phase summation generates the multiplicative factor $(J + 2)\delta_{mn}$. Furthermore, use of the trace identities of Appendix B one squeezes the whole trace down to the trace of interacting part with a multiplicative factor of $\frac{1}{2}(N/2)^{J-1}$ (See Appendix B for a similar application of the trace identities). The

final answer can be written as,

$$\begin{aligned}
\langle O_\mu^n(x) \bar{O}_\nu^m(y) \rangle_1 &= \partial_\mu^q \partial_\nu^{\bar{r}} \langle \text{Tr}(\phi Z^{J+1}) \text{Tr}(\bar{\phi} \bar{Z}^{J+1}) \rangle_1 \\
&= G(x, y)^J \frac{1}{2} (N/2)^{J-1} (J+2) \delta_{mn} \frac{1}{4} (1-q)(1-\bar{r}) \langle \text{Tr}(J_\mu(x) \bar{J}_\nu(y)) \rangle.
\end{aligned}
\tag{3.20}$$

Radiative corrections to this current correlator arise from three sources: D-term quartic vertex, gluon exchange and self energies. It is easy to see that D-term contribution vanishes identically by the antisymmetry of J_μ under exchange of two incoming Z particles. This is shown in Appendix A. self-energy contributions are straightforward to calculate with Differential Renormalization method [34] and calculations are explicitly shown in Appendix A.

However, gluon exchange contribution to $\langle J \bar{J} \rangle$ is notoriously difficult to evaluate by direct methods. Fortunately, there is the following trick ¹: Suppose that one computes the true flavor-current correlator of scalar QED, $\langle j \bar{j} \rangle$ with $j = \bar{Z} \overleftrightarrow{\partial} Z$ instead. Feynman rules treat these two correlators equivalently except than an overall minus sign (J and j differs only by replacement of a Z with a \bar{Z} then color factors at external vertices give rise to a minus sign) and the appropriate color factors at the vertices. Hence one can obtain the anomalous dimension which arise from gluon exchange graph by considering the vacuum polarization graphs of scalar QED at two-loop order as we explain below. There are four Feynman diagrams that are shown in Fig. 3-4. Note that, the anomalous dimension arises from the sub-divergent pieces of the gluon exchange graph (when the internal vertices come close to x or y .) Now, the Ward identity of scalar QED requires that the sub-divergent logarithmic pieces of graph I, II and III cancels each other out (IV do not contribute to anomalous dimension.) This fact allows us to compute gluon exchange in terms of I and II which are easy enough to evaluate directly as shown in Appendix A. When the smoke clears one obtains the total anomalous dimension arising from D-term and self-energy part

¹We are grateful to Dan Freedman for pointing out this idea.

of the Lagrangian as,

$$\langle O_\mu^n(x) \bar{O}_\nu^m(y) \rangle_1 = -\frac{5}{8} \lambda' n^2 \delta_{mn} \log((x-y)^2 \Lambda^2) \frac{J_{\mu\nu}(x,y)}{(x-y)^2} G(x,y)^{J+2} \quad (3.21)$$

with the correct normalization of the vector operators.

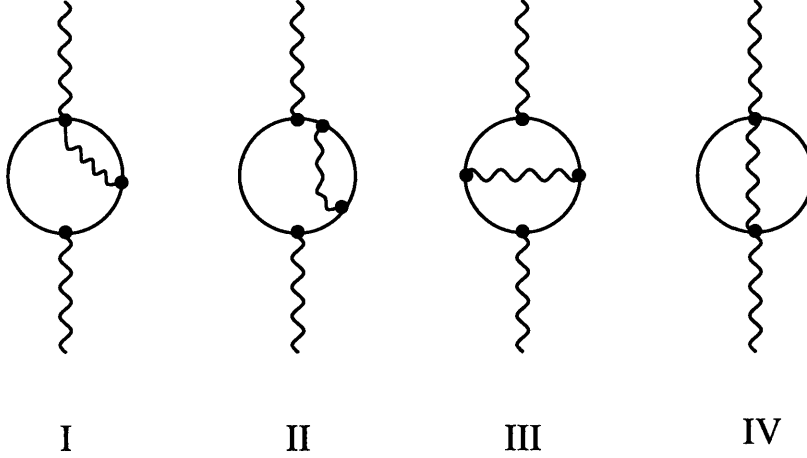


Figure 3-4: Two-loop diagrams of vacuum polarization in scalar QCD. Treatment of other four diagrams obtained by replacing the scalar lines with gluons can be separately and do not affect our argument.

3.3.3 External gluons

There are two topologically different classes of planar diagrams which involve external gluons at $\mathcal{O}(g_{YM}^2)$ order. First class, shown in Fig. 3-5, which arise from contracting external gluons of O_μ^n and \bar{O}_ν^m do not involve any internal vertex to be integrated over, hence do not give rise to log terms. By considering all possible Wick contractions and employing the trace identities of Appendix B, sum over all of these diagrams yield (in Feynman gauge),

$$\langle O_\mu^n(x) \bar{O}_\nu^m(y) \rangle_2 \rightarrow g_{YM}^2 (1-q)(1-\bar{r}) \delta_{\mu\nu} \frac{\delta_{mn}}{(x-y)^2} (J+2)(N/2)^{J+3} G(x,y)^{J+2}. \quad (3.22)$$

Therefore this class does not contribute to the anomalous dimension.

Second class of diagrams which involve one external gluon and one internal cubic vertex are depicted in Fig. 3-6. Diagrams where external gluon belongs to \bar{O}_ν^m will give

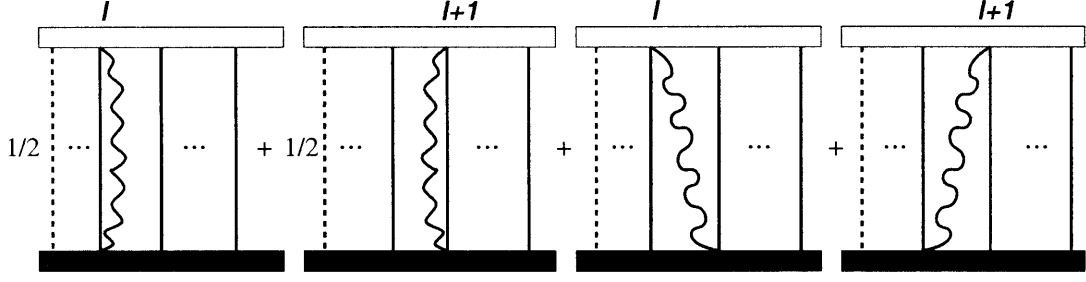


Figure 3-5: First class of $\mathcal{O}(g_{YM}^2)$ diagrams involving external gluons. These do not yield anomalous dimension as there are no internal vertices.

identical contributions to those in fig. 3-6, hence need not be considered separately. Minimal coupling in the covariant derivative in \overline{O}_ν^m can again be dropped since we are interested in $\mathcal{O}(g_{YM}^2)$. Let us first consider graph I in Fig. 3-6. Total contribution to correlator is obtained by taking $\partial_\nu^{\bar{r}}$ of this diagram and performing the phase sum over all possible positions $l \in \{0, \dots, J+1\}$. Define,

$$\text{---} \overset{\text{a}}{\curvearrowright} \overset{\text{b}}{\text{---}} = N\delta_{ab}C_\mu(x, y). \quad (3.23)$$

Using the identity, $\bar{r}^{J+2} = 1$ one easily obtains the $\partial_\nu^{\bar{r}}$ of Graph I with the result,

$$(q\bar{r})^l G(x, y)^J \frac{1}{4} (N/2)^J N^3 \{ \partial_\nu C_\mu(x, y) G(x, y) - \partial_\nu G(x, y) C_\mu(x, y) \}$$

where we again used the trace identities of Appendix B. Summation over l yields,

$$G(x, y)^J \frac{1}{4} (N/2)^J N^3 (J+2) \delta_{mn} \left\{ G(x, y) \overleftrightarrow{\partial}_\nu C_\mu \right\}. \quad (3.24)$$

Graph II gives identical contribution except than a factor of $q\bar{r}$. In Appendix A, we compute $C_\mu(x, y)$ and conclude that graphs I and II give the following contribution to the anomalous dimension (including the equal contribution from the reflected graph where external gluon belongs to \overline{O}_ν^m),

$$\text{Graph I + II} \rightarrow -\frac{3}{8} (1 + q\bar{r}) \frac{g_{YM}^2 N}{4\pi^2} \delta_{mn} \frac{J_{\mu\nu}(x, y)}{(x-y)^2} \log((x-y)^2 \Lambda^2) G(x, y)^{J+2}. \quad (3.25)$$

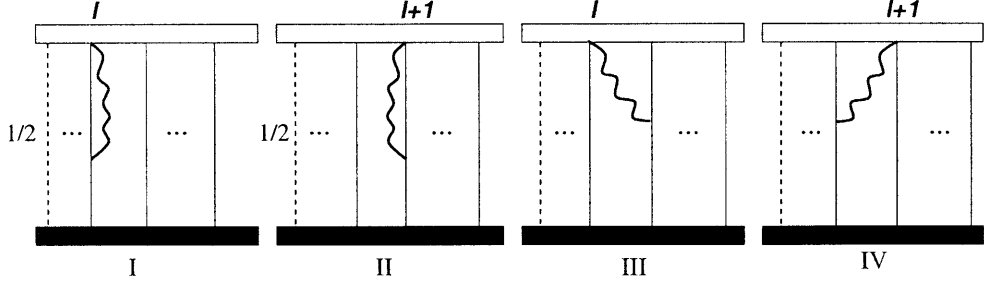


Figure 3-6: Second class of diagrams which involve one external gluon. Derivative of the \bar{O}_ν^J can be placed at any position. Integration over the internal vertex yields a contribution to anomalous dimension.

To handle graph III in Fig. 3-6, let us write,

$$\begin{array}{c} a' \\ \curvearrowright \\ a \end{array} \begin{array}{c} b' \\ \curvearrowleft \\ b \end{array} = -(f^{pab} f^{pa'b'} + f^{pab'} f^{pa'b}) C_\mu(x, y) G(x, y). \quad (3.26)$$

By the same token, $\partial_\nu^{\bar{r}}$ of graph III can be written as (at planar level),

$$\begin{aligned} & -\frac{1}{2}(N/2)^{J-1} G(x, y)^{J-1} \left(\frac{N^4}{8} \right) (q\bar{r})^l \left\{ \partial_\nu^{\bar{r}} (G(x, y) C_\mu(x, y)) G(x, y) - \right. \\ & \quad \left. -(1 + \bar{r}) \partial_\nu G(x, y) G(x, y) C_\mu(x, y) \right\} \\ & = \frac{1}{2} (N/2)^{J-1} G(x, y)^J (q\bar{r})^l \bar{r} \left(\frac{N^4}{8} \right) \left\{ G(x, y) \overleftrightarrow{\partial}_\nu C_\mu(x, y) \right\} \end{aligned}$$

where $\frac{N^4}{8}$ comes from the the color factor, $f^{pab} f^{pa'b'} \text{Tr}(T^a T^{a'} T^{b'} T^b)$. Second color combination in (3.26) gives torus level contribution hence negligible at planar level. Summing over l and using the expression for C_μ which is evaluated in Appendix A, one gets the following contribution,

$$\text{Graph III} \rightarrow -\frac{3}{8} \frac{g_{YM}^2 N}{4\pi^2} \bar{r} \delta_{mn} \frac{J_{\mu\nu}(x, y)}{(x-y)^2} \log((x-y)^2 \Lambda^2) G(x, y)^{J+2} \quad (3.27)$$

where we included the equal contribution coming from the horizontal reflection of graph IV. Graph IV and horizontal reflection of III gives (3.27) with \bar{r} is replaced by

q , giving all in all,

$$\begin{aligned}
\langle O_\mu^J(m; x) \bar{O}_\nu^J(n; y) \rangle_2 &= -\frac{3}{8} \frac{g_{YM}^2 N}{4\pi^2} (1 - q - \bar{r} + q\bar{r}) \delta_{mn} \log \left((x - y)^2 \Lambda^2 \right) \frac{J_{\mu\nu}(x, y)}{(x - y)^2} G(x, y)^{J+2} \\
&= -\frac{3}{8} \frac{g_{YM}^2 N}{4\pi^2} (1 - q)(1 - \bar{r}) \delta_{mn} \log \left((x - y)^2 \Lambda^2 \right) \frac{J_{\mu\nu}(x, y)}{(x - y)^2} G(x, y)^{J+2} \\
&= -\frac{3}{8} \lambda' n^2 \delta_{mn} \log \left((x - y)^2 \Lambda^2 \right) \frac{J_{\mu\nu}(x, y)}{(x - y)^2} G(x, y)^{J+2} \quad (3.28)
\end{aligned}$$

as the total contribution to anomalous dimension from external gluons, after normalizing according to (3.2).

As an aside let us make an important observation which will be used in section 4. In the previous section we concluded that D-term and self-energy contributions to the vector correlator can be organized in terms of the current two-point function $\langle J_\mu \bar{J}_\nu \rangle$ where $J_\mu = Z \overleftrightarrow{\partial}_\mu Z$. Curiously enough, the external gluons result, eq. (3.28) can exactly be reproduced (in order $\mathcal{O}(g_{YM}^2)$) by promoting the ordinary derivative of J_μ in (3.20) to the covariant derivative. Therefore, *one can neatly represent the contributions of D-term, self-energy and external gluons to the anomalous dimension in terms of radiative corrections to the current correlator* $\langle \text{Tr}(U_\mu(x) \bar{U}_\nu(y)) \rangle$ where U_μ is the *gauge-covariant but non-conserved current*, $U_\mu = Z \overleftrightarrow{D}_\mu Z$. Had U_μ been conserved there would not be any radiative corrections to the correlator and the corresponding non- F term contributions to anomalous dimension would vanish identically. By using the equations of motion one can easily see that the “non-conservation” of U_μ is of $\mathcal{O}(g_{YM})$ hence one expects first order corrections to $\langle U\bar{U} \rangle$ be $\mathcal{O}(\lambda')$. Indeed, combining (3.21) and (3.28) one obtains,

$$\langle O_\mu^n(x) \bar{O}_\nu^m(y) \rangle_{1+2} = G(x, y)^J \delta_{mn} \frac{1}{4} (1 - q)(1 - \bar{r}) \langle \text{Tr}(U_\mu(x) \bar{U}_\nu(y)) \rangle \quad (3.29)$$

$$\rightarrow -\lambda' n^2 \delta_{mn} \log \left((x - y)^2 \Lambda^2 \right) \frac{J_{\mu\nu}(x, y)}{(x - y)^2} G(x, y)^{J+2} \quad (3.30)$$

Notice that anomalous dimension is in units of the correct effective 't Hooft coupling associated with the BMN limit *i.e.* $\lambda' = g_{YM}^2 N/J^2$, and tensorial form of the correlator indicates that conformal primary nature of O_μ^J operators is preserved by planar

radiative corrections.

This result proves our previous claim that F-term contribution (which is calculated in Appendix B) and the rest (D-term, self-energy and external gluons) are equal hence the total planar two-point function of vector operators with $\mathcal{O}(\lambda')$ radiative corrections can be written as,

$$\langle O_\mu^n(x) \bar{O}_\nu^m(y) \rangle = \left(1 - \lambda' n^2 \log\left((x-y)^2 \Lambda^2\right)\right) \delta_{mn} \frac{2J_{\mu\nu}(x,y)}{(x-y)^2} G(x,y)^{J+2} \quad (3.31)$$

which shows that *the vector operators possess the same anomalous dimension as BMN operators, as required by the consistency of the BMN conjecture.* This concludes our first test on the BMN conjecture.

3.4 Anomalous dimension on the torus

In the previous section we noted that F-term contribution to planar anomalous dimension of vector operators is just half of the BMN case because vector operators involve one scalar impurity field compared to two impurities of BMN operators. Similarly, one can easily show the effect of F-term interactions on the torus which arise from the ϕ impurity produces half of the BMN torus dimension. Furthermore, we will show that D-term and external gluon contributions combine neatly into the form $\langle \text{Tr}(U_\mu \bar{U}_\nu) \rangle$ as in the planar case, hence yield the same torus anomalous dimension as the F-terms. Therefore, the total torus anomalous dimension of BMN and vector operators are the same as well. As in the previous section we will group the interactions into D-term, external gluon and F-terms but before that it is convenient to classify topologically different torus diagrams which will show up in each of these interaction classes. Notice that all of these interactions will result in two interaction loops which are in contact with each other at the interaction vertex, fig. 3-7. Therefore, one can classify torus diagrams [24] which are leading order in J , *i.e.* $\mathcal{O}(J^3)$, according to whether

1. both of the loops are contractible,

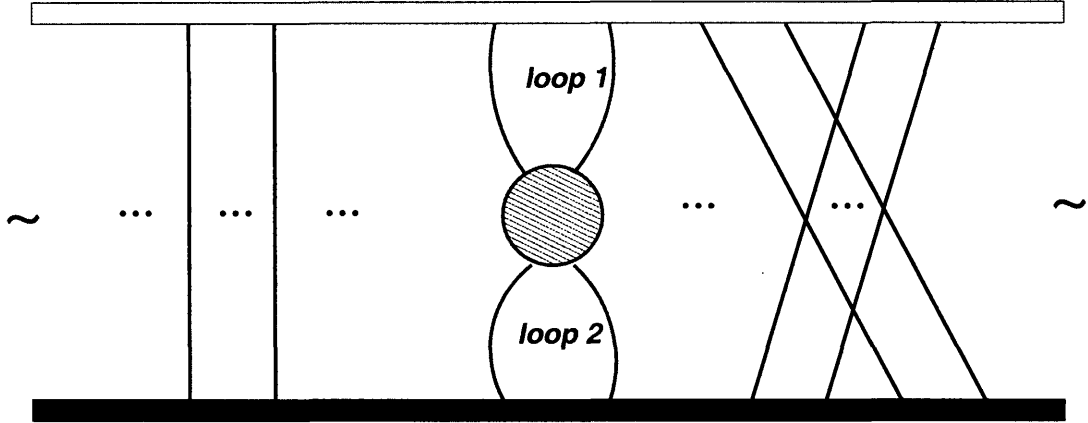


Figure 3-7: A generic $\mathcal{O}(g_{YM}^2)$ interaction on a torus diagram. The internal vertex generates two interaction loops in space-time graphs.

2. only one is non-contractible,
3. both are non-contractible on the same cycle of torus,
4. both are non-contractible on different cycles of torus.

We will call these groups as *contractible*, *semi-contractible*, *non-contractible* and *special* respectively. We called the last class *special* because it is possible only for D-term interactions as we demonstrate below. First three of these classes were discussed in [24] in detail where they were called as *nearest*, *semi-nearest* and *non-nearest* respectively. In what follows, we shall demonstrate that only the “non-contractible” class gives rise to a torus anomalous dimension.

3.4.1 Contractible diagrams

A generic contractible diagram is displayed on the cylinder and on the periodic square in Figs. 3-8 and 3-9 respectively. As in planar interactions, we combined D-term quartic vertex with gluon exchange and self energies into the total vertex, see fig. 3-2.

Let us first consider the contractible contribution to the chiral primary correlator, $\langle O_\phi^J \bar{O}_\phi^J \rangle$ where O_ϕ^J is defined in (2.34). This of course will vanish by the non-renormalization theorem of section 4.1. Still, it will be helpful for illustrative purposes

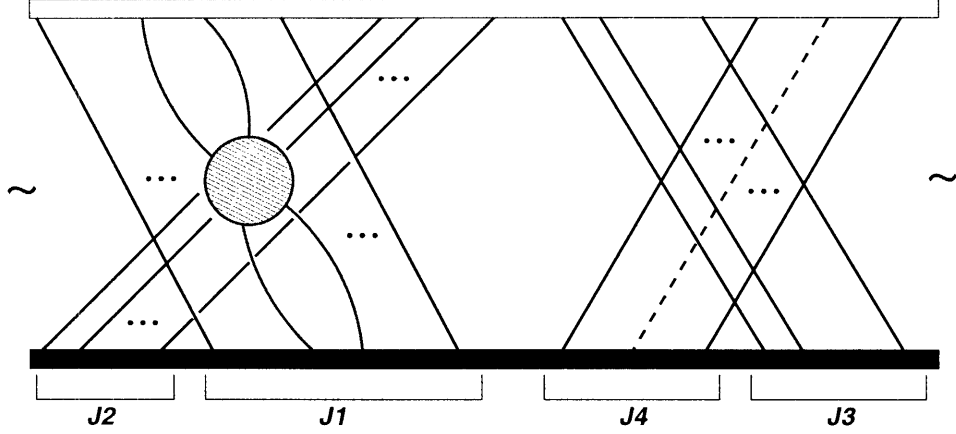


Figure 3-8: A generic contractible diagram. Total vertex includes, D-term quartic vertex, gluon exchange and self-energy corrections.

to discuss this case first because we will obtain $\langle O_\mu^n \bar{O}_\nu^m \rangle$ by taking q -derivatives of the chiral primary correlator. To obtain this contribution we would sum the diagrams similar to Fig. 3-8 with all possible contractible insertions of the this vertex. By the use of trace identities of Appendix B, one gets,

$$\langle O_\phi^J(x) \bar{O}_\phi^J(y) \rangle \propto (B(x, y) + A(x, y)) G(x, y)^{J+2} N^{J+1} J^5. \quad (3.32)$$

Total vertex gives the $B+A$ factor as in (3.16), power of N indicates that this is a torus level (to be compared with N^{J+3} dependence at planar level) and the dependence on J is coming from two observations: there are $\sim J^4$ free diagrams that can be drawn on a torus and the interaction vertex can be inserted at $\sim J$ different positions respecting the contractibility of the diagram. This, of course vanishes by the non-renormalization theorem, (3.17). One obtains correlator of vector operators simply by taking ∂_μ^q and $\partial_\nu^{\bar{r}}$ of fig. 3-8. By the same reasoning as in our planar calculation, one sees that the only non-vanishing case occurs when both of the derivatives hit legs of the total vertex. In that case one arrives at the following expression,

$$\frac{1}{4} q^l \bar{r}^{\sigma(l)} (1-q)(1-\bar{r}) \langle \text{Tr}(J_\mu \bar{J}_\nu) \rangle G^J N^{J-3}.$$

Phase summation $\sum_{l=0}^{J+1} q^l \bar{r}^{\sigma(l)}$ is identical to (3.7) yielding the phase factor, $A_{n,m}$, in

eq. (3.10). As we are interested in the anomalous dimension, we consider the case $n = m$ and get,

$$\langle O_\mu^n(x) \bar{O}_\nu^n(y) \rangle = \frac{A_{n,n}}{4} (1-q)(1-\bar{r}) \langle \text{Tr}(J_\mu \bar{J}_\nu) \rangle G^J N^{J-3}. \quad (3.33)$$

Apart from the phase factor associated with the topology of these diagrams the

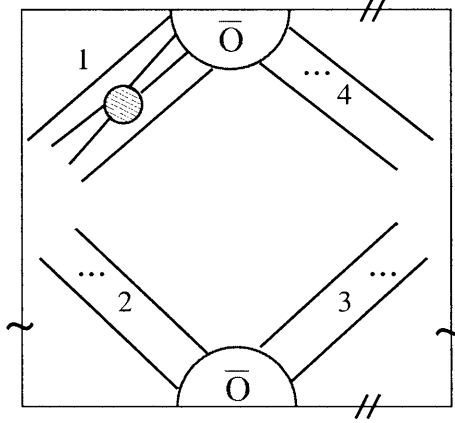


Figure 3-9: Same diagram as Fig.8, but represented on a periodic square.

calculation is identical to the planar case. Therefore, together with the contribution from external gluons and F-term quartic vertex (which is only possible between ϕ and adjacent Z 's) the final answer can be written as,

$$\langle O_\mu^n(x) \bar{O}_\nu^n(y) \rangle_{contractible} = -g_2^2 \lambda' n^2 \log [(x-y)^2 \Lambda^2] A_{nn} \frac{2J_{\mu\nu}(x,y)}{(x-y)^2} G(x,y)^{J+2}. \quad (3.34)$$

where we included the normalization associated with the torus correlator. We conclude that contractible diagrams *do not* contribute to torus anomalous dimension because their sole effect is to modify the normalization of the two point function by the factor of $A_{n,n}$.

3.4.2 Semi-contractible diagrams

An example of the second class of diagrams which might potentially contribute to torus anomalous dimension is shown on the cylinder and the periodic square in figs.

3-10 and 3-11. However, we will now show that sum over all possible semi-contractible diagrams actually vanishes. Last figure explicitly shows that the interaction loop which is formed by two adjacent Z lines connected to O_μ^n is contractible whereas the other interaction loop formed by \bar{Z} lines connected to O_ν^m is surrounding a cycle of the torus. A glance at either figures show that there are 8 possible positions that one can put in such a semi-contractible vertex—as opposed to J possible insertions of contractible vertex—hence the multiplicity of this class of graphs is order J less than the contractible class, that is $\mathcal{O}(J^4)$. As we explain next, the phase summation provides a factor of $\mathcal{O}(1/J)$ rendering semi-contractible class leading order in J *i.e.* $\mathcal{O}(J^3)$. To

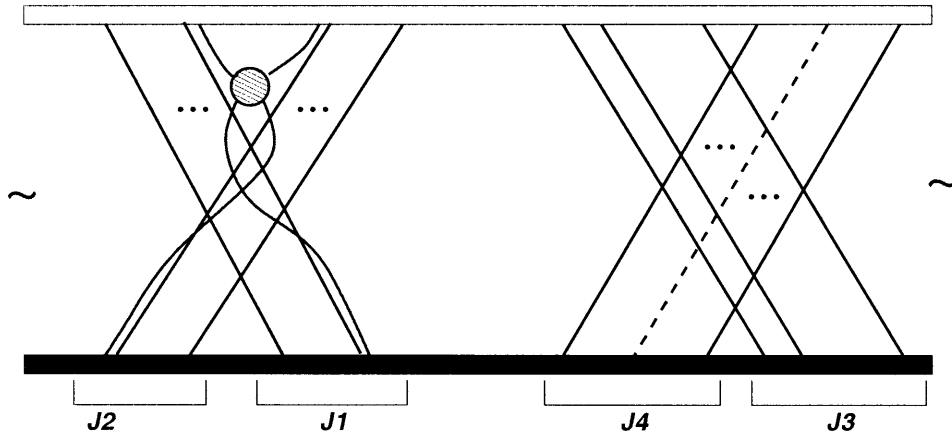


Figure 3-10: A semi-contractible diagram shown on the cylinder.

compute the contribution of fig. 3-10 to the total anomalous dimension one can use the same trick as above. One first combines D-term, gluon exchange and self energies under the total vertex of fig. 3-2. Then, insertion of derivatives in all possible ways with the phases shows that,

$$\langle O_\mu^n(x) \bar{O}_\nu^m(y) \rangle \propto (1 - q)(1 - \bar{r}^{J_1 + J_2}) \langle \text{Tr}(J_\mu \bar{J}_\nu) \rangle$$

for the fixed position of ϕ as in fig. 3-10 and fixed $J_1 \dots J_4$. Contributions from the external gluons are shown in fig. 3-12. Not surprisingly, they add up with total

vertex to modify the above result as,

$$\langle O_\mu^n(x) \bar{O}_\nu^m(y) \rangle \propto (1 - q)(1 - \bar{r}^{J_1 + J_2}) \langle \text{Tr}(U_\mu \bar{U}_\nu) \rangle.$$

One similarly computes the contributions from 7 other semi-contractible graphs with

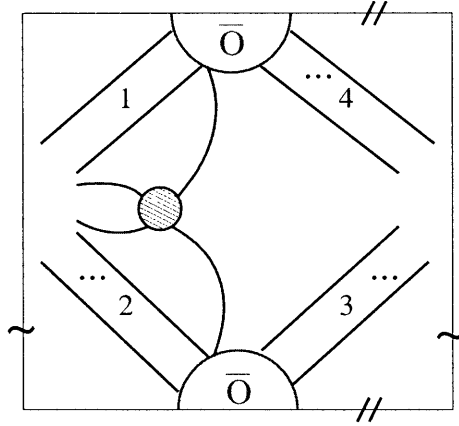


Figure 3-11: Same diagram as Fig. 3-10, but represented on a periodic square.

the *same* $J_1 \dots J_4$ and the *fixed* position of ϕ , and finds that phase factors conspire exactly to cancel out the total result. F-term contributions also give rise to same phase factors and cancel out in exactly the same way as described above.

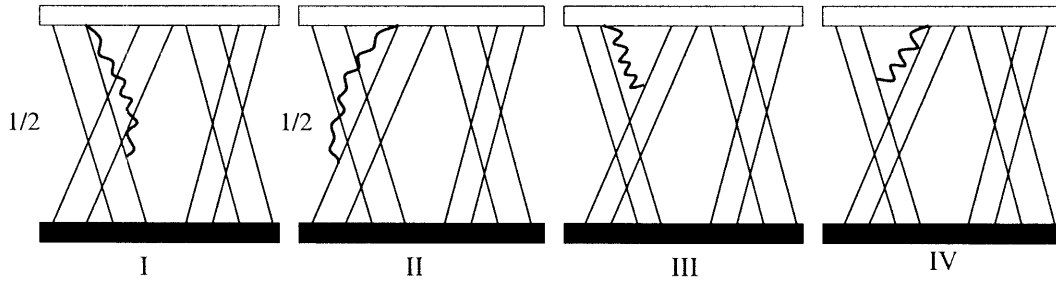


Figure 3-12: External gluon interactions with semi-contractible topology.

3.4.3 Non-contractible diagrams

As advertised in the beginning of this section, we will now show that non-contractible diagrams, figs. 3-13 and 3-14, yield a finite contribution to torus anomalous dimen-

sion. As one can observe in fig. 3-14, to join the legs of the interaction vertex while both interaction loops surround the same cycle of the torus, it is necessary that one of the 4 possible Z -blocks be absent (block 3 is absent in fig. 3-14). Therefore the multiplicity of this class is $1/J$ lower than the semi-contractible class, that is $\mathcal{O}(J^3)$. However phase summation will not change this order essentially because upper and lower legs of the interaction vertex are separated by a macroscopic number of Z lines. One concludes that non-contractible diagrams are also $\mathcal{O}(J^3)$ *i.e.* leading order.

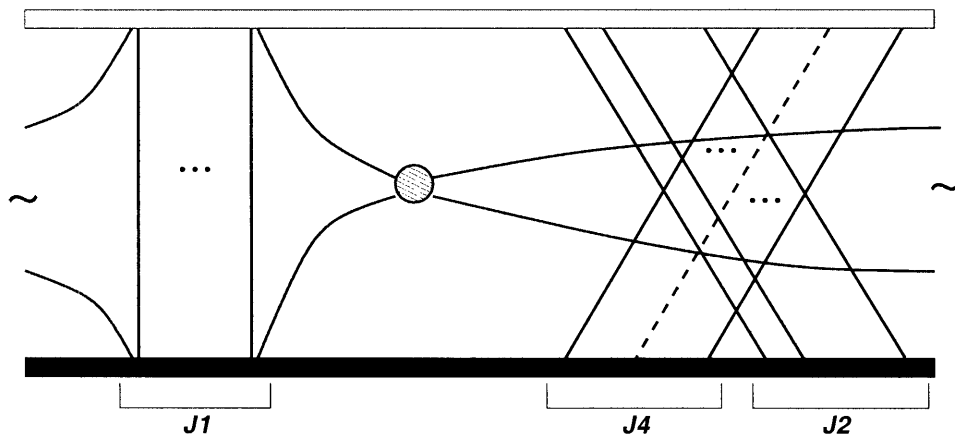


Figure 3-13: Non-contractible diagrams on the cylinder.

fig. 3-15 shows non-contractible external gluon diagrams. Having gained experience with previous calculations one can immediately write down the contribution of the total D-vertex and external gluons (for the fixed position of ϕ shown in figures) as,

$$\frac{1}{4}(1 - q^{J_1})(1 - \bar{q}^{J_1})\bar{q}^{J_2}\langle\text{Tr}(U_\mu(x)\bar{U}_\nu(y))\rangle G(x, y)^J N^{J-3}.$$

This result should be summed over all positions of the scalar impurity ϕ and finally over J_1, \dots, J_4 . Clearly no relative phase will be associated when ϕ is in the first vertical block in fig. 3-13. When it is in the second block, relative distance of ϕ and $\bar{\phi}$ to the interaction vertex is J_3 , hence a nontrivial phase, q^{J_3} arises. The last case, when ϕ propagator is in the third block was already considered above and yields the phase q^{-J_2} . Replacing the sum over J_i (with $J_1 + J_2 + J_3 = J$) by an integral over

$j_i = J_i/J$ (with $j_1 + j_2 + j_3 = 1$), one arrives at the integral

$$\int_0^1 dj_1 dj_2 dj_3 \delta(j_1 + j_2 + j_3 - 1) (j_2 e^{2\pi i n j_3} + j_3 e^{-2\pi i n j_2} + j_1) |1 - e^{2\pi i n j_1}|^2 = \frac{1}{3} + \frac{5}{2\pi^2 n^2} \quad (3.35)$$

(for $n \neq 0$). Using the result for current correlator from Appendix A, one finds the following D-term and external gluon contribution from the non-contractible diagrams,

$$\langle O_\mu^n(x) \bar{O}_\nu^m(y) \rangle \rightarrow \left(\frac{1}{3} + \frac{5}{2\pi^2 n^2} \right) G(x, y)^J \ln(\Lambda^2(x-y)^2) \frac{J_{\mu\nu}(x-y)}{(x-y)^2}. \quad (3.36)$$

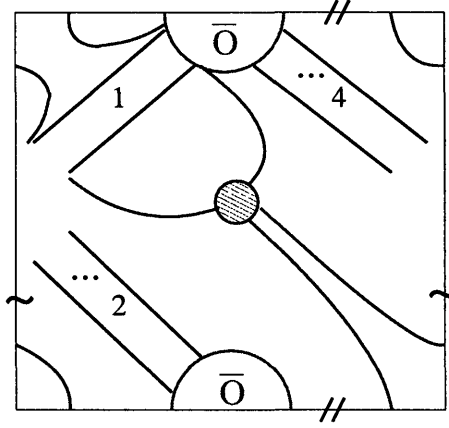


Figure 3-14: A Non-contractible diagram on the periodic square. Note that 3rd block of Z -lines is missing.

The non-contractible F-term contribution in fig. 3-13 arises when ϕ (and $\bar{\phi}$) impurity is at the first or last positions of the first block where one replaces the total vertex with an F-term quartic vertex. Note that the integral over this vertex gives the logarithmic scaling,

$$\frac{1}{(4\pi^2)^4} \int \frac{d^4 u}{(x-u)^4 (y-u)^4} = 2\pi^2 \ln(\Lambda^2(x-y)^2) G(x, y)^2. \quad (3.37)$$

Now, one should dress this diagram by all possible locations of the derivatives. When both ∂_μ and ∂_ν hit the same line, the phase summation is equivalent to the situation discussed above. A double derivative line replaces the ϕ impurity whose position is to be summed over as in (3.35) and one again finds out the factor $(\frac{1}{3} + \frac{5}{2\pi^2 n^2})$ together

with the space-time dependence, $\partial_\mu \partial_\nu \frac{1}{(x-y)^2}$. The case where ∂_μ and ∂_ν hits different lines is handled in the same way as in section 2. One first considers a fixed position of ∂_μ , say l , and sum over position of ∂_ν from $l' = 0$ to $J + 1$ with the condition $l' \neq \sigma(l)$. This yields a factor $-q^l \bar{q}^{\sigma(l)}$ which is then summed over l and finally over J_1, \dots, J_4 resulting in the same phase factor (3.35) up to a minus sign but with a different space-time dependence, $\partial_\mu \frac{1}{(x-y)^2} \partial_\nu \frac{1}{(x-y)^2}$. Combining these cases one gets,

$$\left(\frac{1}{3} + \frac{5}{2\pi^2 n^2}\right) \frac{J_{\mu\nu}(x-y)}{(x-y)^2}$$

where we used (3.9). Therefore F-term contribution to anomalous part of the torus correlator is exactly the same as (3.36) and the total result involving D-term, external gluon and F-term contribution simply becomes,

$$\langle O_\mu^n(x) \bar{O}_\nu^m(y) \rangle_{D\text{-term}} \rightarrow \frac{\lambda' g_2^2}{4\pi^2} \left(\frac{1}{3} + \frac{5}{2\pi^2 n^2}\right) G(x, y)^J \ln(\Lambda^2(x-y)^2) \frac{2J_{\mu\nu}(x-y)}{(x-y)^2}. \quad (3.38)$$

This torus dimension is exactly the same as torus anomalous dimension of BMN operators, [24].

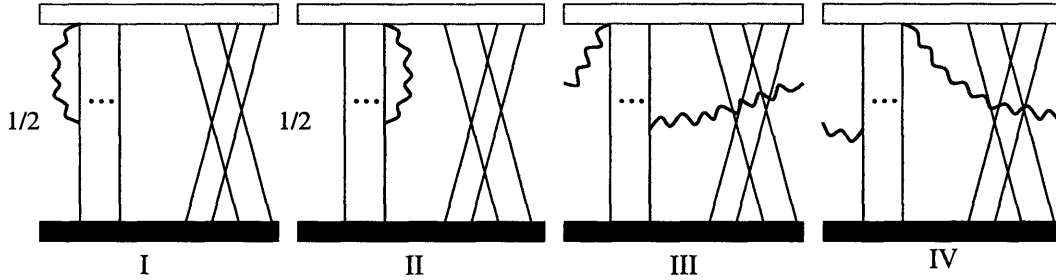


Figure 3-15: External gluon interactions with non-contractible topology.

3.4.4 Special diagrams

All of the topological classes of Feynman graphs that have been discussed so far were available both for F-term and D-term parts of the Lagrangian (3.11). However, the special Feynman graphs on the torus are formed when the interaction loops wind around different cycles and are present only if the interaction is a D-term quartic

vertex (and their external gluon cousins). To see this, one should specify the orientation of the scalar propagator line $Z\bar{Z}$ (and $\phi\bar{\phi}$) by putting an arrow on it (not to be confused by derivatives). We choose the convention where scalar propagation is from O towards \bar{O} . With specification of the orientations, the F-term and D-term quartic vertices can be represented as in fig. 3-16. One observes that the vertex where *adjacent lines have the opposite orientation* is only possible for D-terms. Using such a vertex one can draw 4 different special graphs on a torus. One of these possibilities is shown in figs. 3-17 or 3-18. Here the shaded circle represents the total vertex, fig. 3-2 as before. Special graphs can also be formed by external gluons as in fig. 3-19. In general, special graphs are formed by combining either first or last lines of blocks 1 and 3 or blocks 2 and 4.

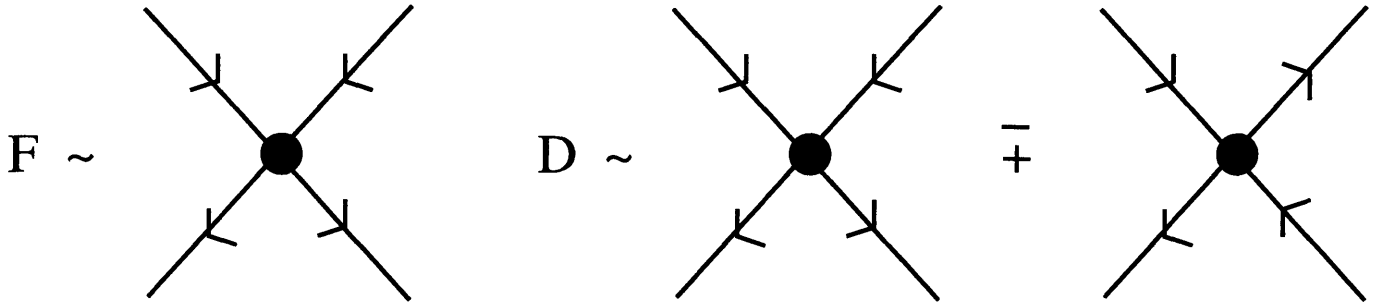


Figure 3-16: Orientations of F-term and D-term quartic vertices.

However, one makes a disturbing observation about special graphs: They are $\mathcal{O}(J^4)$ therefore all of the graphs we have considered so far are sub-leading with respect to them! Even worse, this extra power of J seems to be unsuppressed in the BMN limit, hence the presence of such graphs imply the breakdown of BMN perturbation theory!? Hopefully, as we shall demonstrate next, contribution of special graphs to the anomalous dimension is zero when one adds up all such possible graphs (fig. 3-17) just as in the semi-contractible case.

Let us consider a fixed position of ϕ at the last line of the first block and fixed J_1, \dots, J_4 . By use of trace identities given in Appendix B and q -derivation tricks described above, one can easily boil down the special D-graphs into our familiar $\langle J\bar{J} \rangle$ correlator. Let us first consider the special contribution to the chiral primary

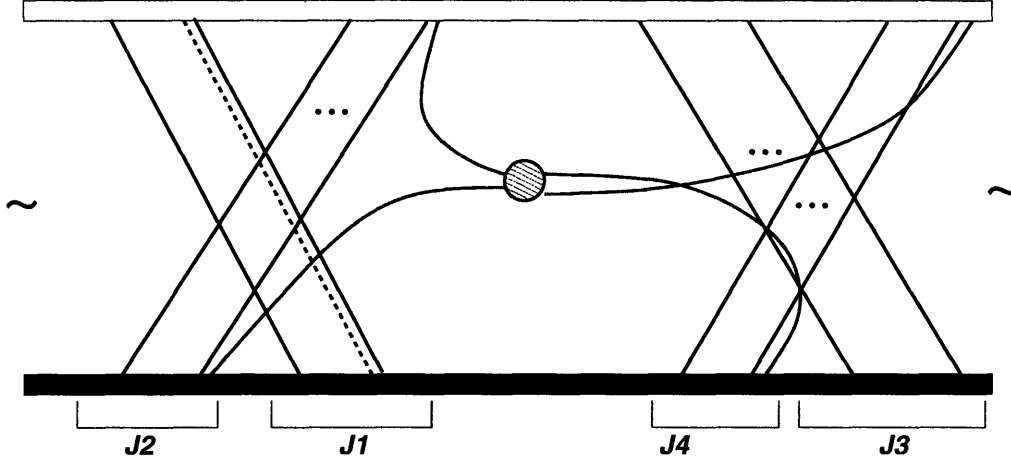


Figure 3-17: Special diagrams shown on a cylinder.

correlator, \mathcal{O}_ϕ^J . The trace identities show that fig. 3-17

$$\sim (B + A)G^{J+2}N^{J+1}$$

hence special graph contribution to chiral primary correlator vanishes by non-renormalization theorem. Reader will find the details of this calculation in Appendix B. Next we put in the q -derivatives on this graph to obtain the special contribution to $\langle \mathcal{O}_\mu^n \bar{\mathcal{O}}_\nu^m \rangle$ and observe that the only positions which yield a non-vanishing result is when both ∂_μ and ∂_ν act on the total vertex. Proof of this fact is exactly analogous to our argument in section 4.2. The algebraic tricks familiar from previous calculations are then used to express the result as

$$\sim q^{-J_2} \bar{r}^{J_1} (1 - q^{-J_2 - J_3}) (1 - \bar{r}^{-J_3 - J_4}) \langle J_\mu(x) \bar{J}_\nu(y) \rangle G^J N^{J+1}.$$

Similarly, the external gluon contributions shown in fig. 3-19 can be shown to have the same form and total result—which follows from combining D-term, external gluon and self-energy contributions—becomes,

$$\sim q^{-J_2} \bar{r}^{J_1} (1 - q^{-J_2 - J_3}) (1 - \bar{r}^{-J_3 - J_4}) \langle U_\mu(x) \bar{U}_\nu(y) \rangle G^J N^{J+1}.$$

This was for the diagram in fig. 3-17. A second special graph is obtained when

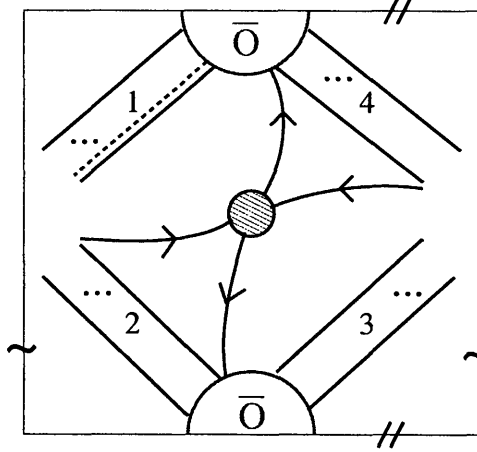


Figure 3-18: Periodic square representation of Special diagrams.

the legs of the total vertex stretches out into the last line of block 1 and last of block 3. Similarly a third graph is formed by first line in block 2 with first of 4 and a fourth graph by the first of 1 with first of 3. Let us now read off the phase factors of these four graphs respectively,

$$\begin{aligned} (1 - q^{-J_4 - J_3})(1 - \bar{r}^{-J_1 - J_4})q^{-J_2} \bar{r}^{J_1}, & \quad (1 - q^{-J_2 - J_3})(1 - \bar{r}^{-J_3 - J_4}), \\ (1 - q^{-J_2 - J_3})(1 - \bar{r}^{-J_1 - J_2})\bar{r}^{-J_3 - J_4}, & \quad (1 - q^{-J_2 - J_1})(1 - \bar{r}^{-J_1 - J_4})q^{J_1} \bar{r}^{J_1}, \end{aligned}$$

respectively. Hence the contribution from 1st graph cancels out 4th graph and the 2nd cancels out th 3rd. *We conclude that contribution of special diagrams to both the vector anomalous dimension (the case $n = m$) and the operator mixing (the case $n \neq m$) vanishes* although it seems to be divergent as $J \rightarrow \infty$ at first sight. This shows that the only non-vanishing contribution is arising from non-contractible class of diagrams and the total correlator including $\mathcal{O}(\lambda')$ corrections both at the planar and the torus levels can now be written as,

$$\begin{aligned} \langle O_\mu^n(x) \bar{O}_\nu^n(y) \rangle &= \left\{ (1 + g_2^2 A_{nn})(1 - n^2 \lambda' \ln(\Lambda^2(x - y)^2)) + \frac{\lambda' g_2^2}{4\pi^2} \left(\frac{1}{3} + \frac{5}{2\pi^2 n^2} \right) \ln(\Lambda^2(x - y)^2) \right\} \\ &\quad \times G(x, y)^{J+2} \frac{2J_{\mu\nu}(x, y)}{(x - y)^2}. \end{aligned} \quad (3.39)$$

This result clearly shows that the total contribution to the anomalous dimension

of the vector type operator at $\mathcal{O}(g_{YM}^2)$ and up to genus-2 level is exactly the same as the BMN anomalous dimension, that is,

$$\Delta = J + 2 + \lambda' n^2 - \frac{g_2^2 \lambda'}{4\pi^2} \left(\frac{1}{3} + \frac{5}{2\pi^2 n^2} \right). \quad (3.40)$$

As mentioned before, from the string theory point of view, the torus anomalous dimension is identified with the genus-one mass renormalization of the corresponding state.

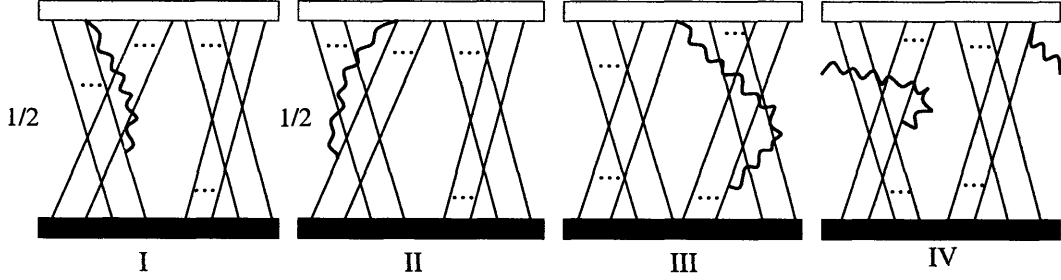


Figure 3-19: External gluons with special diagram topology.

Let us briefly describe how the non-vanishing of torus level anomalous dimension implies the non-vanishing of the $\mathcal{O}(\lambda')$ interacting three-point functions,

$$\langle \bar{O}_\mu^{n,J} O_\nu^{m,J'} O^{J-J'} \rangle \quad \text{and} \quad \langle \bar{O}_\mu^{n,J} O_\nu^{J'} O_\phi^{J-J'} \rangle$$

through the unitarity sum. Here the relevant supergravity operators are defined in (2.34) and (2.35). As mentioned in the introduction, this is puzzling since string field theory result of [36] shows that the three point function coefficient vanishes for vector operators.

It was argued in [24] that one can handle the string interactions effectively with non-degenerate perturbation theory of a quantum mechanical system. Unitarity sum gives the following 2nd order shift in the energy of the string state with momentum n ,

$$E_n^{(2)} = \sum_{m \neq n} \frac{|\langle i' | P^- | j' k' \rangle|^2}{E_n^{(0)} - E_m^{(0)}}. \quad (3.41)$$

Here $|i'\rangle$ is the string excitation with momentum n and $|j'k'\rangle$ represents all possible

intermediate states with momentum m . In the case of $|i'\rangle = \alpha_n^{\phi\dagger} \alpha_{-n}^{\mu\dagger} |0, p^+\rangle$ which is the dual of vector operator (3.3), there are two possibilities for the intermediate states:

1. $|j'\rangle = \alpha_m^{\phi\dagger} \alpha_{-m}^{\mu\dagger} |0, p_1^+\rangle$ and $|k'\rangle = |0, p_2^+\rangle$ with $p_1^+ + p_2^+ = p^+$. Corresponding operators are, $O_{\nu}^{m, J'}$ and $O^{J-J'}$ respectively.
2. $|j'\rangle = \alpha_0^{\phi\dagger} |0, p_1^+\rangle$ and $|k'\rangle = \alpha_0^{\mu\dagger} |0, p_2^+\rangle$. Corresponding operators are the BPS operators, $O_{\nu}^{J'}$ and $O_{\phi}^{J-J'}$.

Therefore the sum in (3.41) involves a sum over these two cases together with sub-summations over m and J' . Vanishing of $\langle i' | P^- | j' k' \rangle$ for both of the cases above implies that $E_n^{(2)} = (\Delta - J)_{torus} = 0$ for the vector operator. A loophole in this argument is that we only considered the cubic string vertex in the effective description whereas the *contact terms* may also contribute the mass renormalization of the string states hence give rise to a non-zero torus level anomalous dimension in the dual theory. We come back to this issue in the last section.

3.5 A SUSY argument

The fact that BMN and vector operators (which belong to separate $SO(4)$ sectors of the gauge theory) have equal anomalous dimensions both at planar and torus levels suggests that there might be a $\mathcal{N} = 4$ SUSY transformation relating these two operators. Whereas the equality of the planar anomalous dimensions of these operators is required by the consistency of BMN conjecture, there is no *a priori* reason to believe that this equality persists at higher genera. A SUSY map, however, would protect $\Delta_{BMN} - \Delta_{vector} = -1$ at all loop orders and all genera.

In this section, we will see that indeed there is such a transformation which maps the BMN operator onto vector operator plus a correction term. We will argue that the correction is negligible in the BMN limit and hence expect the equality of anomalous dimensions, *both at planar and torus levels*.

The supersymmetry transformations of $\mathcal{N} = 4$ SYM has recently been derived in [16]. In $SU(4)$ symmetric notation, the transformations of the scalars and chiral spinors read,

$$\delta_\epsilon X^{AB} = -i(-\bar{\epsilon}_-^A \theta_+^B + \bar{\epsilon}_-^B \theta_+^A + \epsilon^{ABCD} \theta_{+C} \epsilon_{-D}) \quad (3.42)$$

$$\delta_\epsilon \theta_+^A = \frac{1}{2} F_{\mu\nu} \gamma^{\mu\nu} \epsilon_+^A + 2D_\mu X^{AB} \gamma^\mu \epsilon_{-B} + 2i[X^{AC}, X_{CB}] \epsilon_+^B. \quad (3.43)$$

in which $A = 1, \dots, 4$ is an $SU(4)$ index and $X^{AB} = -X^{BA}$.

We will use these transformation rules in a somewhat schematic way, since the information we need can be obtained more simply by classifying all fields and supercharges with respect to the decomposition $SU(4) \rightarrow U(1) \times U(1) \times U(1)$. The three commuting $U(1)$ charges can be viewed as J_{12} , J_{34} and J_{56} in $SO(6)$. All fermionic quantities are taken as 2 component Weyl spinors. The four spinor fields are denoted by $\theta_\phi, \theta_\psi, \theta_Z, \theta_{A_\mu} = \lambda$ where the subscript indicates their bosonic partner in an $\mathcal{N} = 1$ decomposition of $\mathcal{N} = 4$ SUSY. The fermionic transformation rule above may be interpreted as,

$$\{\bar{Q}_{+B}, \theta^A\} \sim F_{\mu\nu} \gamma^{\mu\nu} \delta_A^B + \dots,$$

showing that \bar{Q}_{+A} has the same $U(1)$ quantum numbers as θ^A . In general fermions and anti-fermions have opposite $U(1)$ charges, as in the case of conjugate bosons. The product of these 3 charges is positive on the \bar{Q}_{+A} . With these remarks in view, we can write the following table of $U(1)$ charges.

	ϕ	ψ	Z	A_μ	θ_ϕ	θ_ψ	θ_Z	λ	Q^1	Q^2	Q^3	Q^4
J_{12}	1	0	0	0	1/2	-1/2	-1/2	1/2	-1/2	1/2	1/2	-1/2
J_{34}	0	1	0	0	-1/2	1/2	-1/2	1/2	1/2	-1/2	1/2	-1/2
J_{56}	0	0	1	0	-1/2	-1/2	1/2	1/2	1/2	1/2	-1/2	-1/2

We now apply the transformation rules (3.42) and (3.43) in the $U(1) \times U(1) \times U(1)$ basis in which all transformations which conserve the $U(1)$ charges are allowed. Consider the action of Q_α^2 on the BMN operator (2.37). We see that ϕ and Z 's are

left unchanged whereas ψ is transformed into a gaugino λ , *i.e.*

$$[Q^2, O_{\phi\psi}^n] \propto \sum_{l=0}^J e^{\frac{2\pi i n l}{J}} \text{Tr}(\phi Z^l \lambda Z^{J-l})$$

Next we act on this with another anti-chiral supercharge \bar{Q}_α^3 with quantum numbers $(-1/2, -1/2, +1/2)$. According to table 1 and transformation rules given in (3.43), Z 's again remain unchanged, λ is transformed into $D_\mu Z^2$ and ϕ is transformed into $\bar{\theta}_\psi$, *i.e.*

$$\begin{aligned} \{\bar{Q}_\alpha^3, [Q^2, O_{\phi\psi}^n]\} &\propto \sum_{l=0}^J e^{\frac{2\pi i n l}{J}} \text{Tr}(\phi Z^l (D_\mu Z) Z^{J-l}) \\ &+ \sum_{l=0}^J e^{\frac{2\pi i n l}{J}} \text{Tr}(\bar{\theta}_\psi Z^l \lambda Z^{J-l}) \equiv \tilde{O}_\mu^n + O_f^n. \end{aligned} \quad (3.44)$$

Therefore supersymmetry guarantees that $\tilde{O}_\mu^n + O_f^n$ has the same $\Delta - J$ with the BMN operator.

Note that the first term is not quite the same as the vector operator of (3.3) but there are two differences. However, for large but finite J , the difference between contributions of \tilde{O}_μ^n and O_μ^n to the correlators is $\mathcal{O}(1/J)$. This is because the exceptional piece in (3.3) where D_μ is acting on the impurity ϕ is $\mathcal{O}(1/J)$ with respect to the first term of (3.3) hence negligible in the dilute approximation. Secondly, the difference between the definitions of q for \tilde{O}_μ^n and O_μ^n , *i.e.* $q^J = 1$ and $q^{J+2} = 1$ respectively, is also $\mathcal{O}(1/J)$.

Now consider computing the dimension of $\tilde{O}_\mu^n + O_f^n$ at the planar level. This would be the same as the dimension of only \tilde{O}_μ^n provided that the transition amplitude $\langle \tilde{O}_\mu^n \bar{O}_f^m \rangle$ is negligible. Let us first consider the correlator $\langle O_\mu^n \bar{O}_f^m \rangle$ instead. Above we explained that the difference between the contributions of \tilde{O}_μ^n and O_μ^n to the anomalous dimension is $\mathcal{O}(1/J)$, therefore conclusions made for $\langle O_\mu^n \bar{O}_f^m \rangle$ will also be valid for $\langle \tilde{O}_\mu^n \bar{O}_f^m \rangle$ as $J \rightarrow \infty$ in the BMN limit. The leading contribution to this transition amplitude in $\mathcal{O}(\lambda')$ arises from Z - λ - $\bar{\theta}$ (5th term in (3.11)) and the

²The last term in (3.43) which is quadratic in the scalars does not give correct quantum numbers for $J_{12} \dots J_{56}$ hence is not present.

Yukawa interaction (6th term in (3.11)): One of the Z 's in O_μ^n splits into a θ_Z and $\bar{\lambda}$ and θ_Z gets absorbed by ϕ turning into $\bar{\theta}_\psi$ through the Yukawa interaction. See fig. 3-20 for the analogous interaction at the torus level. Note that contribution to the *planar* dimension requires the Z that is taking place in the interaction and ϕ be adjacent. Note also that the derivative in O_μ^n can be at any position. Before acting with the q -derivative, the integration over the internal vertices together with the scalar propagators yields,

$$\sim \ln((x - y)^2 \Lambda^2) G^J.$$

Since the anomalous dimension is the coefficient of the log term, anomalous contributions arise when the ∂_μ act on G 's but not on the log. Therefore any position of the derivative in O_μ^n in the planar diagram (also any position of the derivative in fig. 3-20 in torus case) gives the same contribution,

$$\sim \ln((x - y)^2 \Lambda^2) G^{J+1},$$

regardless it is acting on the fields participating in the interaction or not. Then the phase sum over the position of ∂_μ gives (using $q^{J+2} = 1$),

$$\sum_{l=0}^{J+1} q^l = 0.$$

Therefore the transition amplitude $\langle O_\mu^n \bar{O}_f^m \rangle_{planar}$ vanishes identically! As we described above this implies that, for large but finite J , $\langle \tilde{O}_\mu^n \bar{O}_f^m \rangle_{planar}$ do not vanish but suppressed with a factor of $1/J$ with respect to $\langle \tilde{O}_\mu^n \bar{\tilde{O}}_\mu^n \rangle_{planar}$ in the BMN limit. Therefore we see that *supersymmetry together with large J suppression is capable to explain why vector and BMN anomalous dimensions are equal at the planar level.*

This argument can easily be extended to the torus level. In section 5.4 it was proven that the only torus level contribution for the vector correlator $\langle O_\mu^n \bar{O}_\nu^m \rangle_{torus}$ comes from the non-contractible diagram, fig. 3-13. Recall that this diagram is of $\mathcal{O}(J^3)$ because there are three blocks of Z lines and no phase suppression (unlike

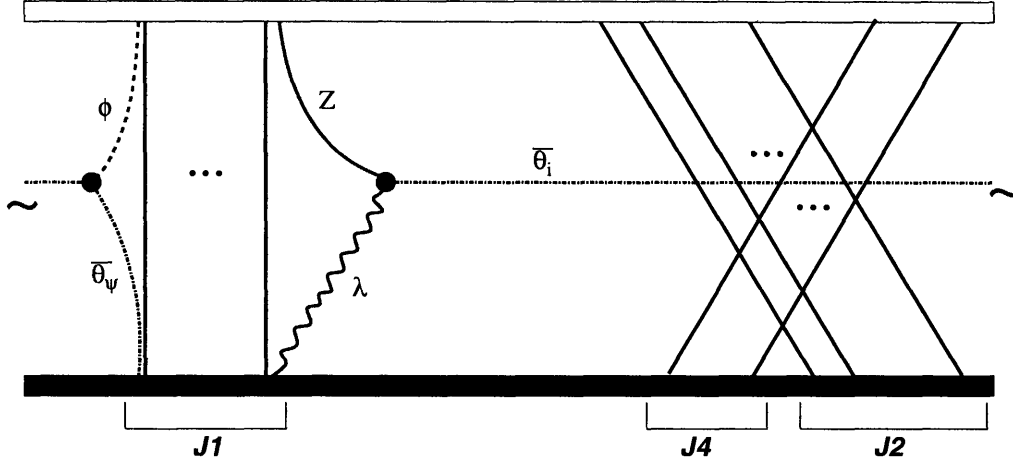


Figure 3-20: Torus level non-contractible contribution to $\langle O_\mu^n \bar{O}_f^m \rangle$ transition amplitude. Derivative in O_μ^n can be placed on any line connected to O_μ^n , although it is not shown explicitly. There is a similar graph obtained by interchanging internal vertices.

contractible or semi-contractible cases). Including the $1/(JN^2)$ normalization factor we found out that the diagram is of $\mathcal{O}(g_2^2)$. We want to see how the transition amplitude at the torus level, $\langle \tilde{O}_\mu^n \bar{O}_f^m \rangle_{torus}$ goes with J . Instead, let us again consider the correlator $\langle O_\mu^n \bar{O}_f^m \rangle_{torus}$. One can easily see that (with the same argument presented in the beginning of section 5) all possible torus diagrams of $\langle O_\mu^n \bar{O}_f^m \rangle$ can be divided into four separate classes of section 5. Let us consider the non-contractible diagram for example. The diagram is shown in fig. 3-20. The derivative in O_μ^n can be at any position. Hence the phase summation over the position of the derivative vanishes identically just as in the planar case. For the same reason the external gluon contribution vanishes as well (together with other torus diagrams: contractible, semi-contractible and special). One concludes that for large but finite J , $\langle \tilde{O}_\mu^n \bar{O}_f^m \rangle_{torus}$ is again $1/J$ suppressed with respect to $\langle O_\mu^n \bar{O}_f^m \rangle_{torus}$. We see that *supersymmetry in the BMN limit, is also capable to explain the equality of vector and BMN anomalous dimensions at the torus level*. However we emphasize that this equality is not exact but only holds in large J limit. Therefore, whether this reasoning can be extended to higher orders in genus remains as an interesting question.

As an aside we state another important conclusion. The fact that the transition amplitude is negligible with respect to $\langle O_\mu^n \bar{O}_f^m \rangle$ shows that *the vector operator O_μ^n and the fermionic impurity BMN operator O_f^n has the same planar and torus anomalous*

dimensions. This gives an easy method to generate all BMN operators which carry the same anomalous dimension as the scalar operator by acting on it with the supercharges Q^I arbitrary times *and* making sure that the transition amplitudes among all of the pieces in the end-product is negligible in the BMN limit.

3.6 Discussion and outlook

In this chapter we computed the two-point function of vector impurity type BMN operator at planar and torus levels, for small λ' (large $\mu p^+ \alpha'$). In this regime, SYM is weakly coupled and we only considered interactions at $\mathcal{O}(\lambda')$ order in SYM interactions. Our result for the total anomalous dimension is given in eq. (3.40). This turns out to be exactly the same as scalar impurity type anomalous dimension which was computed in [24] *both at planar and torus levels*. This result provides two tests on the recent conjectures. This equality at the planar level constitutes a non-trivial check on the BMN conjecture. Secondly, the non-zero torus anomalous dimension is a field theory prediction which should match the string theory result for the mass renormalization of the vector states. We mentioned at the end of section 5 however that this non-zero torus dimension raises a puzzle since the string field theory cubic vertex for vector the string states vanishes[36]. Our results are further supported by the SUSY argument given in the previous section.

We would like to briefly address some possible resolutions of this contradiction between string field theory and gauge theory results. Generally speaking, there is another type of interaction in light-cone string field theory [37] apart from the cubic string vertex. This arises from the *contact terms* and was not taken into account in the calculation of [36]. In the context of IIB strings in pp-wave background this issue was discussed in [38]. Contact terms arise from a quartic string vertex whose presence is required by supersymmetry [39][40]. Contribution of contact terms to mass renormalization is $\mathcal{O}(g_s'^2)$ and there seems no *a priori* reason to ignore it. In case these terms are indeed non-negligible they might give rise to a non-zero torus anomalous dimension in the dual field theory.

Another resolution ³ of the gauge/string contradiction would be that perturbative gauge theory calculations for the interacting three-point function are not capable to probe the short distance ($< 1/\mu$) physics on the world-sheet. Recall that [36] it is the *prefactor* of cubic vertex which suggests the vanishing of $\langle i'|P^-|j'\rangle|k'\rangle$ in case of the vector state: Spradlin and Volovich have pointed out that the short distance limit on the world-sheet and the weak gauge coupling limit ($\mu \rightarrow \infty$) do not commute. To be able to obtain the *prefactor* one should first take the short distance limit. Then one takes large μ limit to obtain an expression for the weakly coupled three-point function. This procedure expects vanishing of $\langle i'|P^-|j'\rangle|k'\rangle$. On the other hand, exchanging the limits, hence loosing the contribution of *prefactor* would suggest non-zero interacting three-point function also for the vector operator. It is a possibility that perturbative SYM is not able to “discover” the *prefactor* of string field theory but able to see only a $1/\mu$ expansion of the delta-functional. This would be another line of reasoning to explain why our perturbative calculation produced a non-zero torus anomalous dimension for the vector operator. Clearly, a perfect understanding of the map between weakly coupled string/gauge theories should resolve this apparent contradiction.

³I am Grateful to L. Motl for mentioning this idea to me.

Chapter 4

Analysis of Multi-Trace Operators

In this chapter, we consider the family of single- and multi-trace operators with two scalar “impurity” fields $\phi(x), \psi(x)$ and J “substrate” fields $Z(x)$,

$$\mathcal{O}_n^{J_0} = \frac{1}{\sqrt{J_0 N^{J_0+2}}} \sum_{l=0}^{J_0} e^{\frac{2\pi i n l}{J_0}} \text{Tr}(\phi Z^l \psi Z^{J_0-l}). \quad (4.1)$$

and

$$\mathcal{O}_n^{J_0, J_1, \dots, J_k} =: O_n^{J_0} O^{J_1} \dots O^{J_k} :, \quad (4.2)$$

with $J = J_0 + J_1 + \dots + J_k$. Here O^J is the chiral primary operator,

$$O^J = \frac{1}{\sqrt{J N^J}} \text{Tr}(Z^J). \quad (4.3)$$

The states of superconformal $\mathcal{N} = 4$ gauge theory on $R \times S^3$ which correspond to these operators¹ are dual to states of the Type IIB superstring quantized in light-cone gauge in the background pp-wave metric and 5-form (2.13)(2.14).

The dual string states are those obtained from the ground state $|p^+\rangle$ with light-cone momentum p^+ by the action of creation operators $a_\phi^*(n)$, $a_\psi^*(n)$ with world-sheet momentum n . More specifically one considers single- and multi-string states:

$$a_\phi^*(n) a_\psi^*(-n) |p^+\rangle \quad (4.4)$$

¹We use the terms states and operators as if synonymous in the gauge theory.

and

$$a_\phi^*(n)a_\psi^*(-n)|p_0^+\rangle \otimes |p_1^+\rangle \otimes \cdots |p_k^+\rangle \quad (4.5)$$

where light-cone momenta p_i^+ of individual string states are related to corresponding R -charges by $\mu p_i^+ \alpha' = \frac{J_i}{\sqrt{g_{YM}^2 N}}$.

After establishing the validity of our method for the single-trace BMN operators, one can ask for the $\mathcal{O}(g_2^2)$ eigenvalues of higher trace BMN operators. We consider this problem in this chapter. A rigorous investigation yields an unexpected result: *Eigenvalues of all multi-trace BMN operators are solely determined by the eigenvalue Δ_1 of single-trace operator as,*

$$\Delta_i = \left(\frac{J_1}{J}\right)^2 \Delta_1.$$

This result is essentially due to the suppression of connected GT correlators $\langle \bar{\mathcal{O}}_i \bar{\mathcal{O}}_j \rangle$ by a power of J as $J \rightarrow \infty$ in the BMN limit. It is found that disconnected GT diagrams are less suppressed in this limit and in fact only non-zero contributions to a generic correlator of BMN operators arise from fully disconnected pieces. The connected correlators will contribute to eigenvalues to higher order in g_2 .

Utilizing the correspondence of $\Delta - J$ with P^- in the string theory we show that this fact translates into the absence of $\mathcal{O}(g_s^2)$ contact terms between states higher than single-string states. If the correspondence with P^- at the level of matrix elements holds, this also implies that a particular class of tree-level string processes that would contribute to the matrix elements on the PP-wave are suppressed in the large μ limit. This conclusion is valid for processes in which the the external string states that have two excitations along $i = 1, 2, 3, 4$ transverse directions (that correspond to scalar impurities in BMN operators).

It is also interesting to investigate the the duality of P^- and $\Delta - J$ at the level of matrix elements. Using the method of [27] to fix the basis transformation into “string basis” at $\mathcal{O}(g_2^2)$, we study the correlators of double and triple operators in this basis and obtain predictions for the matrix elements of P^- at $\mathcal{O}(g_s^2)$, in double-double and single-triple sectors. These matrix elements are given by remarkably simple

expressions and solely determined by the “non-contractible” contribution to $\langle \bar{O}_i O_j \rangle$ correlator just as in the case of single-single matrix element [26][27]. On the ST side, in the single-string sector the matrix element is determined by the ”contact” interaction between two single-string states [28][26]. Our study suggests a generalization of this fact: a one-to-one map between non-contractible contributions to GT correlation functions and contact interactions of the corresponding states in SFT. These are explicit gauge theory results that are subject to check by a direct SFT calculation.

We organize the chapter as follows. In the next section we demonstrate the invalidity of non-degenerate perturbation theory in determining the eigen-operators and eigenvalues of $\Delta - J$. Taking into account the mixing with triple-trace operators we obtain the mostly single-trace eigen-operator at $\mathcal{O}(g_2^2)$. We briefly outline our conjecture that use of degenerate and non-degenerate perturbation theory leads us to the same results concerning the anomalous dimensions of particular eigen-states that correspond to \tilde{O}_n^J and \tilde{O}_i^J in the BMN limit. This section also introduces necessary notation and presents single-double, single-triple and double-triple trace BMN correlators. In section 2, we discuss the scaling behavior of arbitrary multi-trace correlators of BMN operators with g_2 and J . We demonstrate that connected contributions to all of the correlators of this sort are suppressed as $J \rightarrow \infty$. In section 3, we utilize this result to obtain the anomalous dimension of an i -trace BMN operator at $\mathcal{O}(g_2^2 \lambda')$. We also discuss some implications for the corresponding processes in string theory in this section. Last section studies the duality between P^- and $\Delta - J$ at the level of matrix elements.

Appendix C proves the scaling behaviour that we discuss in section 2. Appendix D deals with the basis transformation which takes from the BMN basis into string basis in GT. Using the inputs from [26] and [27] we derive new decomposition identities relating various multi-trace inner products with the product of smaller order inner products. In particular, the free single-triple inner product decomposes into single-double and double-triple inner products as,

$$G^{13} = \frac{1}{2} G^{12} G^{23}.$$

Similarly we derive the identity,

$$G^{22} = \frac{1}{2}(G^{21}G^{12} + G^{23}G^{32})$$

and discuss immediate generalizations. We emphasize that these identities are derived by relating the basis transformations proposed in [27] and [26], therefore subject to explicit GT computations. These computations which involve non-trivial summations are outlined in Appendix E and these identities are proven there. In this appendix, we also explain evaluation of other sums that are used in sections 2,4 and 5. Appendix F computes $\mathcal{O}(g_2^2)$ and $\mathcal{O}(g_2^2\lambda')$ contributions to single-triple and $\mathcal{O}(g_2)$ and $\mathcal{O}(g_2\lambda')$ contributions to double-triple correlation functions.

4.1 Operator mixing at g_2^2 level

In this section we shall carry out the diagonalization procedure of the multi-trace BMN operators including the mixing with triple trace operators. This is achieved by extending the method of [29] to include the $\mathcal{O}(g_2^2)$ and $\mathcal{O}(g_2^2\lambda')$ effects in the diagonalization. In [29], it was shown that the procedure of determining the eigenvectors and eigenvalues of the mixing matrix of single and double trace operators (which is $\mathcal{O}(g_2\lambda')$) is equivalent to first order non-degenerate perturbation theory. To include the mixing with triple trace operators one needs to go one step further in perturbation expansion, i.e. to second order perturbation theory.

Let us first outline the method of [29] briefly. Consider the eigenvalue problem,

$$M_j^i e_{(k)}^j = \lambda_{(k)} e_{(k)}^i \quad (4.6)$$

where M is the $3 \times \infty$ dimensional mixing matrix of single, double and triple trace operators. ² Here i, j is a collective index labeling the state of a BMN operator, e.g. for a triple trace, $i = \{m, y, z\}$ where $y = J_1/J$ and $z = J_2/J$ in (4.2) for $i = 3$.

²In the next section we explain why BPS type double and triple trace operators do not affect the following discussion.

The order in g_2 of the various blocks of M is indicated by,

$$M = \begin{pmatrix} 1 & g_2 & g_2^2 \\ g_2 & 1 & g_2 \\ g_2^2 & g_2 & 1 \end{pmatrix}.$$

Therefore it is possible to solve the eigenvalue problem order by order in g_2 . Expanding M , e and λ as

$$\begin{aligned} M_j^i &= \rho_i d_j^i + g_2 M^{(1)j}_i + g_2^2 M^{(2)j}_i \\ e_{(k)}^i &= d_k^i + g_2 e^{(1)i}_{(k)} + g_2^2 e^{(2)i}_{(k)} \\ \lambda_{(k)} &= \lambda_{(k)}^{(0)} + g_2 \lambda_{(k)}^{(1)} + g_2^2 \lambda_{(k)}^{(2)}, \end{aligned}$$

we obtain,

$$\begin{aligned} 0 &= (\rho_k - \lambda_{(k)}^{(0)}) d_k^i + g_2 \left(\rho_i e^{(1)i}_{(k)} + M^{(1)j}_k - \lambda_{(k)}^{(0)} e^{(1)i}_{(k)} - d_k^i \lambda_{(k)}^{(1)} \right) \\ &\quad + g_2^2 \left(\rho_i e^{(2)i}_{(k)} + M^{(2)j}_k + M^{(1)j}_i e^{(1)i}_{(k)} - \lambda_{(k)}^{(0)} e^{(2)i}_{(k)} - \lambda_{(k)}^{(1)} e^{(1)i}_{(k)} - \lambda_{(k)}^{(2)} d_k^i \right) \end{aligned} \quad (4.7)$$

At zeroth order one gets $\lambda_{(k)}^{(0)} = \rho_k$. Using this in the next order for $i \neq k$ yields the first order eigenvectors,

$$e^{(1)i}_{(k)} = \frac{M^{(1)j}_k}{\rho_k - \rho_j},$$

whereas for $i = k$ we learn that $\lambda_{(k)}^{(1)} = 0$.

Using these results, $\mathcal{O}(g_2^2)$ piece of (4.7) for $i = k$ gives,

$$\lambda_{(k)}^{(2)} = \sum_j \frac{M^{(1)k}_j M^{(1)j}_k}{\rho_k - \rho_j}, \quad (4.8)$$

and for $i \neq k$ we obtain the second order contribution to the eigenvectors,

$$e^{(2)i}_{(k)} = \frac{1}{\rho_k - \rho_i} \left(M^{(2)j}_k + \sum_j \frac{M^{(1)j}_i M^{(1)j}_k}{\rho_k - \rho_j} \right). \quad (4.9)$$

Using above expressions for $e^{(1)}$ and $e^{(2)}$, we obtain the single-trace eigen-operator modified at $\mathcal{O}(g_2^2)$ as,

$$\begin{aligned}\tilde{O}_n^J &= O_n^J + g_2 \sum_{my} \frac{\Gamma_n^{my}}{n^2 - (m/y)^2} O_{my}^J \\ &+ g_2^2 \sum_{myz} \frac{1}{n^2 - (m/y)^2} \left(\Gamma_n^{myz} + \sum_{m'y'} \frac{\Gamma_{m'y'}^{myz} \Gamma_n^{m'y'}}{n^2 - (m'/y')^2} \right) O_{myz}^J.\end{aligned}\quad (4.10)$$

Here,

$$\Gamma_j^i = G^{ik} \Gamma_{kj}$$

are the matrix of anomalous dimensions where G^{ij} denotes the inverse metric on the field space. The metric, G_{ij} is determined by the correlation functions $\langle \bar{O}_i O_j \rangle$ at the free level whereas $\mathcal{O}(\lambda')$ radiative corrections to this correlator yield Γ_{ij} . To wit,

$$\langle \bar{O}_i O_j \rangle = G_{ij} - \lambda' \Gamma_{ij} \ln(x^2 \Lambda^2). \quad (4.11)$$

G and Γ should be expanded in powers of g_2 . Instead of denoting the order in g_2 on G and Γ , we will show g_2 dependence explicitly in what follows.

Again, using above expressions for first and second order eigenvectors, $e^{(1)}$ and $e^{(2)}$, one obtains the double-trace eigen-operator as,

$$\tilde{O}_{ny}^J = O_{ny}^J + g_2 \sum_m \frac{\Gamma_{ny}^m}{(n/y)^2 - m^2} O_m^J + g_2 \sum_{myz} \frac{\Gamma_{ny}^{myz}}{(n/y)^2 - (m/y')^2} O_{myz'}^J. \quad (4.12)$$

A very important point is to notice that these expressions are valid when the coefficients in front of O_i on the RHS are finite for all values of external and internal momenta. In particular one needs to check the finiteness of (4.10) when the incoming and outgoing world-sheet energies are equal, $n = \pm(m/y)$ and also at $n = \pm(m'/y')$ for the internal denominator in the third term. Note that, the danger of degeneracy is absent only for the case $n = 1$. Therefore without checking the finiteness at $\mathcal{O}(g_2^2)$ one can assume the validity of (4.10) and (4.12) only for the very particular case of $n = 1$! We will now demonstrate that the last term in (4.10) is indeed divergent at the pole![41]

Finiteness of the $\mathcal{O}(g_2)$ piece of (4.10) was demonstrated in ([29]) where the coefficient was found to be,

$$\frac{\Gamma_n^{my}}{n^2 - (m/y)^2} = -\frac{m/y}{n + (m/y)} G_{n;my}^{12}. \quad (4.13)$$

Here, $G_{n;my}$ denotes the tree-level inner product between single and double trace operators which was first computed in [24],

$$G_{n;my}^{12} = \frac{g_2}{\sqrt{J}} \sqrt{\frac{1-y}{y}} \frac{\sin^2(\pi ny)}{\pi^2 (n - (m/y))^2}. \quad (4.14)$$

We will also make abundant use of the radiative corrections to single-double correlator which was also obtained in [29],

$$\Gamma_{n;my}^{12} = \left(\left(\frac{m}{y}\right)^2 - n\frac{m}{y} + n^2 \right) G_{n;my}^{12}. \quad (4.15)$$

Let us now investigate $\mathcal{O}(g_2^2)$ part of (4.10). First of all, it is not hard to show that there is no divergence at $n = \pm m'/y'$ in the second sum of the second term. These internal poles are canceled out by zeros of the numerator. Similarly one can show that (4.10) is finite at the external pole $n = -m/y$. This is done at the end of this section. However we shall shortly demonstrate that the external pole at $n = +m/y$ give rise to a divergence [41] hence render the use of non-degenerate perturbation theory invalid for $n > 1$.³

To go further we need (in addition to matrix elements already computed in the literature) the $\mathcal{O}(g_2^2)$ contributions to

$$G_{n;myz}^{13} \quad \text{and} \quad \Gamma_{n;myz}^{13}$$

and $\mathcal{O}(g_2)$ contributions to

$$G_{ny;my'z'}^{23} \quad \text{and} \quad \Gamma_{ny;my'z'}^{23}.$$

³For $n = 1$ it is impossible to satisfy the degeneracy condition $n = m/y$.

Necessary computations are summarized in Appendix F and the results read,

$$G_{n;myz}^{13} = \frac{g_2^2}{\pi^2 J} \sqrt{\frac{z\bar{z}}{y}} \frac{1}{(n-k)^2} \left((1-y) \sin^2(\pi n y) + y(\sin^2(\pi n z) + \sin^2(\pi n \bar{z})) \right. \\ \left. - \frac{1}{2\pi(n-k)} (\sin(2\pi n y) + \sin(2\pi n z) + \sin(2\pi n \bar{z})) \right) \quad (4.16)$$

$$\Gamma_{n;myz}^{13} = \lambda'(n^2 + k^2 - nk) G_{n;myz}^{13} + B_{n;myz}^{13}. \quad (4.17)$$

Here $k = m/y$ is the world-sheet momentum of the double-string state and we defined $\bar{z} = 1 - y - z$.

Let us digress to underline an important detail. As we showed in Appendix F, among the contributions to the radiative corrections to single-triple correlator there are contractible, semi-contractible and non-contractible Feynman diagrams (see Appendix F for definition of contractibility in planar diagrams). The contributions of the first two are summarized in the first term above, whereas $B_{n;myz}^{13}$ denotes the non-contractible contribution,

$$B_{n;myz}^{13} = \frac{2g_2^2 \lambda'}{\pi^3 J} \frac{1}{(n - m/y)} \sqrt{\frac{z\bar{z}}{y}} \sin(\pi n z) \sin(\pi n \bar{z}) \sin(\pi n (1 - y)). \quad (4.18)$$

Double-triple coefficients receive $\mathcal{O}(g_2)$ only from disconnected diagrams where the 2-3 process is separated as 1-1 and 1-2. Therefore these require somewhat simpler computations and the results are,

$$G_{ny';myz}^{23} = y'^{3/2} G_{n;my/y'}^{12} (d_{y',y+z} + d_{y',1-z}) + \frac{g_2}{\sqrt{J}} d_{mn} d_{yy'} \sqrt{(1-y)z\bar{z}} \quad (4.19)$$

$$\Gamma_{ny';myz}^{23} = \frac{n^2}{y'^2} G_{ny';myz}^{23} + y'^{3/2} (d_{y',y+z} + d_{y',1-z}) \frac{m}{y} (m/y - n/y') \quad (4.20)$$

$$= \left(\frac{n^2}{y'^2} - \frac{n}{y'} \frac{m}{y} + \frac{m^2}{y^2} \right) G_{ny';myz}^{23}. \quad (4.21)$$

We now move on to compute the $\mathcal{O}(g_2^2)$ term in (4.10). First of all one shows the curious fact⁴ that

$$\Gamma_n^{myz} = 0. \quad (4.22)$$

⁴which finds a natural explanation in the formulation of [41]

Γ_n^{myz} is decomposed as,

$$\Gamma_n^{myz} = G^{myz;m'} \Gamma_{m';n} + G^{myz;m'y'} \Gamma_{m'y';n} + G^{myz;m'y'z'} \Gamma_{m'y'z';n}. \quad (4.23)$$

One can easily invert $3 \times \infty$ dimensional matrix G_{ij} , by solving the equation $G^{ik} G_{kj} = d_j^i$ order by order in g_2 . To $\mathcal{O}(g_2^2)$ one finds,

$$G^{ij} = \begin{pmatrix} d_{mn} + G_{m;py''}^{12} G_{py'';n}^{12} & -G_{m;ny'}^{12} & \frac{1}{2} G_{m;py''}^{12} G_{py'';ny'z'}^{23} - \frac{1}{2} G_{m;ny'z'}^{13} \\ -G_{my;n}^{12} & d_{mn} d_{y,y'} + G_{my;p}^{12} G_{p;ny'}^{12} + \frac{1}{2} G_{my;py''z''}^{23} G_{py''z'';ny'}^{23} & -\frac{1}{2} G_{my;ny'z'}^{23} \\ \frac{1}{2} G_{myz;py''}^{23} G_{py'';n}^{12} - \frac{1}{2} G_{myz;n}^{13} & -\frac{1}{2} G_{myz;ny'}^{23} & \frac{1}{4} d_{m,n} d_{y,y'} (d_{z,z'} + d_{z,\bar{z}'}) + \frac{1}{4} G_{myz;py''}^{23} G_{py'';ny'z'}^{23} \end{pmatrix}.$$

By the use of decomposition identities listed in Appendix E, one can prove that (4.23) vanishes (see App. E for details).

Let us now consider the last term in (4.10). A calculation similar to the one that leads to (4.13) gives,

$$\Gamma_{py'}^{myz} = \frac{1}{2} k' (k' - p) \frac{G_{p;my/y'}^{12}}{\sqrt{y'}} (d_{y',y+z} + d_{y',y+\bar{z}}), \quad (4.24)$$

where $k' = my'/y$. The other necessary ingredient, $\Gamma_n^{py'}$ was already computed in [29]

$$\Gamma_n^{py'} = k(k-n) G_{n;py'}$$

where $k = p/y'$. Inserting these expressions into (4.10), we get the whole coefficient in front of O_{myz}^J as,

$$I = \frac{1}{n^2 - (m/y)^2} \int_0^1 dy' \sum_{p=-\infty}^{\infty} \frac{k'(k'-p)k(k-n)}{2\sqrt{y'}(n^2 - (p/y')^2)} G_{p;my/y'} G_{n;py'} (d_{y',y+z} + d_{y',y+\bar{z}}). \quad (4.25)$$

Despite the appearance of $n^2 - (p/y')^2$ in the denominator there is no divergence at $n = \pm p/y'$ because $G_{n;py'}$ in the numerator also vanishes at these intermediate poles. We will now show however that I is divergent at $n = m/y$ [41]. The residue of I at $n = m/y$ is,

$$(n - m/y)I \Big|_{n=m/y} = -\frac{g_2^2}{4\pi^4 J} \sqrt{\frac{z\bar{z}}{y}} \int_0^1 dy' \frac{1}{y'} (d_{y',y+z} + d_{y',y+\bar{z}}) \sin^2(\pi n y')$$

$$\sum_{p=-\infty}^{\infty} \frac{p}{y'} \frac{\sin^2(\pi p y/y')}{(n^2 - (p/y')^2)(n - p/y')^2}.$$

We emphasize that the infinite series in this expression is a prototype for the non-trivial sums that appear in the computations involving triple-trace BMN operators. We explain the computation of this one and other similar sums which will be necessary for the next section in Appendix E. ⁵ The result is,

$$\sum_{p=-\infty}^{\infty} \frac{p}{y'} \frac{\sin^2(\pi p y/y')}{(n^2 - (p/y')^2)(n - p/y')^2} = y' \left(\frac{\pi^3 y^2}{2} \cot(\pi n y') - \frac{\pi^2 y}{4n} \right). \quad (4.26)$$

Inserting this in the above expression for the residue and evaluating the integral gives,

$$(n - m/y)I \Big|_{n=m/y} = \frac{g_2^2}{J} \frac{y}{8n\pi^2} \sqrt{\frac{z\bar{z}}{y}} \sin(\pi n z) \sin(\pi n \bar{z}).$$

Since the residue does not vanish at $n = +m/y$, (4.10) becomes divergent at this pole.

To see that there is no further divergence in (4.10) let us consider what happens at the other pole $n = -m/y$. It is easy to see from (4.13) that the second term is finite because G^{12} in the numerator linearly goes to zero as well as the denominator. The complicated second piece in the last term of (4.10) seems to be divergent at the first sight. Let us look at the residue at this pole,

$$(n + m/y)I_2 \Big|_{n=-m/y} = -\frac{g_2^2}{4\pi^4 J} \sqrt{\frac{z\bar{z}}{y}} \int_0^1 dy' \frac{1}{y'} (d_{y',y+z} + d_{y',y+\bar{z}}) \sin^2(\pi m y'/y)$$

⁵Unfortunately none of the well-known symbolic computation programs is helpful.

$$\times \sum_{p=-\infty}^{\infty} \frac{p}{y'} \frac{\sin^2(\pi p y / y')}{((m/y)^2 - (p/y')^2)^2}.$$

This sum vanishes thanks to the antisymmetry of the summand. Thus we saw that all of the terms in (4.10) is finite at the pole $n = -m/y$ ⁶.

The fact that $I = \infty$ at $n = m/y$, hence (4.10) is ill-defined at this pole hints that *one should rather use degenerate perturbation theory to handle the diagonalization problem* [41]. Although somewhat disappointing, this result is by no means unexpected. On the GT side one can reason as follows.⁷ 't Hooft limit suggests that anomalous dimensions of observables be expanded in powers of g_2^2 where $g_2 = 1/N$ in 't Hooft limit and $g_2 = J^2/N$ in the BMN double scaling limit. Had single-trace BMN operators been degenerate with double-trace BMN operators one would expect an $\mathcal{O}(g_2)$ shift in the single-trace anomalous dimension. This would be unexpected for the 't Hooft expansion of the observables hence might have indicated an inconsistency in the BMN theory. However the degeneracy of single and triple-trace BMN operators, at most, gives rise to an $\mathcal{O}(g_2^2)$ shift in Δ_1 which is not inadmissible. By the same token, one generally expects degeneracy among BMN operators with only odd-numbered traces and only even-numbered traces separately. At order g_2^2 , this result indeed follows by the scaling law of GT correlators derived in the next section provided that there is no degeneracy between single and double-traces and there is degeneracy between single and triple traces. Hence, at this order the degenerate subspace of BMN operators are divided into two subspaces which include odd and even numbered traces separately.

On the string theory side the degeneracy of single and triple-trace operators indicate that a single-string state can decay into a triple-string state the same world-sheet momentum $m = ny$. Furthermore, as we mentioned in the introduction, correspondence of trace number in GT and string number in ST loses its meaning for finite g_2 . Therefore the general conclusion is that an initial string state that is composed of states of different string number but all on the same “momenta-shell”, $n = m/y$,

⁶Of course one has to worry about finiteness of (4.12) at $n = \pm m/y$. But this requires much little effort to see from the expressions for Γ^{23} and Γ^{12} .

⁷This is a suggestive argument due to Dan Freedman.

is generically unstable and can decay into states that are stable at $O(g_s^2)$. These stable states should be in correspondence with the eigen-operators of the degenerate subspaces in GT side. This conclusion is hardly surprising.

We shall not pursue this degeneracy problem further in this paper, but based on some preliminary calculations we make the following conjecture. Consider the degeneracy problem for finite J (which we choose as an odd number for convenience). Then two degenerate subspaces involve $1, 3, \dots, J$ -trace and $2, 4, \dots, J-1$ -trace operators separately. To find whether degeneracy gives rise to a shift in the eigenvalues one should diagonalize the order g_2^2 “transition matrix”, M_i^{i+2} (finite J version of (4.6)) at $n = m/y$ separately for odd and even i . We conjecture that regardless the exact form of M , there exist an eigenstate O'_1 that tend to the BMN operator \tilde{O}_1 (at order g_2^2) as $J \rightarrow \infty$ where \tilde{O}_i is the mostly i -trace eigen-operator of the dilatation generator that is obtained by the non-degenerate formulation at $\mathcal{O}(g_2)$. Furthermore there exist i -trace eigenstates, O'_i in the degenerate subspace whose eigenvalues tend to the anomalous dimensions of \tilde{O}_i that are obtained by naively using the non-degenerate formulation. Therefore the eigenvalues of these particular O'_i will coincide with the anomalous dimensions which can be obtained via non-degenerate theory ignoring the aforementioned mixing. For the case of $i = 1$ this can be understood as a justification of (2.39). For $i > 1$ this leads to a simplification in determination of the higher-trace anomalous dimensions which we employ in section 4. We prefer to leave this assertion as a conjecture in this paper.

In section 4 we will use this conjecture to make predictions about string-theory amplitudes. We will first compute the anomalous dimension of a general i -trace BMN operator, $\Delta_i - J$ by the method of non-degenerate perturbation theory. Since dilatation generator is supposed to correspond to P^- , this will give a prediction for the eigenvalue of P^- in the two-string sector. Next, we will move on to compute the modified mixing matrices, $\tilde{\Gamma}^{22}$ and $\tilde{\Gamma}^{13}$ in the string basis. This will allow us to make predictions for the corresponding matrix elements of P^- .

4.2 Dependence on g_2 and J of an arbitrary gauge theory correlator

As shown by detailed investigation in the recent literature n-point functions of the observables in the BMN limit come with definite dependence on the dimensionless parameters, λ' and g_2 .⁸ Generally, the correlators also have an explicit dependence on J which will turn out to be crucial in drawing conclusions about the corresponding string processes.

In this section we will discuss the g_2 and J dependence of a two-point correlator of multi-trace BMN operators with two scalar impurities:

$$C^{ij} \equiv \langle : \bar{O}_n^{J_1} \bar{O}^{J_2} \dots \bar{O}^{J_i}(x) :: O_m^{J_{i+1}} O^{J_{i+2}} \dots O^{J_{i+j}}(0) : \rangle \Big|_{connected}. \quad (4.27)$$

This scaling law that we find is also valid for the correlators of a more general class of operators,

$$: O_{n_1}^{J_1} \dots O_{n_i}^{J_i} O_\phi^{J_{i+1}} \dots O_\phi^{J_{i+j}} O_\psi^{J_{i+j+1}} \dots O_\psi^{J_{i+j+k}} O^{J_{i+j+k+1}} \dots O^{J_{i+j+k+l}} :,$$

for arbitrary i, j, k, l and also for the n-point functions involving same type of operators. This should be clear from the discussion in Appendix C.

The space-time dependence of (4.27) is trivial: $(4\pi^2 x^2)^{-J-2}$ in free theory and $(4\pi^2 x^2)^{-J-2} \ln(x^2 \Lambda^2)/(8\pi^2)$ at $\mathcal{O}(\lambda')$ where J is the total number of Z fields, *i.e.* $J = J_1 + \dots + J_i = J_{i+1} + \dots + J_{i+j}$ in (4.27). Without loss of generality, one can assume $j \leq i$. There are various connected and disconnected diagrams with different topology that contribute to (4.27). Since the results for disconnected contributions will be given by (4.27) for smaller i and j , it suffices to consider the fully-connected contribution to (4.27). In Appendix C we prove that the fully-connected piece of (4.27) has the

⁸For finite g_2 proof exist only at linear order in λ' although it is very likely to hold at higher loops. For $g_2 = 0$, [42] showed that sum of radiative corrections to single-single BMN correlator at all orders in $\mathcal{O}(g_{YM}^2)$ can be expressed as a function only λ' .

following general form,

$$C^{ij} = \frac{g_2^{i+j-2}}{J^{(i+j)/2-1}} \left\{ G^{ij} \frac{1}{(4\pi^2 x^2)^{J+2}} - \lambda \Gamma^{ij} \frac{1}{(4\pi^2 x^2)^{J+2}} \ln(x^2 \Lambda^2) \right\}. \quad (4.28)$$

Here the “free” and “anomalous” matrix elements, G and Γ are functions of world-sheet momenta, m, n and of the ratios J_s/J for $s = 1, \dots, i + j$. Disconnected pieces are less suppressed by J . Note that *suppression of C^{ij} in the BMN limit is absent only when $i = j = 1$* . We state the conclusion as,

- *Connected contributions to C^{ij} are suppressed in the BMN limit for i and/or j larger than 1.*

Let us briefly discuss the case of BPS type multi-trace operators. A BPS type multi-trace operator which involve two scalar type impurities is defined as,

$$O_{i;\phi\psi}^J =: O_\phi^{J_1} O_\psi^{J_2} O^{J_3} \dots O^{J_i} :, \quad (4.29)$$

where,

$$O_\phi^J = \frac{1}{\sqrt{N^{J+1}}} \text{Tr}(\phi Z^J) \quad (4.30)$$

and a similar definition for O_ψ^J .

One observes that a generic matrix element between BMN and BPS i -trace operators (both having the same number of traces) at all orders in g_2 are suppressed by a power of J . This can be seen by noting that these correlators should necessarily be partially connected (since both $O_\psi^{J'_1}$ and $O_\phi^{J'_2}$ in the BPS type i -trace operator should connect to the same $O_n^{J_1}$ in the i -trace BMN operator) and therefore suppressed by at least a factor of J with respect to BPS-BPS or BMN-BMN correlators of the same number of traces. Above scaling law tells us that, in the latter cases suppression at an arbitrary order in g_2 can only be avoided by completely disconnected graphs with an arbitrary number of loops. This simple observation allowed us to ignore BPS type double and triple operators in the previous section that would otherwise contribute in the intermediate sums.

4.3 Anomalous dimension of a general multi-trace BMN operator at $\mathcal{O}(g_2^2)$

The fact that disconnected contributions to the multi-trace correlators are suppressed as $J \rightarrow \infty$ has direct consequences for the scale dimension of multi-trace operators both at order g_2^2 and higher.

Call the i -trace BMN operator in (4.27) as O_i . Here i is a collection of labels, $i = \{n, y_1, \dots, y_i\}$ with $y_1 \equiv \frac{J_1}{J}$, etc. Because of the non-vanishing mixing, $\langle \bar{O}_i O_j \rangle$ with multi-trace operators of different order ($i \neq j$), O_i is *not* an eigen-operator of $\Delta - J$ and a non-trivial diagonalization procedure is required to obtain the true scale dimension. Eigenvectors at $\mathcal{O}(g_2)$ is affected only by mixing of O_i with $O_{i\pm 1}$. The diagonalization procedure is essentially equivalent⁹ to non-degenerate perturbation theory [29] and as in section 2 one obtains the mostly i -trace eigen-operator as,

$$\tilde{O}_i = O_i + g_2 \sum_{j=i\pm 1} \frac{\Gamma_i^j}{\rho_i - \rho_j} O_j, \quad (4.31)$$

where $\Gamma_i^j = G^{jk} \Gamma_{ki}$ and ρ_k is the $\mathcal{O}(g_2^0)$ eigenvalue of the k -trace operator ($\rho_i = (n/y_1)^2$ in case of O_i in (4.27))¹⁰. To compute the eigenvalue we need, (using (4.31)),

$$\langle \bar{\tilde{O}}_i \tilde{O}_i \rangle = \langle \bar{O}_i O_i \rangle + 2g_2 \sum_{j=i\pm 1} \frac{\Gamma_i^j}{\rho_i - \rho_j} \langle \bar{O}_j O_i \rangle + g_2^2 \sum_{j,k=i\pm 1} \frac{\Gamma_i^j}{\rho_i - \rho_j} \frac{\Gamma_i^k}{\rho_i - \rho_k} \langle \bar{O}_j O_k \rangle. \quad (4.32)$$

Call the $\mathcal{O}(g_2^2)$ part of this quantity as,

$$\langle \bar{\tilde{O}}_i \tilde{O}_i \rangle \Big|_{g_2^2} = \tilde{G}_{ii} - \lambda \tilde{\Gamma}_{ii} \ln(x^2 \Lambda^2). \quad (4.33)$$

Generalizing the method described in [29] to the case of multi-trace operators, we

⁹see the discussion at the end of section 2 for the effects of mixing with higher trace BMN operators

¹⁰The proof of the validity of non-degenerate perturbation theory at $\mathcal{O}(g_2^2)$ is illustrated in case of single-trace and double-trace operators in section 2. However this proof immediately generalizes to the general case of i -trace operators because of the suppression of connected correlators. Requirement of disconnectedness boils down the required computation to the one presented in section 2.

express the true scale dimension at this order in terms of the above quantities as,

$$\Delta_i \Big|_{g_2^2} = \tilde{\Gamma}_{ii} - \rho_i \tilde{G}_{ii}. \quad (4.34)$$

It is not hard to see that (4.34) is equivalent to (4.8) as it should be. To compute Δ_i from either (4.34) or (4.8) one needs G_{ij} and Γ_{ij} to the necessary order. Although second method is a short-cut we prefer to start from (4.34) because this method makes it clear that modified operators, \tilde{O}_i are true eigen-operators of the dilatation generator.

Now, the crucial point is to recall that the connected contributions to $\tilde{\Gamma}_{ii}$ and \tilde{G}_{ii} are suppressed as $J \rightarrow \infty$ and the evaluation of these quantities reduce to the evaluation of only the fully disconnected pieces. For example the quantity G_{ii} receives non-zero contributions only from the following completely disconnected Wick contractions,

$$\begin{aligned} G_{ii} \Big|_{g_2^2} &= \langle \bar{O}_i O_i \rangle_{g_2^2} = \langle \bar{O}_n^{J_1} O_n^{J_1} \rangle_{g_2^2} \langle \bar{O}^{J_2} O^{J_2} \rangle_{g_2^0} \dots \langle \bar{O}^{J_i} O^{J_i} \rangle_{g_2^0} \\ &+ \langle \bar{O}_n^{J_1} O_n^{J_1} \rangle_{g_2^0} \langle \bar{O}^{J_2} O^{J_2} \rangle_{g_2^2} \dots \langle \bar{O}^{J_i} O^{J_i} \rangle_{g_2^0} + \dots \\ &+ \langle \bar{O}_n^{J_1} O_n^{J_1} \rangle_{g_2^0} \langle \bar{O}^{J_2} O^{J_2} \rangle_{g_2^0} \dots \langle \bar{O}^{J_i} O^{J_i} \rangle_{g_2^2}. \end{aligned} \quad (4.35)$$

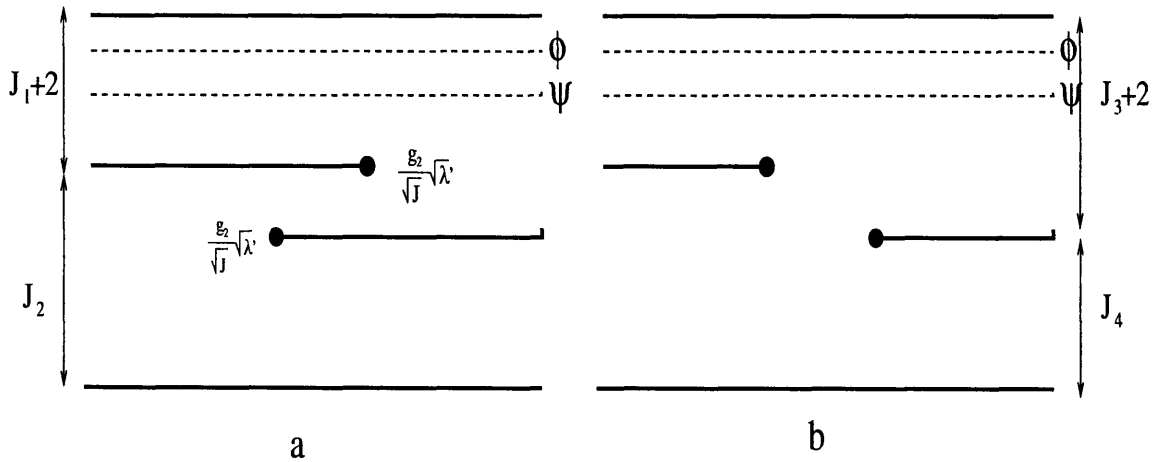


Figure 4-1: Left figure shows that connected contribution to $2 \rightarrow 3 \rightarrow 2$ process is suppressed by $1/J$. Right figure shows similar suppression of mixing of double trace operators with single-traces.

Now, we shall compute Δ_i at $\mathcal{O}(g_2^2)$ for arbitrary i . One first observes that $j = i - 1$ channel in (4.32) necessarily gives connected diagrams hence suppressed by the power of J given by (4.28). More explicitly, the summands in the $(i - 1)$ channel are $\mathcal{O}(g_2^2/J)$ but the intermediate sums do not provide a compensating factor of J unlike in the $(i + 1)$ channel. This is illustrated in Fig. 4-1 in case of $i = 2^{11}$. Similarly the summands in $(i + 1)$ channel are also $\mathcal{O}(g_2^2/J)$, therefore only disconnected $i \rightarrow (i + 1) \rightarrow i$ processes can contribute. This is also illustrated in Fig. 4-2. The conclusion is that,

1. i - $(i - 1)$ mixing does not affect i -trace eigenvalue,
2. Only disconnected $i \rightarrow (i + 1) \rightarrow i$ processes in i - $(i + 1)$ mixing matter. (see Fig. 4-2)

One obtains the quantities, \tilde{G}_{ii} and $\tilde{\Gamma}_{ii}$ that are necessary to evaluate (4.34) from (4.32). The former reads,

$$\begin{aligned} \tilde{G}_{ii} &= G_{ii} + 2 \sum_{i+1} \frac{\Gamma_i^{i+1}}{\rho_i - \rho_{i+1}} G_{i+1,i} + \sum_{i+1,i'+1} \frac{\Gamma_i^{i+1}}{\rho_i - \rho_{i+1}} \frac{\Gamma_i^{i'+1}}{\rho_i - \rho_{i'+1}} G_{i+1,i'+1} \\ &= G_{ii} + \sum_{i+1} \frac{\Gamma_i^{i+1}}{\rho_i - \rho_{i+1}} \left(2G_{i+1,i} + i! \frac{\Gamma_i^{i+1}}{\rho_i - \rho_{i+1}} \right). \end{aligned} \quad (4.36)$$

Here, we use the indices in a schematic sense, for example $(i' + 1)$ and $(i + 1)$ are independent indices that both refer to a collective index which labels an $(i + 1)$ -trace operator, *i.e.* $i + 1 = \{m, y_1, \dots, y_i\}$ and $i' + 1 = \{m', y'_1, \dots, y'_i\}$. In the second line above, we used the expression for the lowest order, free two-point function of $(i + 1)$ -trace BMN operators. For general i , this is easily obtained by recalling the fact that only disconnected pieces contribute. Thus to lowest order, $\mathcal{O}(g_2^0)$, G_{ii} is product of its disconnected pieces summed over all ways of Wick contracting various BPS operators:

$$G_{ii'} = G_{m y_1 \dots y_i; m' y'_1 \dots y'_i} = d_{m m'} d_{y_1 y'_1} \sum_P d_{y_2 y'_{P(2)}} \dots d_{y_i y'_{P(i)}}, \quad (4.37)$$

¹¹For an explanation for these “string-like” transition diagrams see the end of this section

where P runs over all permutations of the set $\{2, \dots, i\}$. We stress that we need the $\mathcal{O}(g_2^2)$ expression for G_{ii} in (4.36) rather than (4.37). Using this formula for $G_{i+1, i'+1}$ in the first line of (4.36) and summing over the indices $i' + 1$ produces a factor of $i!$. To go further we need

$$\frac{\Gamma_i^{i+1}}{\rho_i - \rho_{i+1}}.$$

The only $\mathcal{O}(g_2)$ contributions to the matrix element come from the following two terms,

$$\Gamma_i^{i+1} = G^{i+1, j+1} \Gamma_{j+1, i} + G^{i+1, j} \Gamma_{j, i}.$$

We need to invert the $2 \times \infty$ dimensional matrix of inner products between i -trace and $(i + 1)$ -trace operators.¹² It is not hard to find the inverse perturbatively at $\mathcal{O}(g_2)$ with the result,

$$G^{A, B} = \begin{pmatrix} \frac{G_{i, i'}}{(i-1)!(i-1)!} + \mathcal{O}(g_2^2) & -\frac{G_{i, i'+1}}{(i-1)!i!} + \mathcal{O}(g_2^3) \\ -\frac{G_{i+1, i'}}{(i-1)!i!} + \mathcal{O}(g_2^3) & \frac{G_{i+1, i'+1}}{i!i!} + \mathcal{O}(g_2^2) \end{pmatrix}.$$

We also need *free* i - $(i + 1)$ correlator at $\mathcal{O}(g_2)$. Since it is given by the fully-disconnected contribution, it is obtained as a simple generalization of (4.19):

$$\begin{aligned} G_{m y_1 \dots y_i; m' y'_1 \dots y'_{i+1}}^{i, i+1} &= d_{m, m'} d_{y_1, y'_1} \frac{g_2}{\sqrt{J}} \sum_{P, P'} d_{y_{P(2)}, y'_{P'(2)}} \cdots d_{y_{P(i-1)}, y'_{P'(i-1)}} d_{y_{P(i)}, y'_{P'(i)} + y'_{P'(i+1)}} \\ &\quad \times \sqrt{(1 - y_{P(i)}) y'_{P'(i)} y'_{P'(i+1)}} \\ &+ y_1^{3/2} G_{m, m' y'_1 / y_1}^{12} \sum_P d_{y_2, y'_{P(2)}} \cdots d_{y_i, y'_{P(i)}} d_{y_1, y'_1 + y'_{P(i+1)}}. \end{aligned} \quad (4.38)$$

Here the first term is a generalization of the second term in (4.19) and the second terms is the generalization of the first term in (4.19). The sum P in the first term is over cyclic permutations of the set $\{2, \dots, i\}$ *i.e.* it has dimension $i - 1$ and sum P' is over all possible ways of choosing two indices out of the set $1, \dots, i + 1$ (to form the single-double BPS correlator with $P(i)$ th BPS operator in O_i) and then taking

¹²See section 3 for a justification of our omitting BPS type i -trace and $(i + 1)$ -trace operators in the evaluation of the eigenvalue.

all possible permutations in the rest of the indices, *i.e.* $\dim(P') = (i-2)!i(i-1)/2$.

Finally we need the first order *radiative corrections* to this correlator. Much as in (4.21) this is given as,

$$\begin{aligned}\Gamma_{m y_1 \dots y_i; m' y'_1 \dots y'_{i+1}}^{i, i+1} &= \frac{m^2}{y_1^2} G_{m y_1 \dots y_i; m' y'_1 \dots y'_{i+1}}^{i, i+1} + y_1^{3/2} G_{m, m' y'_1 / y_1}^{12} \frac{m'}{y'_1} \left(\frac{m'}{y'_1} - \frac{m}{y_1} \right) \\ &\quad \times \left\{ \sum_P d_{y_2, y'_{P(2)}} \cdots d_{y_i, y'_{P(i)}} d_{y_1, y'_1 + y'_{P(i+1)}} \right\} \\ &= \left(\frac{m^2}{y_1^2} - \frac{m m'}{y_1 y'_1} + \frac{m'^2}{y_1^2} \right) G_{m y_1 \dots y_i; m' y'_1 \dots y'_{i+1}}^{i, i+1}\end{aligned}\quad (4.39)$$

Eqs. (4.38) and (4.3) are sufficient to determine Γ_i^{i+1} at $\mathcal{O}(g_2)$:

$$\begin{aligned}\Gamma_i^{i+1} &= G^{i+1, j+1} \Gamma_{j+1, i} + G^{i+1, j} \Gamma_{j, i} \\ &= \frac{1}{i!} y_1^{3/2} G_{m, m' y'_1 / y_1}^{12} \frac{m'}{y'_1} \left(\frac{m'}{y'_1} - \frac{m}{y_1} \right) \left\{ \sum_P d_{y_2, y'_{P(2)}} \cdots d_{y_i, y'_{P(i)}} d_{y_1, y'_1 + y'_{P(i+1)}} \right\}\end{aligned}\quad (4.40)$$

We insert this expression in (4.36) and perform the sum over the intermediate $(i+1)$ channel. Most of the terms in the contraction of delta-functions will be suppressed (*e.g.* first term in (4.38) multiplied with Γ_i^{i+1} and summed over $(i+1)$ is suppressed by $1/J$). Result is,

$$\tilde{G}_{ii'} = G_{ii'} - \delta_{ii'} \sum_{ny} y^3 G_{m, ny/y_1}^{12} G_{m', ny/y'_1}^{12} \frac{\binom{n}{y} \left(\frac{n}{y} + \frac{m}{y_1} + \frac{m'}{y'_1} \right)}{\left(\frac{n}{y} + \frac{m}{y_1} \right) \left(\frac{n}{y} + \frac{m'}{y'_1} \right)}.\quad (4.41)$$

Here, $\delta_{ii'}$ is a shorthand for the delta functions that arise from disconnected Wick contractions:

$$\delta_{ii'} = d_{y_1, y'_1} \sum_P d_{y_2, y'_{P(2)}} \cdots d_{y_i, y'_{P(i)}}.$$

A completely analogous computation yields $\tilde{\Gamma}_{ii'}$ as,

$$\tilde{\Gamma}_{ii'} = \Gamma_{ii'} - \delta_{ii'} \sum_{ny} y^3 G_{m, ny/y_1}^{12} G_{m', ny/y'_1}^{12} \frac{\binom{n}{y} \left(\frac{n^3}{y^3} + \frac{m^3}{y_1^3} + \frac{m'^3}{y_1'^3} \right)}{\left(\frac{n}{y} + \frac{m}{y_1} \right) \left(\frac{n}{y} + \frac{m'}{y_1'} \right)}.\quad (4.42)$$

For the same reason as above we only need disconnected contributions to G_{ii} and Γ_{ii} which are trivial to evaluate. In case of $i = 2$ required diagrams are illustrated in Fig. 4-2.b,c and d. In terms of the known expression for single string correlator at $\mathcal{O}(g_2^2)$ and radiative corrections to this [24][22], one readily gets (see (4.35))

$$G_{ii'} = g_2^2 \delta_{ii'} \left(y_1^4 A_{mm'} + \frac{d_{mm'}}{24} \sum_{r=2}^i y_r^4 \right), \quad (4.43)$$

and

$$\Gamma_{ii'} = g_2^2 \delta_{ii'} \left(y_1^2 (m^2 - mm' + m'^2) A_{mm'} + y_1^2 B_{mm'} + \frac{d_{mm'}}{24} \frac{m^2}{y_1^2} \sum_{r=2}^i y_r^4 \right), \quad (4.44)$$

where A and B matrices are first defined in [24] and are reproduced in eqs. (E.1) and (E.2).

Let us digress for a moment to discuss a simpler type of degeneracy in energy eigenvalues that is referred as *momenta-mixing*. So far, we formulated our discussion in terms of the multi-trace BMN operators as given in eqs. (4.2) and (2.37). In doing so we ignored a degeneracy in the energy eigenvalues corresponding to operators with opposite world-sheet momenta, namely O_n^J and O_{-n}^J carry the same energy that is n^2 . To incorporate the effects of this momenta-mixing one should disentangle the degenerate states by going to \pm basis,

$$O_n^{\pm J} = \frac{1}{\sqrt{2}} (O_n^J \pm O_{-n}^J). \quad (4.45)$$

In \pm basis BMN operators with two scalar impurities transform in the singlet and triplet representation under the $SU(2)$ subgroup of the full $SO(4)$ R-symmetry. One can easily reformulate our results in this basis. For example the eigenvalue equation reads,

$$\Delta_{my_1 \dots y_i; my_1 \dots y_i}^{\pm} \Big|_{g_2^2} = \Delta_{my_1 \dots y_i; my_1 \dots y_i} \Big|_{g_2^2} \pm \Delta_{my_1 \dots y_i; -my_1 \dots y_i} \Big|_{g_2^2} \quad (4.46)$$

Using eqs. (4.43), (4.44),(4.41) and (4.42), it is straightforward to see that,

$$\Delta_{my_1\dots y_i; -my_1\dots y_i}\Big|_{g_2^2} = 0. \quad (4.47)$$

Thus, our first observation is that

- *Scaling dimension of all multi-trace BMN operators remain degenerate in \pm channels at $\mathcal{O}(g_2^2)$.*

This fact can be explained by relating the multi-trace BMN operators in $+$ and $-$ channels by a sequence of supersymmetry transformations[12][29][43]. However, we would like to emphasize that this explanation holds only in the strict BMN limit where $J \rightarrow \infty$. The reason is that, although supersymmetry is exact for any J , BMN operators do not exactly transform under long multiplets unless J is strictly taken to ∞ . We would also like to emphasize that degeneracy of multi-trace BMN operators can be viewed as a consistency check on our long computation because our results are valid also for single-trace BMN operators for $i = 1$, where this degeneracy is well-established [30][29].

Having established the degeneracy in \pm basis, we can compute the eigenvalue by using (4.43), (4.44),(4.41) and (4.42) in

$$\Delta_i^\pm\Big|_{g_2^2} = \tilde{\Gamma}_{ii} - \rho_i \tilde{G}_{ii}.$$

Straightforward computation gives,

$$\Delta_{ii}^\pm = y_1^2 \left(g_2^2 B_{mm} - J \int_0^1 dx \sum_{n=-\infty}^{\infty} (G_{m,nx}^{12})^2 \frac{k^2(k^2 - m^2)}{(k+m)^2} \right),$$

where $k = m/x$. Using (4.14) one gets,

$$\Delta_i^\pm\Big|_{g_2^2} = \frac{y_1^2}{4\pi^2} \left(\frac{1}{12} + \frac{35}{32\pi^2 m^2} \right). \quad (4.48)$$

This is exactly the single-trace anomalous dimension that were computed in [30] and [29] up to the normalization factor y_1^2 . This is hardly surprising given the fact

that all Feynman diagrams that contribute to the evaluation of Δ_i separate into completely disconnected pieces. Since the only piece that can contribute to anomalous dimension is coming from the single-trace BMN sub-correlator (BPS sub-correlators are protected), we obtain the single-trace anomalous dimension as a result. However, from a general point of view this is a striking result and is one of the main conclusions of this paper:

- *Scaling dimension of all multi-trace BMN operators are determined by the dimension of the single-trace operator as*

$$\Delta_i^\pm = \left(\frac{J_1}{J}\right)^2 \Delta_{11}.$$

We believe that this result will also hold at higher orders in g_2 because the fact that only disconnected Feynman diagrams survive the BMN limit is still valid for higher orders in genus expansion. We see this by noticing that each g_2 comes along with a factor of $1/\sqrt{J}$ in the expansion, (see eq. (4.28), also Fig. 4-2 below). This should become more clear in the following.

This result establishes a firm prediction for $\mathcal{O}(g_2^2)$ eigenvalues of the light-cone SFT Hamiltonian. When translated into string language, this prediction reads,

$$\langle \psi_i | P^- | \psi_i \rangle = \left(\frac{p_1^+}{p^+}\right)^2 \langle \psi_1 | P^- | \psi_1 \rangle.$$

We would like to emphasize that this prediction is completely independent of the field theory basis which identifies operators that are dual to the string states.

Let us now discuss the implications of our findings for some of the string amplitudes. For this let us represent our discussion about the scaling of correlators with g_2 and J in a diagrammatic way that is suggestive for light-cone SFT. For instance we represent the double-trace correlator in the BMN basis, $\langle \bar{O}_2 O_2 \rangle_{g_2^2 \lambda'}$, as in Fig. 4-2 where Fig. 4-2.a shows the connected contribution to this correlator while Fig. 4-2.b,c d, represent the disconnected contributions at this order. Here each vertex

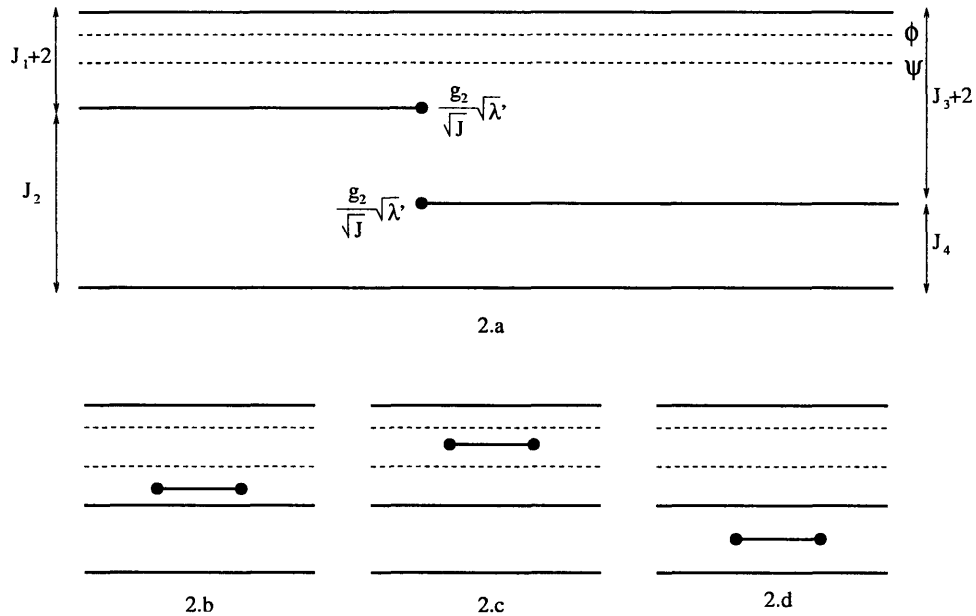


Figure 4-2: A representation of planar contributions to $\langle : \bar{O}_n^{J_1} \bar{O}^{J_2} :: O_m^{J_3} O^{J_4} : \rangle$ at $\mathcal{O}(g_2^2 \lambda')$. Dashed lines represent scalar impurities. We do not show Z lines explicitly. Vertices are of order $g_2 \sqrt{\lambda'/J}$. **a** Connected contribution. **b**, **c**, **d** Various disconnected contributions.

represent a factor of Γ^{12} which is defined as,

$$\langle \bar{O}_1(x) O_2(0) \rangle_{g_2^2} = -\Gamma^{12} \lambda' \frac{\ln(x^2 \Lambda^2)}{(4\pi^2 x^2)^{J+2}}.$$

This quantity was first computed in [29] and given in eqs. (4.15), (4.14) which show that each vertex scale with a factor of $\frac{g_2}{\sqrt{J}}$. It is now clear that one can reproduce all of the information contained in the scaling law of (4.28) by representing the correlators with these diagrams. For instance the connected diagrams in Fig. 4-2.a is $\mathcal{O}(g_2^2/J)$ hence vanishes in BMN limit whereas the disconnected diagrams of the same order in Fig. 4-2.b,c and d scale as g_2^2 therefore they are finite because of the extra J factor provided by the integration over the loop position.

To make contact with light-cone SFT we take this diagrammatic representation seriously with one qualification: The matrix elements of the light-cone Hamiltonian should correspond to the matrix Γ in the *string basis*, not in BMN basis. As discussed in Appendix D, this matrix element is obtained from Γ_{ij} with a unitary transformation, $\tilde{\Gamma} \equiv U \Gamma U^\dagger$. Whatever the correct identification of U is, this transformation will

not change the scaling of Γ because it is independent of J . Therefore we can take the diagrams in Fig. 4-2 seriously as string theory diagrams¹³, where the vertices Γ replaced with $\tilde{\Gamma}$ which scale in the same way as before. For instance, the vanishing of Fig. 4-2.a implies that there is no double-double “contact term” that contributes to $\langle \psi_2 | P^- | \psi_2 \rangle$ at $\mathcal{O}(g_s^2)$. This observation immediately generalize as,

- *There are no $\mathcal{O}(g_s^2)$, i - i contact terms that contribute to $\langle \psi_i | P^- | \psi_i \rangle$.*

However, these contact terms do give contributions at higher orders in g_s^2 . In other words, the suppression of the correlators in (4.28) does not imply the absence of physical information contained in these quantities. They certainly yield non-zero contributions to single-single loop corrections as illustrated in Fig. 4-3.

Let us also observe that the suppression of the diagram in Fig. 4-1.b implies that there is also no $2 \rightarrow 1 \rightarrow 2$ contribution to this matrix element in string perturbation theory. This fact generalizes as,

- *String theory processes where the number of internal propagations is less than i , do not contribute $\langle \psi_i | P^- | \psi_i \rangle$.*

These assertions might seem strong, however one should note the important assumptions that were made in the above discussion. First of all the correspondence with GT, at the perturbative level only holds when $\lambda' \ll 1$ which translates into the condition $\mu \gg 1$ in string theory. Therefore our discussion is valid for large values of μ . Secondly, the string amplitudes we consider involve a very particular class of external string states, namely the states with only two excitations along $i = 1, 2, 3, 4$ directions (corresponding to scalar impurities in the BMN operators). Note however that our discussion does not make any restriction to these particular two scalar excitations in the *internal string states*.

¹³Of course one should replace strips in these 2D figures with tubes for closed SFT

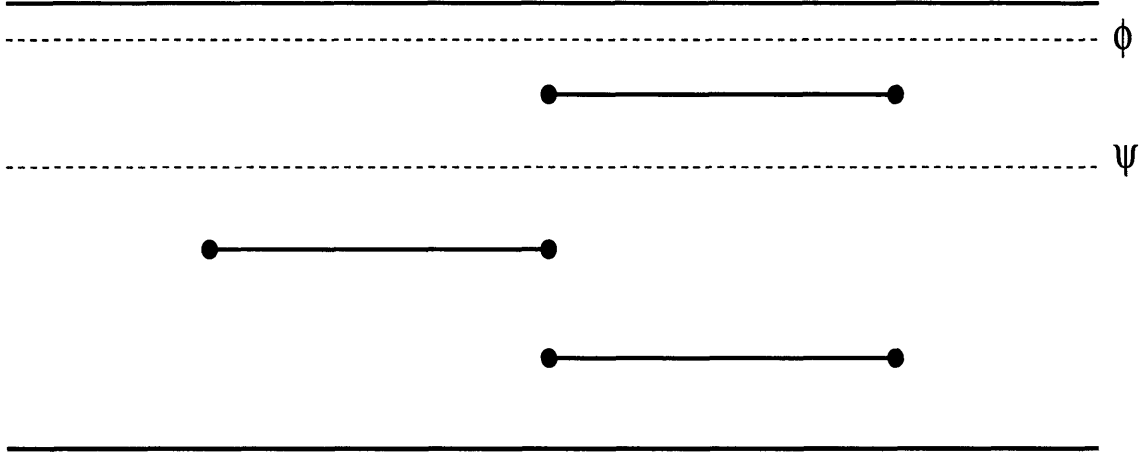


Figure 4-3: Connected contribution to double-triple correlator, $\langle \bar{O}_{ny} O_{mxyz} \rangle$, does give non-zero contribution in $1 \rightarrow 1$ process. For example this diagram will show up in the computation of $\mathcal{O}(g^6)$ scale dimension of single-trace operators.

4.4 Matrix elements of pp-wave Hamiltonian in 2-2 and 1-3 sectors

We will first compute the matrix elements of P^- in the two-string sector by the method of [27]. Assuming the validity of the basis transformation U_G that we discussed in Appendix D, this will allow us to make a gauge theory prediction for SFT. Then, by the same method we will obtain the matrix elements in single-triple string sector. Let us briefly review the method.

In Appendix D we presented a prescription to identify the string basis in field theory by transforming the basis of BMN observables with a real and symmetric transformation which renders the metric G_{ij} diagonal. The conjecture is that, matrix elements of P^- should be in correspondence with the matrix of $\mathcal{O}(\lambda')$ piece of the field theory correlators in the string basis. This is related to the same quantity in the old basis as,

$$\tilde{\Gamma} = U_G \Gamma U_G^\dagger.$$

We are interested in the $\mathcal{O}(g^2 \lambda')$ piece of $\tilde{\Gamma}$. Using (D.2), this reads [27],

$$\tilde{\Gamma}^{(2)} = \Gamma^{(2)} - \frac{1}{2} \{G^{(2)}, \Gamma^{(0)}\} - \frac{1}{2} \{G^{(1)}, \Gamma^{(1)}\} + \frac{3}{8} \{(G^{(1)})^2, \Gamma^{(0)}\} + \frac{1}{4} G^{(1)} \Gamma^{(0)} G^{(1)}, \quad (4.49)$$

where the superscript denotes the order in g_2 . Straightforward algebra gives,

$$\begin{aligned}\tilde{\Gamma}_{m_y; m' y'}^{22} &= \Gamma_{m_y; m_y'}^{22} - \frac{1}{2} \left(\left(\frac{m}{y} \right)^2 + \left(\frac{m'}{y'} \right)^2 \right) G_{m_y; m' y'}^{22} - \frac{1}{2} \left(G^{21} \Gamma^{12} + \Gamma^{21} G^{12} + G^{23} \Gamma^{32} + \Gamma^{23} G^{32} \right)_{m_y; m' y'} \\ &+ \frac{3}{8} \left(G^{21} G^{12} + G^{23} G^{32} \right)_{m_y; m' y'} \left(\left(\frac{m}{y} \right)^2 + \left(\frac{m'}{y'} \right)^2 \right) + \frac{1}{4} \left(G^{12} G^{12} n^2 + G^{23} \Gamma^{33} G^{32} \right)_{m_y; m' y'}\end{aligned}$$

Γ^{22} and G^{22} in the first two terms are $\mathcal{O}(g_2^2)$ pieces of the corresponding matrices and Γ^{33} in the last term is the $\mathcal{O}(1)$ piece. Repeated intermediate indices mean summing over all possible operators that may appear in that intermediate process *e.g.* in the expression $G^{23} G^{32}$ one should sum over both BPS type *and* BMN type triple trace operators. Remarkable simplifications occur, when one recalls that only non-vanishing contributions in the double-double sector comes from disconnected diagrams. A term like $G^{21} G^{12}$ and $G^{21} \Gamma^{12}$ cannot be disconnected hence of $\mathcal{O}(1/J)$ and decouples in the BMN limit. Similarly one only keeps the disconnected contributions to G^{22} and Γ^{22} . All of the necessary ingredients to compute this expression except,

$$\Gamma^{33} = \begin{pmatrix} \frac{1}{2} \left(\frac{m}{y} \right)^2 d_{m, m'} d_{y, y'} (d_{z, z'} + d_{z, 1-y-z'}) & 0 \\ 0 & 0 \end{pmatrix},$$

were presented in section 2. This matrix tells us that there is no anomalous mixing among BPS type and between BMN and BPS type triple-trace operators at the zeroth order in g_2 .

With the help of the decomposition identity (D.4), one obtains,

$$\tilde{\Gamma}_{m_y; m' y'}^{22} = g_2^2 d_{y, y'} \frac{y^2}{4} B_{m, m'}. \quad (4.50)$$

For the definition of matrix B , see Appendix E.

A similar calculation yields the single-triple matrix element in the string basis as,

$$\begin{aligned}\tilde{\Gamma}_{m; m' y' z'}^{13} &= \Gamma_{m; m' y' z'}^{13} - \frac{1}{2} \left(m^2 G^{13} + G^{13} \Gamma^{33} \right)_{m; m' y' z'} - \frac{1}{2} \left(G^{12} \Gamma^{23} + \Gamma^{12} G^{23} \right)_{m; m' y' z'} \\ &+ \frac{3}{8} \left(\Gamma^{11} G^{12} G^{23} + G^{12} G^{23} \Gamma^{33} \right)_{m; m' y' z'} + \frac{1}{4} G_{m; n y''}^{12} (n/y'')^2 G_{n y''; m' y' z'}^{23}.\end{aligned}$$

Again, repeated indices in the intermediate sums imply the inclusion of all possible operators of that given type. For instance in the term $G^{12}G^{23}\Gamma^{33}$, one should use both BMN and BPS type double and triple operators in the intermediate process. A simplification occurs however when one notes that there is no $\mathcal{O}(g_2)$ contribution to G^{23} and Γ^{23} for a BPS type double-trace operator, the lowest order non-zero contribution appearing at $\mathcal{O}(g_2^3)$. By repeated use of the decomposition identities (D.5), (E.12) and (E.13) one obtains the amazingly simple expression,

$$\tilde{\Gamma}_{m;m'y'z'}^{13} = \frac{g_2^2}{4} B_{m;m'y'z'}^{13}.$$

Here B^{13} is the contribution to Γ^{13} from non-nearest neighbour interactions, given by (4.18). Thus we obtain the following GT prediction for the matrix elements of P^- in 1 string-3 string sector:

$$\tilde{\Gamma}_{m;m'y'z'}^{13} = \frac{g_2^2 \lambda'}{2\pi^3 J} \frac{1}{(n - m/y)} \sqrt{\frac{z\bar{z}}{y}} \sin(\pi n z) \sin(\pi n \bar{z}) \sin(\pi n(1 - y)). \quad (4.51)$$

Some comments are in order. First of all we note the striking similarity of $\tilde{\Gamma}^{22}$ and $\tilde{\Gamma}^{13}$ to $\tilde{\Gamma}^{11}$ that was obtained in [26][27]:

$$\tilde{\Gamma}_{m;m'}^{11} = \frac{1}{4} B_{m,m'}.$$

In the 2-2 sector this just follows from the disconnectedness of the GT diagrams, hence the 2-2 matrix element just reduces to 1-1 case up to an overall factor y^2 therefore is hardly surprising. But our result for the 1-3 matrix elements indicates the following generalization. As first computed by Vaman and Verlinde [31] using SBF and then by Roiban, Spradlin and Volovich [28] using rigorous SFT the matrix element $\tilde{\Gamma}^{11}$ represents the “contact term” *i.e.* the $\mathcal{O}(g_s^2)$ matrix element of P^- between two single-string states in the ST side. On the GT side, in all of the cases we considered this matrix element is determined solely by the “non-contractible” contribution to Γ^{ij} . It is tempting to conjecture that the “non-contractible” GT diagram encodes the information for the $\mathcal{O}(g_s^2)$ contact term in PP-wave SFT. To check this conjecture

one should compute $\mathcal{O}(g_s^2)$ matrix element of P^- between a single and a triple-string state and compare with (4.51).

4.5 Discussion and outlook

There are three main results in this chapter. First of all, we demonstrated that non-degenerate perturbation theory becomes invalid at order g_2^2 , as single-trace operators are degenerate with triple-trace operators. This result casts some doubt on the previously computed anomalous dimensions in [29][30]. However we conjectured that some particular eigenstates of the degenerate subspace for finite J , tend to the modified BMN operators \tilde{O}_i in the BMN limit whose eigenvalues coincide with the dimensions of \tilde{O}_i . Therefore the use of non-degenerate perturbation theory can be justified for these particular dilatation eigen-operators. This problem requires further investigation and it will be interesting to explore new effects related to this degeneracy problem in future.

Our second main conclusion is the determination of the anomalous dimensions of all multi-trace BMN operators that include two scalar impurity fields in terms of the single-trace anomalous dimension. We proved this interesting result to order $g_2^2\lambda'$ but the fact that connected field theory diagrams are suppressed also at higher orders in g_2 suggests that the conclusion holds at an arbitrary level in perturbation theory. (Of course, one has to first establish the validity perturbation theory at higher orders.) These predictions for the eigenvalues of P^- are basis independent and therefore provide a firm prediction for SFT. It would be interesting to understand the string theory mechanism that is analogous to the BMN suppression that leads to vanishing of connected field theory diagrams. A natural next step in this analysis is to consider the anomalous dimensions of BMN operators that include higher number of impurities. We believe that suppression of the disconnected GT diagrams will lead to remarkable simplifications also in that problem.

Finally, we obtained predictions for the matrix elements of the light-cone Hamiltonian in 2-2 and 1-3 string sectors. We emphasize that these predictions are sensitive

to the way the string basis in GT is identified, unlike the predictions of section 3 for the *eigenvalues* of P^- . We fixed the basis with the assumption that the form of the basis transformation at $\mathcal{O}(g_2)$ is also valid at $\mathcal{O}(g_2^2)$. Although this assumption passed a non-trivial test in predicting the correct $\mathcal{O}(g_2^2)$ contact term of single-string states [28], there is no obvious reason to believe its validity for instance in the single-triple sector. Thus, our predictions can also be used as a test of the basis identifications of either [26] or [27] which are equivalent to each other at $\mathcal{O}(g_2^2)$.

Chapter 5

Instability and String Decay in BMN Correspondence

5.1 Introduction

Despite the correspondence of notation the string states listed in (4.4,4.5) are not the direct maps of the individual operators in (4.1,4.2). The reason is that the operators mix through nonplanar graphs [29, 30, 44] even in the free field theory whereas the eigenstates of the free string Hamiltonian in (4.5) containing different numbers of strings are orthogonal. An operator S effecting a change of basis in the gauge theory has been identified [14, 45] which makes the gauge theory states in (4.2) orthogonal in the free theory and it is the states obtained by applying S^{-1} to those of (4.2) which map into the string states of (4.5).

Quantitative tests of the correspondence are based on the assumption that the light-cone Hamiltonian $P^- = H$ of string theory corresponds to the field theory operator $\Delta - J$, the difference between dilation and R -charge, through the relation

$$\Delta - J = \frac{1}{\mu} H \tag{5.1}$$

In planar order the eigenstates of $\Delta - J$ are the individual states listed in (4.2), and

the order g_2^0 eigenvalues are

$$\omega(n, J_0, J_1, \dots, J_k) = 2 + \lambda' \frac{n^2}{s_0^2} \quad (5.2)$$

with $s_0 = J_0/J$. Operator mixing appears in order g_2 , and to this order the k -trace eigenoperator acquires order g_2 admixtures of $(k \pm 1)$ -trace operators [29, 30]. The eigenvalue is first corrected in order g_2^2 to

$$\omega(n, J_0, J_1, \dots, J_k) \rightarrow 2 + \lambda' \left[\frac{n^2}{s_0^2} + \frac{g_2^2 s_0^2}{4\pi^2} \left(\frac{1}{12} + \frac{35}{32\pi^2 n^2} \right) \right] \quad (5.3)$$

For $k = 1$ the correction was found in [29, 30] and in [13] for $k > 1$. For $k = 1$, the correction exactly matches the genus 1 energy shift of single-string states calculated in light-cone string field theory [26, 28]. This match provides a basis independent test of the relation (5.1). It has also been shown that related matrix elements of H agree with those of $\Delta - J$ after the basis change is made [26, 27].

The computations of (5.3) in gauge theory used a formalism equivalent to non-degenerate quantum mechanical perturbation theory. Yet it is obvious from (5.2) that the zero order eigenvalues of single-trace operators of momentum n are degenerate with multi-traces of momentum m if $ns_0 = \pm m$. The $n = 1$ state is non-degenerate, since $s_0 = 1$ would be required, and J_1, J_2, \dots, J_k would vanish. But the $n = 2$ single-trace operator is degenerate with multi-traces with $m = \pm 2$, $s_0 = 1/2$. For $n = 3$ we have degeneracy with multi-traces when $m = \pm 2$, $s_0 = 2/3$ and when $m = \pm 1$, $s_0 = 1/3$, and so forth. One must thus question the validity of non-degenerate perturbation theory, and this was discussed in [29]. One signal for breakdown of perturbation theory is a divergence due to a vanishing energy denominator in the summation formulas for shifts of eigenvalues. It was pointed out in [29] that perturbation theory would remain valid if the matrix elements in the numerator happened to vanish at degeneracy, and that the matrix element of the effective interaction between single- and double-trace states does indeed so vanish. This is a necessary condition for the validity of the order g_2^2 calculation leading to (5.3), but it is not sufficient. The single/triple mixing matrix element is of order g_2^2 . If it does not vanish at degeneracy,

it would also require [29] the use of degenerate perturbation theory with possible modification of the result (5.3) even though a divergence would not appear until order g_2^4 .

An effective quantum mechanical formulation for the gauge theory, which simplifies previous computations was developed in [41]. The single/triple matrix element was computed in this formalism, and it **does not** vanish at degeneracy. It is this fact that motivates the present note in which we discuss the consequences for the physics of the BMN correspondence. In string theory single-string states $|(n, -n)p^+\rangle$ with $n > 1$ would be expected to be unstable, with decay to the continuum of $(k+1)$ -string states $|(m, -m)p_0^+, p_1^+, \dots p_k^+\rangle$ in which the total light cone momentum is divided continuously among the $k+1$ strings. The lowest case $k=1$ should correspond to single/double trace mixing in gauge theory, and it has been shown [46] that the relevant string theory matrix element vanishes at order g_2 in agreement with the vanishing gauge theory result mentioned above. Instability would then be expected in string theory via a composite (order g_2^2) process in which the single string first splits into two “virtual” strings and by a further interaction into three final state strings. The non-vanishing single/triple trace mixing matrix element, which is also composite in a sense described below, is the signal of this instability in gauge theory.

More generally the gauge theory has discrete single-trace states \mathcal{O}_n^J embedded in a continuum of multi-traces, since the ratios J_i/J become continuous variables with range 0 to 1 in the BMN limit. It is a well known phenomenon in quantum mechanics that a state which is purely in the discrete sector at time $t=0$ undergoes irreversible decay to the continuum of states which are degenerate in energy. This phenomenon can be derived using time-dependent perturbation theory [47]. The standard derivation must be generalized in the present case because the relevant process is composite. We make this generalization and compute the order g_2^4 contributions to the energy shift and decay width of single trace states with $n \geq 2$. The energy shift is the less significant datum when there is instability, but it agrees with the principal value calculation of [41]. The value we find for the decay width would also emerge from the formalism of [41] if an $i\epsilon$ prescription had been used rather than principal value (as

suggested recently in [48]). We show that the decay amplitude is invariant under the basis change discussed above. It should therefore agree with the amplitude computed in string theory.

The development of the continuous spectrum in the string theory is intimately connected with the Penrose limit which produces the pp-wave spacetime from $\text{AdS}_5 \times \text{S}_5$. For finite radius R of S_5 , the null circle in x^- is compact [38] and there is a discrete spectrum of stable states. In the limit $R \rightarrow \infty$ the null circle becomes non-compact, producing a continuous spectrum and the possibility of instability.

5.2 The Effective Gauge Theory Hamiltonian

Let us denote an operator in the set (4.2) using the generic notation $\mathcal{O}_i(x)$. With one-loop interactions included, the general form of two-point functions is

$$\langle \mathcal{O}_i(x) \mathcal{O}_j(y) \rangle = \frac{1}{(x-y)^{2J+4}} [g_{ij} - h_{ij} \ln(x-y)^2 M^2] \quad (5.4)$$

where $g_{ij} = g_{ji}$ is the free-field amplitude which defines a positive-definite inner product or metric, and $h_{ij} = h_{ji}$ describes the order $\lambda' = g_{YM}^2 N/J$ interactions. We use a real notation for simplicity, but it is accurate since the correlators of our operators are real. The diagonal elements of g_{ij} , h_{ij} are of order $1 + \mathcal{O}(g_2^2)$ while off-diagonal elements between operators containing k and k' traces are of order $g_2^{|k-k'|}$.

One diagonalizes this system via the relative eigenvalue problem

$$h_{ij} v_\alpha^j = \gamma_\alpha g_{ij} v_\alpha^j \quad (5.5)$$

There is a complete set of eigenvectors v_α^i which are orthogonal with respect to the metric, viz. $v_\alpha^i g_{ij} v_\beta^j = \delta_{\alpha\beta}$. The system (5.5) is equivalent to the conventional eigenvalue problem for the ‘‘up-down Hamiltonian’’ $h_j^i = g^{ik} h_{kj}$, namely

$$h_j^i v_\alpha^j = \gamma_\alpha v_\alpha^i, \quad (5.6)$$

but one must remember that h_j^i is not naively Hermitean (symmetric), but Hermitean with respect to g_{ij} , i.e. $g_{ik} h_j^k = h_i^k g_{kj}$.

It is easy to show that the eigenoperators are $\mathcal{O}_\alpha(x) = v_\alpha^i \mathcal{O}_i(x)$ and have diagonal 2-point functions:

$$\langle \mathcal{O}_\alpha(x) \mathcal{O}_\beta(y) \rangle = \frac{\delta_{\alpha\beta}}{(x-y)^{2J+4}} [1 - \gamma_\alpha \ln(x-y)^2 M^2] \quad (5.7)$$

$$\sim \frac{\delta_{\alpha\beta}}{(x-y)^{2\Delta_\alpha}}, \quad (5.8)$$

from which one can read the scale dimension $\Delta_\alpha = J + 2 + \gamma_\alpha$.

A simpler method for field theory computations was developed in [41]. It is a method to compute h_j^i directly with no need for the complicated combinatorics of Feynman diagrams required in earlier work. The resulting effective Hamiltonian has a quite simple and striking structure. The method applies to 2-point functions of the operators of (4.2) and has recently been extended [49] to a wider class of scalar operators.

We refer readers to [41] for an explanation of the method, and we begin our discussion with (11) of that paper. Certain “end-point terms” and other terms which vanish in the BMN limit are neglected in (11), and we note that the omitted terms actually vanish in the channel which is symmetric under exchange $\phi \leftrightarrow \psi$ of the two impurities, so (11) is exact in this channel. Although the BMN limit is taken at an early stage in [41], we use a discrete finite J version of the method and take the limit $J \rightarrow \infty$ at the final stage of computation.

In this method h_j^i is replaced by matrix elements of an effective Hamiltonian $H = H_0 + H_+ + H_-$. The action of H on gauge theory states/operators is given in (11) of [41] in which the operators contain impurities of fixed spacing l , *i.e.* $\mathcal{O}_l^{J_0, J_1, \dots, J_k} \sim \text{Tr}(\phi Z^l \psi Z^{J_0-1}) \text{Tr} Z^{J_1} \dots \text{Tr} Z^{J_k}$. After a discrete Fourier transform with respect to l , which is equivalent to that in (4.2) for large J , one obtains the following equations:

$$\begin{aligned}
H_0 \mathcal{O}_m^{J_0, J_1, \dots, J_k} &= \lambda' \frac{m^2}{s_0^2} \mathcal{O}_m^{J_0, J_1, \dots, J_k} \\
H_+ \mathcal{O}_m^{J_0, J_1, \dots, J_k} &= \lambda' g_2 \sum_{\alpha_{k+1}} V_{\alpha_k}^{\alpha_{k+1}} \mathcal{O}_{m'}^{J_0 - J_{k+1}, J_1, \dots, J_{k+1}} \\
H_- \mathcal{O}_m^{J_0, J_1, \dots, J_k} &= \lambda' g_2 \sum_{i, \alpha'_{k-1}} V_{\alpha_k}^{\alpha_{k-1}} \mathcal{O}_{m'}^{J_0 + J_i, J_1, \dots, J_i, \dots, J_k}
\end{aligned} \tag{5.9}$$

where we introduce a collective index notation in the matrix elements $V_{\alpha_k}^{\alpha_{k\pm 1}}$, namely $\alpha_k = \{m, s_0, \dots, s_k\}$. Here $s_i = J_i/J$ satisfy $\sum_i s_i = 1$.

The right sides of the equations for H define contributions to matrix elements h_j^i . Symbolically, the structure is $H \mathcal{O}_j = h_j^i \mathcal{O}_i$. Note that the interaction terms are purely of order g_2 and describe the splitting/joining of a $(k+1)$ -trace operator into superpositions of $(k+1 \pm 1)$ -trace operators. The Hamiltonian $\tilde{H} = SHS^{-1}$

transformed to string basis agrees [48] with the Hamiltonian of string bit formalism which contains order g_2 splitting/joining interaction and an order g_2^2 contact term.

For large finite J the matrix elements are

$$V_{\alpha_k}^{\alpha'_{k+1}} = \frac{1}{\pi^2 \sqrt{J}(k+1)!} \sqrt{\frac{s_0 - s'_0}{s_0 s'_0}} \left(\frac{m'}{s'_0}\right) \frac{\sin^2(\pi m s'_0 / s_0)}{\frac{m'}{s'_0} - \frac{m}{s_0}} \Delta_{ss'} \quad (5.10)$$

$$V_{\alpha_{k+1}}^{\alpha'_k} = \frac{1}{\pi^2 \sqrt{J}k!} \sqrt{\frac{s'_0 - s_0}{s_0 s'_0}} \left(\frac{m'}{s'_0}\right) \frac{\sin^2(\pi m' s_0 / s'_0)}{\frac{m'}{s'_0} - \frac{m}{s_0}} \Delta_{s's} \quad (5.11)$$

where $\Delta_{ss'}$ is a product of delta functions,

$$\Delta_{ss'} = \sum_{P \in S_{k+1}} \delta_{s_1, s'_{P(1)}} \cdots \delta_{s_k, s'_{P(k)}} \delta_{s_0, s'_0 + s'_{P(k+1)}}. \quad (5.12)$$

It is in this form that we will use these equations. In the BMN limit, matrix elements we calculate agree with those of the continuum formulation of ([41]).

We have also obtained a version of (5.9) valid at any finite J in the $\phi \leftrightarrow \psi$ symmetric channel. Eigenoperators of H_0 are superpositions of those of fixed spacing, namely

$$\mathcal{O}_n^{J_0, J_1, \dots, J_k} = \frac{1}{\sqrt{J_0 + 1}} \sum_{l=0}^{J_0} \cos\left(\frac{\pi n(2l+1)}{J_0 + 1}\right) \mathcal{O}_l^{J_0, J_1, \dots, J_k} \quad (5.13)$$

These operators have eigenvalues of H_0 given by $\frac{g_{YM}^2 N}{\pi^2} \sin^2\left(\frac{\pi n}{J_0 + 1}\right)$ which approaches the eigenvalue in (5.9) as $J_0 \rightarrow \infty$. These results agree with those of [43, 50]. The interaction terms still describe order g_2 splitting/joining of traces, but they are more complicated than those of (5.9). For example when H_+ acts on the the single-trace \mathcal{O}_n^J one obtains a superposition of double-trace operators $\mathcal{O}_m^{J_0, J_1}$ where $J_0 = J - J_1$ with expansion coefficients

$$\frac{g_{YM}^2 \sqrt{J_1}}{\pi^2 \sqrt{(J+1)(J_0+1)}} \sin\left(\frac{\pi m}{J_0 + 1}\right) A(n, m, J_1) \quad (5.14)$$

$$A(n, m, J_1) = \frac{1}{2} \sin\left(\frac{\pi n J_1}{J+1}\right) \left\{ \left[\frac{\sin\left(\pi\left(\frac{nJ'}{J+1} - \frac{m}{J_0+1}\right)\right)}{\sin\left(\pi\left(\frac{n}{J+1} + \frac{m}{J_0+1}\right)\right)} \right] - [m \rightarrow -m] \right\} \quad (5.15)$$

One notes that these coefficients exactly reduce to (5.10) in the symmetric channel

in the $J \rightarrow \infty$ limit. Another thing to note here is that working at finite J does not resolve the degeneracy problem. For example, single- and double-trace operators are degenerate when $\frac{n}{J+1} = \pm \frac{m}{J_0+1}$, and there is a similar degeneracy condition for $(k+1)$ -trace operators. One may also observe that $A(n, m, J')$ does not vanish at degeneracy for finite J , although it does vanish as $J \rightarrow \infty$. In principle, one should apply degenerate perturbation theory to the calculation of eigenvalues of H even before triple-trace operators are included. However, we will ignore this complication, which very likely disappears in the large J limit.

Our primary goal is to apply time-dependent perturbation theory to study the time evolution of a state which is purely single-trace at time $t = 0$. We will calculate the decay rate of such a state into degenerate triple-trace states. We have found it useful to illustrate the essential physics in quantum mechanical toy models and then adapt the results in the models to the BMN limit of the Hamiltonian (5.9).

5.3 Quantum Mechanical Models

Our calculation of the decay rate is based on the treatment of the decay of a discrete state embedded in a continuum in [47]. This treatment needs to be modified for our case, but we first review it to set the basic technique in the context of the present up-down matrix formalism.

We thus consider a quantum mechanical system with a set of discrete states $|n\rangle$ and continuum states $|\alpha\rangle$ where α denote the continuous labels of the state. The Hamiltonian is $H = H_0 + V$ where H_0 and V are given by the following matrices:

$$H_0 = \begin{pmatrix} E_i \delta_j^i & 0 \\ 0 & E_\alpha \delta(\alpha - \beta) \end{pmatrix}, \quad (5.16)$$

$$V = \begin{pmatrix} 0 & V_\alpha^i \\ V_i^\alpha & 0 \end{pmatrix}. \quad (5.17)$$

Note that V has vanishing matrix elements between pairs of discrete or pairs of continuum states in agreement with the interactions H_\pm of (5.9). We look for the

solution of the Schrödinger evolution equation $i \frac{d}{dt} |\Psi(t)\rangle = H |\Psi(t)\rangle$, with $|\Psi(t)\rangle$ given by the formal vector:

$$|\Psi(t)\rangle = \begin{pmatrix} a^i(t) e^{-i E_i t} \\ \phi^\alpha(t) e^{-i E_\alpha t} \end{pmatrix}.$$

and the initial conditions $a^m(0) = \delta_n^m$, $\phi^\alpha(0) = 0$.

It is easy to see that the discrete and continuum components of $|\Psi(t)\rangle$ satisfy:

$$i \frac{d}{dt} a^n(t) = \int d\alpha V_\alpha^i \exp i(E_n - E_\alpha)t \phi^\alpha(t) \quad (5.18)$$

$$i \frac{d}{dt} \phi^\alpha(t) = \sum_m V_m^\alpha \exp i(E_\alpha - E_m)t a^m(t) \quad (5.19)$$

We integrate the second equation using the initial conditions above and substitute the resulting expression for $\phi^\alpha(t)$ in the first equation, obtaining an equation involving only the discrete components, namely

$$\frac{d}{dt} a^n(t) = - \int d\alpha \sum_m \int_0^t dt' \exp i(E_n - E_\alpha)t \exp i(E_\alpha - E_m)t' V_\alpha^n V_m^\alpha a^m(t') \quad (5.20)$$

Next we separate the energy variable in the continuum measure by writing $d\alpha = dE d\beta \rho(\beta, E)$ and define the matrix

$$K_m^n(E) = \int d\beta \rho(\beta, E) V_\alpha^n V_m^\alpha. \quad (5.21)$$

We assume that $K_m^n(E)$ is a slowly varying function of energy whose scale of variation is ΔE . Substituting (5.21) in (5.20), we find

$$\frac{d}{dt} a^n(t) = - \int_0^\infty dE K_m^n(E) \exp i(E_n - E)t \int_0^t dt' \exp i(E_\alpha - E_m)t' a^m(t'). \quad (5.22)$$

We now follow [47] and make the short-time approximation $a^n(t') \approx 1$, $a^m(t') \approx 0$ for $m \neq n$ in (5.22). We encounter the well known integral

$$\int_0^t dt' \exp i(E_n - E)(t - t') = \frac{\exp i(E_n - E)t - 1}{i(E_n - E)}$$

$$\approx \pi\delta(E_n - E) + i\mathcal{P}\left(\frac{1}{E_n - E}\right). \quad (5.23)$$

The last result is strictly correct in the limit $t \rightarrow \infty$, but it is effectively valid within integrals of functions $f(E)$ for times much larger than the inverse scale of variation ΔE .

This approximate treatment of (5.22) thus leads to the result

$$a^n(t) \approx 1 - \left(\frac{\Gamma_n}{2} + i\Delta\omega_n\right)t \quad (5.24)$$

$$\Gamma_n = 2\pi K_n^n(E = E_n) \quad (5.25)$$

$$\Delta\omega_n = \mathcal{P} \int_0^\infty dE \frac{K_n^n(E)}{E_n - E}. \quad (5.26)$$

The quantities Γ_n , $\Delta\omega_n$ are interpreted as the decay width and energy shift of the unstable state to lowest order in the interaction V . The approximations made in the derivation are valid under the conditions: $1/\Delta E \ll t \ll 1/\Gamma_n$, *i.e.* the time t must be long compared to the inverse scale of variation of $K_n^n(E)$ and sufficiently short to justify the short-time approximation to (5.22). Note that it was not necessary to specify a scalar product in Hilbert space. It is necessary to define the measure $d\alpha = dE d\beta d\rho(\beta, E)$ explicitly. In our problem this measure is determined by the BMN limit of the discrete formulation.

There are additional checks of the self-consistency of the method. One can show that the components $a^m(t)$, $m \neq n$ satisfy $a^m(t) \sim t^2$ for small t , and that the unitarity constraint $|a^n|^2 + \int d\alpha |\phi^\alpha| = 1$ is satisfied to order t .

Applied to our problem the treatment above gives the result $\Gamma_n = 0$, since $K_n^n(E_n)$ vanishes at degeneracy¹. This is because triple-trace states enter the dynamics only at higher order in the coupling g_2 . The toy model above must be generalized to include this effect. Note that the energy shift $\Delta\omega_n$ in (5.24) agrees with the order g_2^2 contribution to the scale dimension of single-trace BMN operators in (5.3).

The generalized model includes three types of states: i) the discrete “single-trace” $|n\rangle$, ii) continuous “double-trace” $|\alpha_2\rangle$, and iii) continuous “triple-trace” $|\alpha_3\rangle$. The

¹It is curious that $K_n^n(E) \leq 0$ because $V_n^{\alpha_2}$ is not Hermitean.

free Hamiltonian H_0 is diagonal with energy eigenvalues E_n, E_{α_2} , and E_{α_3} , respectively. The interaction matrix and time-dependent state vector which generalize those of the model above are:

$$V = \begin{pmatrix} 0 & V_{\alpha_2}^i & 0 \\ V_i^{\alpha_2} & 0 & V_{\alpha_3}^{\alpha_2} \\ 0 & V_{\alpha_2}^{\alpha_3} & 0 \end{pmatrix}, \quad (5.27)$$

$$|\Psi(t)\rangle = \begin{pmatrix} a^i(t)e^{-iE_i t} \\ \phi(\alpha_2, t)e^{-iE_{\alpha_2} t} \\ \sigma(\alpha_3, t)e^{-iE_{\alpha_3} t} \end{pmatrix}. \quad (5.28)$$

Again we need the solution of the Schrödinger equation $id/dt|\Psi(t)\rangle = (H_0 + V)|\Psi(t)\rangle$ with initial conditions: $a^m(0) = \delta_n^m$, $\phi^{\alpha_2}(0) = 0$, $\sigma^{\alpha_3}(0) = 0$. The equations linking the components of $|\Psi(t)\rangle$ are

$$i\frac{d}{dt}a^n(t) = \int d\alpha_2 V_{\alpha_2}^n e^{iE_{n\alpha_2} t} \phi^{\alpha_2}(t) \quad (5.29)$$

$$i\frac{d}{dt}\phi^{\alpha_2}(t) = \sum_m V_m^{\alpha_2} e^{iE_{\alpha_2 m} t} a^m(t) + \int d\alpha_3 V_{\alpha_3}^{\alpha_2} e^{iE_{\alpha_2 \alpha_3} t} \sigma^{\alpha_3}(t) \quad (5.30)$$

$$i\frac{d}{dt}\sigma^{\alpha_3}(t) = \int d\alpha_2 V_{\alpha_2}^{\alpha_3} e^{iE_{\alpha_3 \alpha_2} t} \phi^{\alpha_2}(t) \quad (5.31)$$

We use the notation $E_{n\alpha_2} = E_n - E_{\alpha_2}$, etc. for differences of energy.

We now wish to process the information in (5.29-5.31) to obtain a relation describing the coupling of the discrete components of $|\Psi(t)\rangle$ alone. Rather than the exact equation (5.20) in the simpler model, we will obtain a relation which is accurate to fourth order in the potentials. For this purpose we begin in straightforward fashion to integrate (5.31) obtaining an expression for σ^{α_3} in terms of ϕ^{α_2} . We then substitute this in (5.30) and integrate that, and substitute the result in the first equation which becomes

$$\frac{d}{dt}a^n(t) = -\int d\alpha \sum_{m'} \int_0^t dt' e^{iE_{n\alpha} t + iE_{\alpha m'} t'} V_{\alpha}^n V_{m'}^{\alpha} a^{m'}(t') \quad (5.32)$$

$$+i\int d\alpha_2 d\alpha_3 d\alpha'_2 \int_0^t dt' \int_0^{t'} dt'' e^{iE_{n\alpha_2}t+iE_{\alpha_2\alpha_3}t'+iE_{\alpha_3\alpha'_2}t''} V_{\alpha_2}^n V_{\alpha_3}^{\alpha_2} V_{\alpha'_2}^{\alpha_3} \phi^{\alpha_2}(t'')$$

The next step is to substitute for $\phi^{\alpha_2}(t'')$ in the equation above the value obtained by integrating the first term of (5.30) with “source” a^m . The term with “source” ϕ^{α_2} is of higher order in the potentials through (5.31) and can be dropped. This gives us the net contribution of triple-trace intermediate states, denoted by

$$\begin{aligned} \frac{d}{dt} a^n(t)_{triple} &= \sum_m \int d\alpha_2 d\alpha_3 d\alpha'_2 \int_0^t dt' \int_0^{t'} dt'' \int_0^{t''} dt''' e^{iE_{n\alpha_2}t+iE_{\alpha_2\alpha_3}t'} \\ &\quad e^{iE_{\alpha_3\alpha'_2}t''+iE_{\alpha_2\alpha'_2}t'''} V_{\alpha_2}^n V_{\alpha_3}^{\alpha_2} V_{\alpha'_2}^{\alpha_3} V_m^{\alpha'_2} a^m(t''') \end{aligned} \quad (5.33)$$

To obtain the contribution of single-trace intermediate states at order g_2^4 , we integrate the first term of (5.32) to find an expression for $a^n(t)$ (with $n \rightarrow m$). This expression is then reinserted for $a^{m'}(t')$ in (5.32) to obtain the iterated contribution

$$\begin{aligned} \frac{d}{dt} a^n(t)_{single} &= \sum_{m,m'} \int d\alpha_2 d\alpha'_2 \int_0^t dt' \int_0^{t'} dt'' \int_0^{t''} dt''' e^{iE_{n\alpha_2}t+iE_{\alpha_2 m}t'} \\ &\quad e^{iE_{m\alpha'_2}t''+iE_{\alpha_2 m'}t'''} V_{\alpha_2}^n V_m^{\alpha_2} V_{\alpha'_2}^m V_{m'}^{\alpha'_2} a^{m'}(t''') \end{aligned} \quad (5.34)$$

The full expression for $\frac{d}{dt} a^n(t)$ to fourth order is

$$\begin{aligned} \frac{d}{dt} a^n(t) &= -\int d\alpha_2 \sum_{m'} \int_0^t dt' e^{iE_{n\alpha_2}t+iE_{\alpha_2 m'}t'} V_{\alpha_2}^n V_n^{\alpha_2} \\ &\quad + \frac{d}{dt} a^n(t)_{triple} + \frac{d}{dt} a^n(t)_{single} \end{aligned} \quad (5.35)$$

The first term is just the short-time approximation to (5.22) in the simple model in different notation. We will not discuss it further since it does not contribute to the fourth order amplitudes of primary concern in the generalized model.

We now make the short-time approximation $a^n(t') \approx 1$, $a^m(t') \approx 0$ for $m \neq n$ in (5.33) and (5.34). We will present the treatment of the triple-trace part explicitly and then summarize the rather similar steps needed for the single-trace part.

The nested set of time integrals in (5.33) can easily be done, and the result (in-

cluding the overall factor $\exp i(E_{n\alpha_2})t$ is

$$\frac{e^{iE_{n\alpha_3}t} - 1}{E_{\alpha_3 n} E_{\alpha_2 \alpha_3}} - \frac{e^{iE_{n\alpha_2}t} - 1}{E_{\alpha_2 n} E_{\alpha_2 \alpha_3}} + \frac{e^{iE_{n\alpha'_2}t} - e^{iE_{n\alpha_2}t}}{E_{\alpha_2 \alpha'_2} E_{\alpha_3 \alpha'_2}} + \frac{e^{iE_{n\alpha_2}t} - e^{iE_{n\alpha_3}t}}{E_{\alpha_2 \alpha_3} E_{\alpha_3 \alpha'_2}} \quad (5.36)$$

In an obvious fashion we subtract and add 1 in the last two terms of (5.36). We thus obtain six terms with the structure $\exp iEt - 1$ divided by energy denominators. In our discussion of the contribution of these six terms to (5.33) in the short-time limit, we need the fact that all the interaction matrix elements of the actual problem vanish at degeneracy due to the trigonometric factors in (5.10). We assume the same property in the toy model so that all energy integrals which appear when (5.36) is inserted in (5.33) converge despite the singular denominators.

We apply the $i\epsilon$ prescription of the last line of (5.23) in each of the six terms, multiplying and dividing by the energy denominators which are missing in the last four terms. It is easy to see that all contributions cancel pairwise in third and fourth and in the fifth and sixth terms. In the first and second terms we obtain

$$\begin{aligned} \frac{d}{dt} a^n(0)_{triple} = & - \int d\alpha_2 d\alpha_3 d\alpha'_2 V_{\alpha_2}^n V_{\alpha_3}^{\alpha_2} \frac{1}{E_{\alpha_2 \alpha_3}} V_{\alpha'_2}^{\alpha_3} V_n^{\alpha'_2} \frac{1}{E_{\alpha'_2 n}} \\ & [\pi \delta(E_{n\alpha_3}) + i\mathcal{P}(\frac{1}{E_{n\alpha_3}}) - \delta(E_{n\alpha_2}) - i\mathcal{P}(\frac{1}{E_{n\alpha_2}})] \end{aligned} \quad (5.37)$$

We now note that the term with $\delta(E_{n\alpha_2})$ vanishes because $V_{\alpha_2}^n = 0$ at degeneracy. Because of this vanishing one can combine the two principal value terms without ambiguity. The triple-trace contribution to the decay amplitude can then be written as

$$\frac{d}{dt} a^n(0)_{triple} = - \int d\alpha_3 U_{\alpha_3}^n [\pi \delta(E_{\alpha_3 n}) + i\mathcal{P}(\frac{1}{E_{\alpha_3 n}})] U_n^{\alpha_3} \quad (5.38)$$

where we have introduced the effective composite interactions which couple single- and triple-traces, namely

$$U_{\alpha_3}^n = \int d\alpha_2 \frac{V_{\alpha_2}^n V_{\alpha_3}^{\alpha_2}}{E_{n\alpha_2}} \quad (5.39)$$

$$U_n^{\alpha_3} = \int d\alpha_2 \frac{V_{\alpha_2}^{\alpha_3} V_n^{\alpha_2}}{E_{n\alpha_2}}. \quad (5.40)$$

The single-trace contribution (5.34) can be treated similarly. One makes the short-time replacement $a^m(t''') \rightarrow \delta_n^m$. The time integrals are then easily done, but separately for the two cases $m \neq n$ and $m = n$. The contributions of the various terms to $\frac{d}{dt}a^n(t)$ at small t are then analyzed as above. In each case there is one term which contributes at $t = 0$ via the $i\epsilon$ prescription. In each there is a $\delta(E_{n\alpha_2})$ which drops because $V_{\alpha_2}^n = 0$. The contributions of two (non-singular) principal value integrals remain in the final result

$$\frac{d}{dt}a^n(0)_{single} = i \sum_m U_m^n \frac{1 - \delta_{E_{nm}}}{E_{mn}} U_n^m \quad (5.41)$$

$$-i U_n^n \int d\alpha_2 \frac{V_{\alpha_2}^n V_n^{\alpha_2}}{E_{\alpha_n}^2} \quad (5.42)$$

which is largely written in terms of the composite interaction

$$U_m^n = \int d\alpha_2 \frac{V_{\alpha_2}^n V_m^{\alpha_2}}{E_{n\alpha_2}} \quad (5.43)$$

We can now interpret the results (5.37,5.41) in terms of (5.24). We find the decay width

$$\Gamma_n = 2\pi \int d\alpha_3 \delta(E_{\alpha_3 n}) U_{\alpha_3}^n U_n^{\alpha_3} \quad (5.44)$$

and energy shift

$$\begin{aligned} \Delta\omega_n &= U_n^n - \sum_m U_m^n \frac{1 - \delta_{E_{nm}}}{E_{mn}} U_n^m \\ &+ U_n^n \int d\alpha_2 \frac{V_{\alpha_2}^n V_n^{\alpha_2}}{E_{\alpha_2 n}} \\ &- \int d\alpha_3 U_{\alpha_3}^n \mathcal{P}\left(\frac{1}{E_{\alpha_3 n}}\right) U_n^{\alpha_3} \end{aligned} \quad (5.45)$$

We are primarily interested in the decay width, which will be evaluated for the BMN system (5.9, 5.10) in section 5. However, we note that the energy shift agrees with the result of fourth order non-degenerate (time-independent) perturbation theory

for any quantum-mechanical system whose state space and interaction structure are the same as the present model as defined in (5.27) and the discussion above it². Of course, the principal value derived here to resolve the divergence in the last term is not present in conventional perturbation theory. The physical interpretation of our result is that the pole of the resolvent operator $1/(H_0 - E)$ at $E = E_n$ due to the discrete state $|n\rangle$ is shifted to $E = E_n + \Delta\omega_n - i\Gamma/2$ in the complex plane by the interaction in $1/(H_0 + V - E)$. The state $|n\rangle$ is unstable in the full theory.

The goal of the Hamiltonian formulation of [41] was the calculation of anomalous dimensions of BMN operators. In our opinion the calculations undertaken for this purpose should be revised to incorporate degenerate rather than non-degenerate perturbation theory. One may note that the various contributions to our energy shift (5.45) agree exactly with those of (25) of [41]. So the result there should be interpreted as the real part of the shift of a pole rather than the anomalous dimension of an eigenstate of the dilatation operator.

It is interesting that the present time-dependent treatment provides justification for the recent suggestion in [48] of an S -matrix approach to the BMN system (see also [51]) which would require an $i\epsilon$ prescription in the genus two calculations of [41]. The idea of an S -matrix is fully compatible with our interpretation of the instability of the states $|n\rangle$.

5.4 Basis Independence

It is our intention to derive a formula for the decay widths which can be compared with future calculations in light-cone string field theory. We must therefore determine the effect of the change to the basis in which gauge theory and string theory calculations should match. It turns out that the result is not changed by the basis transformation (at least to order g_2^4). Basis independence would be a triviality if it were implemented as a standard “change of representation” in quantum mechanics, since matrix elements

²Most treatments of perturbation theory assume a hermitean Hamiltonian, but the standard formulas remain valid when rewritten in terms of h_j^i

are invariant. However, things are not entirely trivial since states and operators actually transform contragrediently. We follow the recent paper [48], although the same result should emerge from the similar formalism of [27].

The metric g_{ij} defined by the free two-point functions of the \mathcal{O}_i of (5.4) can be referred to local frames using the vielbein

$$g_{ij} = e_i^k \delta_{kl} e_j^l \quad (5.46)$$

We found the usual practice of different fonts for the “frame” and “coordinate” indices confusing in the present application, so we prefer to emphasize that the same physical variables are indexed by both upper and lower indices. The inverse vielbein is denoted by f_k^i , so that *e.g.* $f_k^i e_j^k = \delta_j^i$. The operators with diagonal free two-point functions are

$$\tilde{\mathcal{O}}_k = f_k^i \mathcal{O}_i \equiv S^{-1} \mathcal{O}_k \quad (5.47)$$

where we have defined the Hilbert space operator S^{-1} by the last equality. Our S^{-1} has exactly the properties of $S^{-1/2}$ in [48]. In particular the string basis Hamiltonian is

$$\tilde{H} = S H S^{-1} \quad (5.48)$$

which was shown to be exactly the Hamiltonian of the string bit formalism [31, 45] whose order g_2 splitting/joining interaction agrees with string field theory and order g_2^2 contact term also agrees (if a certain truncation of intermediate states is made) [28].

The toy models of Section 3 can now be described in a new notation in which the states \mathcal{O}_i and $\tilde{\mathcal{O}}_j$ span different bases of the Hilbert space, the gauge theory basis and the string basis, respectively. The time evolution problems treated in Section 3 as models for gauge theory can be described as follows. We found (approximately) the state

$$|\Psi(t)\rangle = \sum_i a^i(t) \mathcal{O}_i \quad (5.49)$$

which evolves with time by the Hamiltonian H and satisfies an initial condition

$a^i(0) = 1$ for $i = i_0$ and $a^i(0) = 0$ for $i \neq i_0$. From the Schrödinger equation $i \frac{d}{dt} |\Psi(t)\rangle = H |\Psi(t)\rangle$ we easily derive the component evolution

$$i \frac{d}{dt} a^i(t) = H_j^i a^j(t). \quad (5.50)$$

In string basis we would instead be interested in the state

$$|\tilde{\Psi}(t)\rangle = \sum_i \tilde{a}^i(t) \tilde{\mathcal{O}}_i \quad (5.51)$$

which evolves in time by the Hamiltonian \tilde{H} with the initial conditions $\tilde{a}^i(0) = 1$ for $i = i_0$ and $\tilde{a}^i(0) = 0$ for $i \neq i_0$.

We now attempt to relate the time-dependent expansion coefficients $a^i(t)$ and $\tilde{a}^i(t)$. The Schrödinger equation $i \frac{d}{dt} |\tilde{\Psi}(t)\rangle = \tilde{H} |\tilde{\Psi}(t)\rangle$ can be expanded as

$$i \frac{d}{dt} \sum_i \tilde{a}^i(t) S^{-1} \mathcal{O}_i = \sum_m \tilde{a}^m(t) \tilde{H} S^{-1} \mathcal{O}_i. \quad (5.52)$$

We apply S to both sides and obtain the component equations

$$i \frac{d}{dt} \sum_i \tilde{a}^i(t) = (S \tilde{H} S^{-1})_j^i \tilde{a}^j(t) \quad (5.53)$$

$$= (S^2 H S^{-2})_j^i \tilde{a}^j(t) \quad (5.54)$$

We now consult Sec. 4 of [48] and learn that $S^2 H S^{-2} = H^\dagger$. Thus the string basis components evolve via

$$i \frac{d}{dt} \sum_i \tilde{a}^i(t) = (H^\dagger)_j^i \tilde{a}^j(t), \quad (5.55)$$

a curious and useful fact!

To apply this fact we simply go back to the expressions for the decay amplitude in (5.38 - 5.45) and observe that these results remain unchanged if we replace every matrix element V_j^i of the potential by that of the adjoint $(V^\dagger)_j^i = V_i^j$. Thus the results obtained in Section 3 in the gauge theory basis exactly describe the decay amplitude in string basis!

5.5 Computation of the decay rate

In Section 3 we derived a formal expression for the decay rate that we reproduce here,

$$\Gamma_n = 2\pi \int d\alpha_3 U_{\alpha_3}^n U_n^{\alpha_3} \delta(E_{\alpha_3} - E_n). \quad (5.56)$$

We explain the evaluation of this expression in some detail. Let us begin with the computation of the effective composite interaction matrices $U_{\alpha_3}^n$ and $U_n^{\alpha_3}$. Triple-trace state is labelled as $\alpha_3 = \{m, s_0, s_1\}$. For convenience, let us also define $s_2 = 1 - s_0 - s_1$. Because of the δ -function in (5.56), we need this matrix element only at degeneracy, $E_{\alpha_3} = E_n$, where the computation simplifies and has already appeared in [13] and [41]. Using the perturbation coefficients (5.10) in (5.40) one finds,

$$U_n^{ms_0s_1} = \frac{\lambda' g_2^2 n}{2\pi^4 J} \sqrt{\frac{s_1 s_2}{s_0}} \int_0^1 ds'_0 \frac{1}{s'_0} (\delta_{s'_0, s_0+s_1} + \delta_{s'_0, s_0+s_2}) \sin^2(\pi n s'_0) \sum_{p=-\infty}^{\infty} \frac{p}{s'_0} \frac{\sin^2(\pi p s_0 / s'_0)}{(n^2 - (p/s'_0)^2)(n - p/s'_0)^2}.$$

The evaluation of the sum in the second line is explained in Appendix C of [13]. Finally performing the integral over s'_0 one arrives at the result,

$$U_n^{\alpha_3} = -\frac{\lambda' g_2^2}{4\pi^2 J} \sqrt{s_1 s_2 s_0} \sin^2(\pi n s_1). \quad (5.57)$$

A similar computation using (5.11) in (5.39) gives the result³ $U_{\alpha_3}^n = 2U_n^{\alpha_3}$ when $E_{\alpha_3} = E_n$. Inserting (5.57) into (5.56) one obtains,

$$\Gamma_n = \frac{\lambda' g_2^4}{4\pi^3 J^2} \sum_{m=-\infty}^{\infty} J \int_0^1 ds_0 J \int_0^{1-s_0} ds_1 s_1 s_2 s_0 \sin^4(\pi n s_1) \delta(n^2 - (\frac{m}{s_0})^2). \quad (5.58)$$

We evaluate this expression for $n > 0$ for simplicity but the final expression will be valid also for $n < 0$. The integral over s_1 can be done analytically with the result,

$$\Gamma_n = \frac{\lambda' g_2^4}{128 n^2 \pi^5} \sum_{m=1}^{\infty} \int_0^1 ds_0 \delta(n^2 - (\frac{m}{s_0})^2) s_0 (1 - s_0) (15 + 4\pi^2 n^2 (1 - s_0)^2). \quad (5.59)$$

³The factor of 2 arises from the $(k+1)!$ and $k!$ prefactors in (5.10) and (5.11).

Let us denote the solutions to the degeneracy condition,

$$n^2 = \frac{m^2}{s_0^2},$$

by $\{m^*, s_0^*\}$. One then performs the integral over s_0 using the δ -function,

$$\delta(n^2 - (\frac{m}{s_0})^2) = \frac{m}{2n^3} \delta(s_0 - \frac{m}{n}).$$

This gives,

$$\Gamma_n = \frac{\lambda' g_2^4}{256\pi^5 n^7} \sum_{m^*=1}^{n-1} m^{*2} (n - m^*) (15 + 4\pi^2 (n - m^*)^2). \quad (5.60)$$

Here range of the sum is set by positive solutions to the degeneracy condition above. For example, when $n = 3$ there are two solutions $\{m^*, s_0^*\} = \{1, 1/3\}$ and $\{2, 2/3\}$. The sum in (5.60) is easily done for general n and one arrives at the final result,

$$\Gamma_n = \frac{\lambda' g_2^4}{3840\pi^3 n^5} (n^2 - 1)(n^2 + 1 + \frac{75}{4\pi^2}). \quad (5.61)$$

We observe that decay width vanishes for $n = \pm 1$ and it shrinks as the excitation mode n increases.

5.6 Discussion

The viewpoint we have taken is somewhat simplified in that we have incorporated the degeneracy of single- and triple-trace operators \mathcal{O}_n^J and $\mathcal{O}_m^{J_0, J_1, J_2}$ when $m = \pm n J_0 / J$, but we have ignored further degeneracies, such as that of $\mathcal{O}_m^{J_0, J_1, J_2}$ with the five-trace $\mathcal{O}_p^{J'_0, J_1, J_2, J_3, J_4}$ when $p = \pm m J'_0 / J_0$. Indeed the state $\mathcal{O}_m^{J_0, J_1, J_2}$ is stable only when $m = \pm 1$, so our calculation gives the true order g_2^2 amplitude for decay of \mathcal{O}_n^J to $\mathcal{O}_{m=\pm 1}^{J_0=J/|n|, J_1, J_2}$. The rate is given by the $m^* = 1$ term in the sum (5.60). For $|n| > 2$ and $|m| > 2$, one must envisage a sequential decay process, *e.g.*

$$\mathcal{O}_{n=3}^J \rightarrow \mathcal{O}_{m=2}^{J_0, J_1, J_2} \rightarrow \mathcal{O}_{p=1}^{J'_0, J_1, J_2, J_3, J_4}$$

with $J_0/J = 2/3$ and $J'_0/J_0 = 1/2$. For general n , there can be a cascade up to $(2|n| - 1)$ -trace states. We have not studied transition amplitudes such as $3 \rightarrow 5$ or sequential decays explicitly, but we expect that the amplitude of the $1 \rightarrow 3 \rightarrow 5$ process is of order g_2^4 . Thus we believe that the order g_2^2 decay amplitude we have calculated is meaningful for general n, m and that it can be readily compared with string field theory calculations.

Readers should note that most statements made in this paper about vanishing amplitudes hold for the lowest order contributions only. One expects non-vanishing higher order corrections. For example, the decay amplitude for $1 \rightarrow 2$ of order g_2^3 is expected to be non-vanishing at degeneracy, and there should be a non-vanishing $1 \rightarrow 4$ amplitude of the same order. On the other hand the elementary order g_2 amplitude $V_{\alpha_3}^{\alpha_4}$ in (5.10) vanishes at degeneracy because it is disconnected, *viz.* the delta functions in (5.12).

As we stated in the Introduction, the computation of anomalous dimensions of BMN operators requires degenerate perturbation theory with possible modification of the order g_2^2 result (5.3). We now briefly describe our preliminary study of this question in which we work at large finite J . In general there are order g_2^2 transition amplitudes which do not vanish at degeneracy between a single trace operator \mathcal{O}_n^J of momentum n and triple-trace operators with several values of m . The triple-traces in turn mix with 5-trace operators, 5-trace with 7-trace, etc., with termination only at the maximal J -trace level. Note that each “band” of k -trace operators involves a finite fraction of J distinct operators. Nevertheless one can derive the precise statement that to order $\lambda'g_2^2$ the anomalous dimensions of operators in this large set are the eigenvalues of $H_0 + \lambda'g_2^2U$ where U is the effective composite interaction whose non-vanishing matrix elements are,

$$U_{\alpha_k}^{\alpha'_{k\pm 2}} = \int d\alpha_{k\pm 1} \frac{V_{\alpha_k \pm 1}^{\alpha_{k\pm 2}} V_{\alpha_k}^{\alpha_{k\pm 1}}}{E_{n\alpha_{k\pm 1}}}, \quad U_{\alpha_k}^{\alpha'_k} = \sum_{j=\pm 1} \int d\alpha_{k+j} \frac{V_{\alpha_{k+j}}^{\alpha'_k} V_{\alpha_k}^{\alpha_{k+j}}}{E_{n\alpha_{k+j}}}. \quad (5.62)$$

Note that single-triple matrix elements appeared in Sec. 3. For large J this is a very large but sparse matrix.

We have studied a reasonably accurate “model” of this matrix to determine the large J limit of eigenvalues and eigenvectors. The results indicate that there is a single eigenvector which is “mostly single trace” as $g_2^2 \rightarrow 0$, and its eigenvalue is that of (5.3) for $k = 0$. Similarly, there are some “mostly k-trace” eigenvectors for which (5.3) is also correct. But there are also some “collective” eigenvectors which are superpositions of many multi-trace operators and whose eigenvalues do not agree with (5.3). Thus our model indicates that (5.3) is correct for most states in the system but not correct for all multi-trace states.

We close by noting that the gauge theory result (5.3) for “mostly k-trace” operators has not yet been confirmed in light cone string field theory. The complication of degenerate perturbation theory described above in the gauge theory will be mirrored in string theory. Thus we expect that the string theory computation can be organized to produce a composite interaction matrix at degeneracy which should agree with (5.62) after change to string basis.

Appendix A

D-term and external gluon contributions at $\mathcal{O}(\lambda')$

The aim of this appendix is to prove equation (3.21) showing the planar level contribution to the vector anomalous dimension which arise from the D-term part of the lagrangian, (3.11). In section 3 we explained how one can express this result in terms of the the correlator of a non-conserved current, $J_\mu = Z \overleftrightarrow{\partial} Z$. Here, we shall compute D-term contributions to this correlator at the one loop level. In the following we will first show that D-term quartic vertex do not contribute to $\langle J\bar{J} \rangle$ at all. Then we will explain how to compute the self-energy contributions. Finally we shall consider the contribution arising from the gluon exchange graph fig. 3-4I by employing the trick of relating it to simpler diagrams figs 3-4II, 3-4III, 3-4IV as we described at the end of section 3.2.

The most direct and painless way to compute these Feynman diagrams is the beautiful method of differential renormalization (DR) [34]. The main idea is to compute n -point functions $\langle O_1(x_1) \cdots O_k(x_k) \rangle$ directly in space time rather than Fourier transforming to momentum space, and adopting a certain differential regularization scheme when the space-time expressions become singular, *i.e.* as $x_i \rightarrow x_j$. Note that, away from the contact points $x_i \rightarrow x_j$, the n -point function is well-defined and can be Fourier transformed back to momentum space. However as x_i approaches to x_j for $i \neq j$, most expressions become too singular to admit a Fourier transform. Yet,

one can easily rewrite the singular expressions in terms of derivatives of less singular expressions hence render the Fourier transform possible. The only such rewriting we will use here is the following formula [34],

$$\frac{1}{(x_1 - x_2)^2} = -\frac{1}{4} \square \frac{\ln((x_1 - x_2)^2 \Lambda^2)}{(x_1 - x_2)^2} \quad (\text{A.1})$$

where Λ^2 is the renormalization scale. We also remind the Green's equation in our conventions,

$$\square \frac{1}{(x_1 - x_2)^2} = -4\pi^2 \delta(x_1 - x_2). \quad (\text{A.2})$$

A nice feature of DR is that one can adopt a renormalization scheme where one ignores all tadpole diagrams, simply by setting them to zero. We will work with the Euclidean signature throughout the appendices in which case the space-time Feynman rules for $\mathcal{N} = 4$ SYM are read off from (3.11). Scalar, gluon and fermion propagators read

$$\frac{\delta_{ab}}{4\pi^2(x-y)^2}; \quad \frac{\delta_{ab}\delta_{\mu\nu}}{4\pi^2(x-y)^2}; \quad \frac{\delta_{ab}}{4\pi^2} \partial_x \frac{1}{(x-y)^2}.$$

The interaction vertices are shown in fig. A-1.

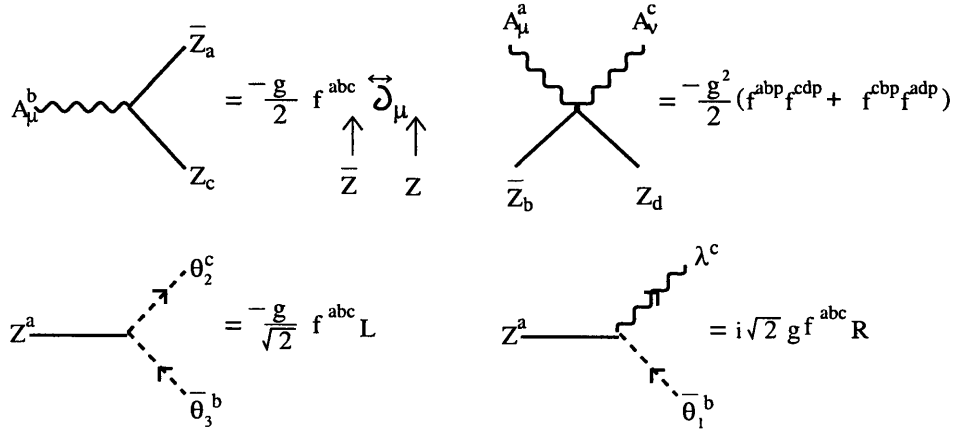


Figure A-1: Feynman rules for vertices. Same rules hold when Z is replaced by ϕ . In the θ - Z - $\bar{\theta}$ vertex, exchanging chiral fermion flavor 2 with 3 gives a minus sign and replacing Z with \bar{Z} changes the chirality projector from L to R . The analogous \bar{Z} - $\bar{\lambda}$ - θ vertex is obtained by replacing R with $-L$.

It is very easy to see that D-term contribution vanishes.

$$\begin{aligned} \langle \text{Tr}(J_\mu J_\nu) \rangle_D &= \frac{g_{YM}^2}{4\pi^2} (f^{abd} f^{ace} + f^{abe} f^{acd}) \text{Tr}(T^a T^b T^c T^d) \\ &\int d^4 u \left(\frac{1}{(x-u)^2} \overleftrightarrow{\partial}_\mu \frac{1}{(y-u)^2} \overleftrightarrow{\partial}_\nu \frac{1}{(y-u)^2} \right) = 0. \end{aligned}$$

To find the self-energy contribution to $\langle J\bar{J} \rangle$ let us first compute self-energy corrections to scalar propagator. These arise from three sources: a gluon emission and reabsorbtion, chiral-chiral fermion loop and chiral-gluino fermion loop. We will not need the exact value of the first contribution as will be explained below. Let us begin with chiral-chiral loop which is shown in fig. A-2. Calling this graph SE_1 , Feynman rules yield,

$$\begin{aligned} SE_1 &= -2 \frac{1}{4\pi^2} f^{acd} \left(-\frac{g}{\sqrt{2}} \right) f^{bdc} \left(\frac{g}{\sqrt{2}} \right) \int d^4 u d^4 v \frac{1}{(x-u)^2} \frac{1}{(y-v)^2} \text{Tr} \left[L \not{\partial}_u \frac{1}{(u-v)^2} R \not{\partial}_v \frac{1}{(u-v)^2} \right] \\ &= -2 \frac{g_{YM}^2 \delta^{ab} N}{4\pi^2} \int d^4 u d^4 v \frac{1}{(x-u)^2} \frac{1}{(y-v)^2} \not{\partial}_\alpha^u \frac{1}{(u-v)^2} \not{\partial}_\alpha^v \frac{1}{(u-v)^2} \end{aligned}$$

where factor of 2 in the first line comes from summing over two fermion flavors θ_1 and θ_2 . We will show the evaluation of integral here for future reference. By parts in u gives,

$$\begin{aligned} I_1(x, y) &= \int d^4 u d^4 v \left\{ \frac{1}{(x-u)^2} \frac{1}{(y-v)^2} (-4\pi^2) \frac{\delta(u-v)}{(u-v)^2} + \frac{1}{2} \frac{1}{(x-u)^2} \frac{1}{(y-v)^2} \square \frac{1}{(u-v)^4} \right\} \\ &\rightarrow -\frac{1}{8} \int d^4 u d^4 v \frac{1}{(x-u)^2} \frac{1}{(y-v)^2} \square_u \square_v \frac{\ln((u-v)^2 \Lambda^2)}{(u-v)^2} \\ &= -\frac{1}{8} (-4\pi^2)^2 \int d^4 u d^4 v \delta(x-u) \delta(y-v) \frac{\ln((u-v)^2 \Lambda^2)}{(u-v)^2} \\ &= -\frac{(4\pi^2)^2 \ln((x-y)^2 \Lambda^2)}{8 (x-y)^2} \end{aligned} \tag{A.3}$$

In passing to second line we omitted the first term which is supposed to cancel out with tadpole contributions in DR. Second and third equalities use (A.1) and (A.2). Hence,

$$SE_1 = \frac{g_{YM}^2 N}{4(4\pi^2)^2} \delta_{ab} \frac{\ln((x-y)^2 \Lambda^2)}{(x-y)^2}. \tag{A.4}$$

An analogous computation for the gluino-chiral fermion loop gives,

$$SE_2 = -\frac{g_{YM}^2 N}{2(4\pi^2)^2} \delta_{ab} \frac{\ln((x-y)^2 \Lambda^2)}{(x-y)^2}. \quad (\text{A.5})$$

Although we will not need it, let us give here the total self-energy correction to the scalar propagator for reference (including gluon emission-reabsorbtion),

$$SE = -\frac{g_{YM}^2 N}{8(4\pi^2)^2} \delta_{ab} \frac{\ln((x-y)^2 \Lambda^2)}{(x-y)^2}. \quad (\text{A.6})$$

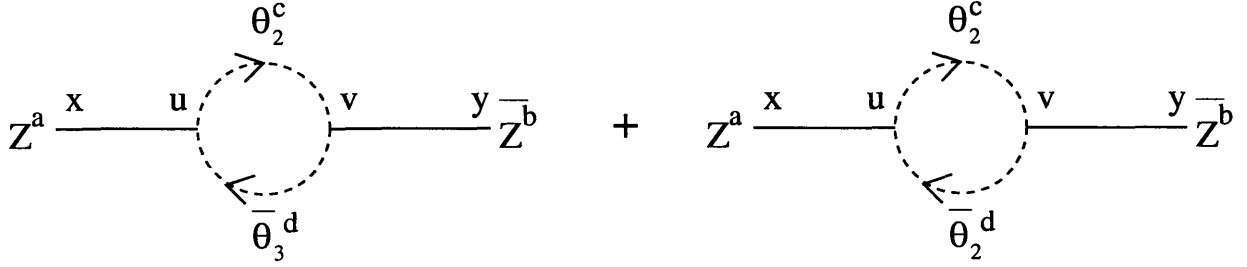


Figure A-2: Chiral fermion loop contributions to self-energy of Z .

Turning to gluon exchange contribution to $\langle J\bar{J} \rangle$, we recall our trick to express it as gluon exchange correction to gluon propagator in scalar QED, fig. 3-4III,

$$\begin{aligned} \langle \text{Tr}(J_\mu(x)\bar{J}_\nu(y)) \rangle_{g.e.} &= \frac{\delta_{ab}}{2} \langle J_\mu^a(x)\bar{J}_\nu^b(y) \rangle_{g.e.} \\ &= -\frac{N^4}{g_{YM}^2} \langle A_\mu(x)A_\nu(y) \rangle_{g.e.} \end{aligned} \quad (\text{A.7})$$

where $J_\mu^a = if^{abc}Z^b\partial_\mu Z^c$. In the second line we divided out by a factor of $(g/2)^2$ to compensate for the coupling of incoming and outgoing gluons to the loop and there is an overall -1 w.r.t. $\langle J\bar{J} \rangle$ because of the antisymmetric derivative in scalar-gluon vertex. We also took into account the color factors at four vertices,

$$fcge f^dac ffdg fehf = \delta^{ab} \frac{N^2}{2}.$$

Now, the sub-divergent piece of this diagram cancels out the sub-divergent pieces of

graphs I and II in fig 3-4. Hence the contribution to anomalous dimension is,

$$\langle A_\mu(x)A_\nu(y) \rangle_{g.e.} \rightarrow -4 \times \text{Fig.3} - 4\text{I} - 2 \times \text{Fig.3} - 4\text{II}.$$

When we include the self-energy corrections to $\langle J\bar{J} \rangle$ second term will be canceled out by gluon emission-reabsorption part of the self energies and one is left with,

$$\langle \text{Tr}(J_\mu \bar{J}_\nu) \rangle_{g.e.+s.e.} = -\frac{N^4}{g_{YM}^2} \{-4 \times \text{Fig.3} - 4\text{a} - 2 \times \text{F.S.E.}\} \quad (\text{A.8})$$

with ‘‘FSE’’ being only the fermion loop contributions to the self energy of $\langle J\bar{J} \rangle$,

$$\text{FSE} = -\frac{g_{YM}^2 N^4}{16\pi^2} \frac{J_{\mu\nu}}{(x-y)^2} \ln((x-y)^2 \Lambda^2) G(x,y)^2. \quad (\text{A.9})$$

Note that we included 1/2 factor coming from our counting of self energies, (see fig. 3-2). Arousal of conformal factor, $J_{\mu\nu}$, is explained below. Let us now compute the contribution of fig. 3-4a including the color factors in conversion to $\langle J\bar{J} \rangle$. Using the Feynman rules for in fig. A-1,

$$\begin{aligned} \text{Fig 3} - 4\text{a} &\rightarrow -\frac{g_{YM}^2}{2} (f^{acp} f^{dhp} + f^{dcp} f^{ahp}) \left(-\frac{g}{2} f^{edh}\right) \left(-\frac{g}{2} f^{cbe}\right) \\ &\quad \frac{1}{(4\pi^2)^4} \int \frac{d^4 u}{(x-u)^2} \left(\frac{1}{(x-y)^2} \overset{\leftrightarrow y}{\partial}_\nu \frac{1}{(y-u)^2} \overset{\leftrightarrow u}{\partial}_\mu \frac{1}{(x-u)^2} \right) \\ &= -N^2 \delta^{ab} \frac{9}{32} \frac{g^4}{(4\pi^2)^4} \frac{1}{(x-y)^2} \overset{\leftrightarrow}{\partial}_\nu \partial_\mu I_2(x,y) \end{aligned}$$

where the integral is

$$I_2(x,y) = \int \frac{d^4 u}{(x-u)^4 (y-u)^2} = \pi^2 \frac{\ln((x-y)^2 \Lambda^2)}{(x-y)^2} \quad (\text{A.10})$$

again by use of (A.1) and (A.2). The anomalous contribution is obtained by keeping terms proportional to \ln in (A.10) which gives,

$$\text{Fig 3} - 4\text{a} \rightarrow -\frac{9}{64} \frac{g^4}{4\pi^2} \delta^{ab} N^2 \ln((x-y)^2 \Lambda^2) \frac{J_{\mu\nu}(x,y)}{(x-y)^2} G(x,y)^2.$$

Putting this in (A.8) together with (A.9) one gets,

$$\begin{aligned}
\langle \text{Tr}(J_\mu \bar{J}_\nu) \rangle_{g.e.+s.e.} &= -\frac{2}{g_{YM}^2} \delta_{ab} \left(4 \times \frac{9}{64} - \frac{1}{4}\right) \delta^{ab} \frac{g_{YM}^2}{4\pi^2} N^2 \\
&\quad \ln((x-y)^2 \Lambda^2) \frac{J_{\mu\nu}(x,y)}{(x-y)^2} G(x,y)^2 \\
&= -\frac{5g_{YM}^2 N}{4\pi^2} \left(\frac{N}{2}\right)^3 \ln((x-y)^2 \Lambda^2) \\
&\quad \frac{J_{\mu\nu}(x,y)}{(x-y)^2} G(x,y)^2. \tag{A.11}
\end{aligned}$$

This is the total contribution to $\langle J\bar{J} \rangle$ from D-term, gluon exchange and self energies. Insertion of this result into (3.20) yields the desired result, (3.21).

Our next task is to fill in the details in the computation of section 3.3 that leads to the contribution of external gluons to the $\mathcal{O}(\lambda')$ anomalous dimension, (3.28). These contributions are shown in fig. 3-6. To evaluate Graph I and II of fig. 3-6, we will need the function C_μ which was defined in (3.23). Recall that external gluon is coming from the commutator $ig[A_\mu, Z]$ which contributes $-gf^{acd}$ at the external vertex where c is associated with the gluon, d with Z -line and a is the color factor of the external vertex. Use of the Feynman rule in fig. A-1. for the internal vertex gives,

$$\begin{aligned}
\begin{array}{c} \text{a} \\ \text{---} \end{array} \begin{array}{c} \text{b} \\ \text{---} \end{array} &= (-gf^{acd}) \left(-\frac{g}{2} f^{dcb} \frac{1}{(4\pi^2)^3} \int \frac{d^4 u}{(x-u)^2} \left(\frac{1}{(x-u)^2} \overleftrightarrow{\partial}_{u\mu} \frac{1}{(y-u)^2} \right)\right) \\
&= -\frac{g_{YM}^2}{2} N \delta^{ab} \frac{1}{(4\pi^2)^3} (-\partial_\mu^y + \frac{1}{2} \partial_\mu^x) I_2(x,y) \\
&= \frac{3}{16} \frac{g_{YM}^2 N}{4\pi^2} \delta^{ab} \partial_\mu^y \left(\ln((x-y)^2 \Lambda^2) G(x,y) \right)
\end{aligned}$$

Hence we read off

$$C_\mu = \frac{3}{16} \frac{g_{YM}^2}{4\pi^2} \partial_\mu^y \left(\ln((x-y)^2 \Lambda^2) G(x,y) \right).$$

Inserting this into (3.24) yields the total contribution to $\langle O_\mu^n \bar{O}_\nu^m \rangle$ from Graph I,

$$\left(\frac{N}{2}\right)^{J+2} (J+2) \delta_{nm} \frac{3}{16} \frac{g_{YM}^2 N}{4\pi^2} G(x,y)^J G(x,y) \overleftrightarrow{\partial}_\nu \partial_\mu^y \left(\ln((x-y)^2 \Lambda^2) G(x,y) \right).$$

We add to this the contribution of Graph II which is identical except a phase factor of $q\bar{r}$ and their horizontal reflections which doubles the total answer. Anomalous contribution is obtained by keeping terms proportional to \log which is (3.25) after correctly normalizing according to (3.3). Contributions of Graph III and IV (and their horizontal reflections) are identical to above except one the factor $1 + q\bar{r}$ is replaced by $-q - \bar{r}$, hence the final answer is (3.28).

Appendix B

Trace identities and F-term contribution at $\mathcal{O}(\lambda')$

Here, we first present the trace identities which were used throughout the calculations and work out an example to show how to use them in calculations of n -point functions. The example we choose is the special diagram—section 4.4—which arises in D-term contribution to torus two-point functions. As another application of the trace identities we compute the F-term contribution to anomalous dimension of vector operators.

Let us fix the convention by,

$$\mathrm{Tr}(T^a T^b) = \frac{1}{2} \delta^{ab}$$

and trivially extend $SU(N)$ structure constants, f^{abc} , to $U(N)$ by adding the $N \times N$ matrix $T^0 = \frac{I}{\sqrt{2N}}$. For notational simplicity let us denote all explicit generators by their index values, *i.e.* $T^a \rightarrow a$ and replace explicit trace of an arbitrary matrix M by $\mathrm{Tr}(M) \rightarrow (M)$.

Results derived in [52] can be used to prove the following trace identities.

$$\begin{aligned} (MaM'a) &= \frac{1}{2}(M)(M') & (ab) &= \frac{1}{2}\delta^{ab} \\ (Ma)(aM') &= \frac{1}{2}(MM') & (a) &= \sqrt{N/2}\delta^{a0} \end{aligned} \tag{B.1}$$

$$aa = \frac{1}{2}NI \quad () = N$$

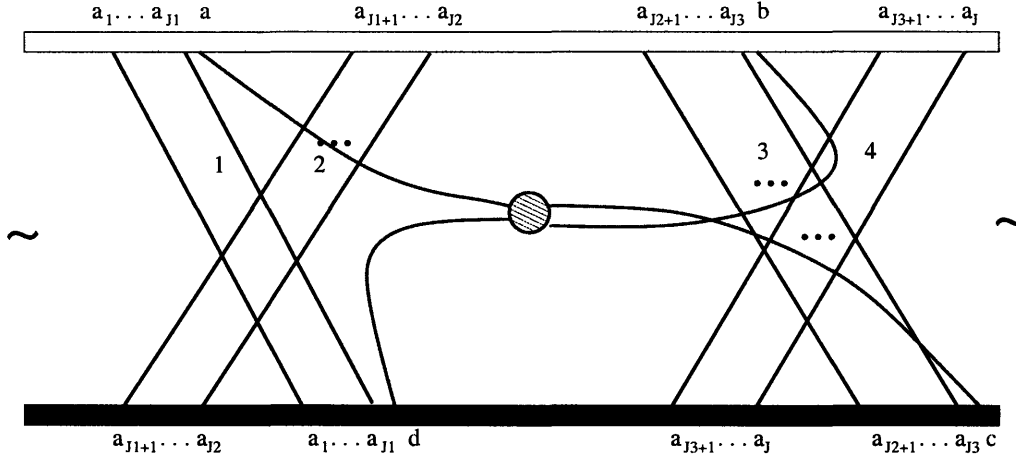


Figure B-1: A torus level diagram with “special” topology.

Let us use these identities on the example of fig. B-1. This shows a D-term interaction in a special diagram. We would like to show that the total trace involved in this graph boils down to a trace over the four interacting legs and eventually to show that this diagram is indeed at torus level by algebraic methods. In fig B-1, the color indices carried by the block of Z -lines are a_1, \dots, a_{J_1} , $a_{J_1+1}, \dots, a_{J_2}$, $a_{J_2+1}, \dots, a_{J_3}$ and a_{J_3+1}, \dots, a_J respectively. Color indices of the interacting lines are denoted as a, b, c, d . Then the color factor associated with the vertex is $f^{acp} f^{dbp}$. Interestingly, untwisting the b and c lines in fig. B-1 which give the other color combination, $f^{abp} f^{dcp}$ turns out to be a genus-2 diagram! That’s why we draw the special and semi-contractible diagrams of section 4 with twists. Use of (B.1) in fig. B-1 goes as follows,

$$\begin{aligned}
& (a_1 \cdots a_{J_1} a a_{J_1+1} \cdots a_{J_2} a_{J_2+1} \cdots a_{J_3} b a_{J_3+1} \cdots a_J) \\
& \quad \cdot (c a_{J_3} \cdots a_{J_2+1} a_J \cdots a_{J_3+1} d a_{J_1} \cdots a_1 a_{J_2} \cdots a_{J_1+1}) \\
= & \frac{1}{2} (N/2)^{J-J_3-1} (a_1 \cdots a_{J_1} a a_{J_1+1} \cdots a_{J_2} a_{J_2+1} \cdots a_{J_3} b d a_{J_1} \cdots a_1 a_{J_2} \cdots a_{J_1+1} c a_{J_3} \cdots a_{J_2+1}) \\
= & \frac{1}{2} (N/2)^{J-J_3-1} (b d a_{J_1} \cdots a_1 a_{J_2} \cdots a_{J_1+1} c) \\
& \quad \cdot (a_{J_3-1} \cdots a_{J_2+1} a_1 \cdots a_{J_1} a a_{J_1+1} \cdots a_{J_2} a_{J_2+1} \cdots a_{J_3-1}) \\
= & \frac{1}{2} (N/2)^{J-J_2-2} (b d a_{J_1} \cdots a_1 a_{J_2} \cdots a_{J_1+1} c) (a_1 \cdots a_{J_1} a a_{J_1+1} \cdots a_{J_2})
\end{aligned}$$

$$\begin{aligned}
&= \frac{1}{2}(N/2)^{J-J_2+J_1-3}(a_{J_2} \cdots a_{J_1+1}cbdaa_{J_1+1} \cdots a_{J_2}) \\
&= (N/2)^{J-3}(cbda).
\end{aligned}$$

Contraction with the vertex color, $f^{acp}f^{dbp}$ gives $(N/2)^{J+1}$.

Same interaction in a planar diagram, fig. B-2 would give,

$$(a_1 \cdots a_{J_1} a b a_{J_1+1} \cdots a_J)(a_J \cdots a_{J_1+1} c d a_{J_1} \cdots a_1) = \frac{1}{2}(N/2)^{J-1}(abcd)$$

Contraction with the color factor of the vertex, $f^{adp}f^{bcp}$ gives, $(N/2)^{J+3}$ as the final color factor. Comparison of this result with the special graph result shows that special graph is indeed at torus level.

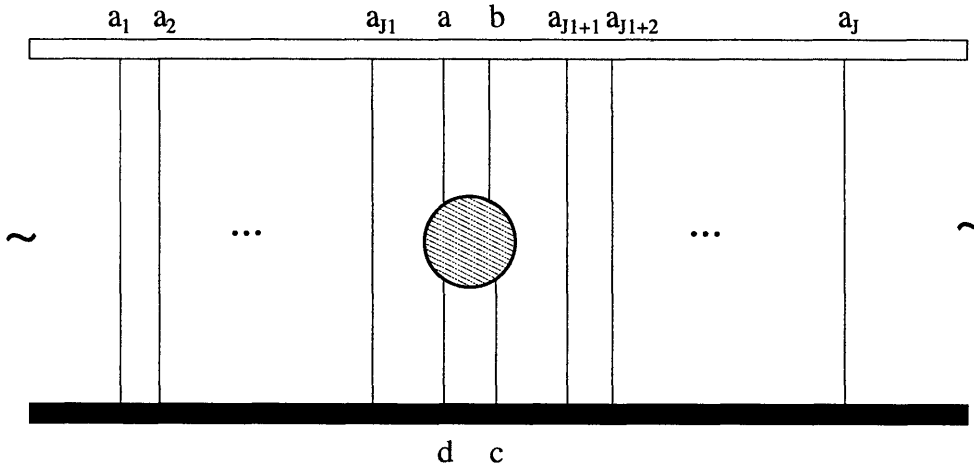


Figure B-2: A planar diagram with same interaction vertex as fig. B-1.

Let us move on to compute the F-term contribution at the planar level. Since we are interested in the anomalous dimension we consider equal momenta, $n = m$ for simplicity. Unlike in the case of D-terms there is a nice algebraic method to tackle with the calculation: Effective operator method [24]. We define the effective operator as the contraction of the vector operator

$$O_\mu^n = \partial_\mu^q(\phi Z^{J+1}) = (\partial_\mu \phi Z^{J+1}) + q \sum_{l=0}^J q^l (\phi Z^l \partial_\mu Z Z^{J-l})$$

with $f^{pab}\bar{Z}^a\phi^b$:

$$\begin{aligned}
O_{eff} &= -i \sum_{m=0}^J ([a, p] Z^m a Z^{J-m}) G \partial_\mu G \\
&- iq \sum_{l=0}^J q^l \sum_{m=0}^{l-1} ([a, p] Z^m a Z^{l-m-1} \partial_\mu Z Z^{J-l}) G^2 \\
&- iq \sum_{l=0}^J q^l \sum_{m=0}^{J-l-1} ([a, p] Z^l a \partial_\mu Z Z^{J-l-m-1} Z^m) G^2 \\
&- iq \sum_{l=0}^J q^l ([a, p] Z^l a Z^{J-l}) G \partial_\mu G.
\end{aligned} \tag{B.2}$$

Planar level contribution arises from the nearest-neighbour interactions, $m = 0, J$ in the first term, $m = 0$ in the second and third terms and $l = 0, J$ in the last term:

$$O_\mu^{eff} = i(q - \bar{q})(N/2)G\partial_\mu G(pZ^J) + iq(q - 1)(N/2)G^2 \sum_{l=0}^{J-1} q^l (pZ^l \partial_\mu Z Z^{J-l-1}) \tag{B.3}$$

where we used (B.1) and $q^{J+2} = 1$. We obtain the two-point function as, $\langle O_\mu^n \bar{O}_\nu^n \rangle = \langle O_\mu^{eff} \bar{O}_\nu^{eff} \rangle$. To compute various terms we will need additional contraction identities,

$$\begin{aligned}
\text{Tr}(Z^a \bar{Z}^a) &= N^{a+1} + \mathcal{O}(N^{a-1}) \\
\text{Tr}(Z^a) \text{Tr}(\bar{Z}^a) &= aN^a + \mathcal{O}(N^{a-2})
\end{aligned} \tag{B.4}$$

which are derived by counting the number of ways one may perform the Wick contractions within each trace structure while obtaining a maximal power of N . Leading order terms show the planar level contributions.

Among the four pieces in $\langle O_\mu^{eff} \bar{O}_\nu^{eff} \rangle$ the term arising from contraction of second term in O_μ^{eff} with second term in \bar{O}_ν^{eff} is the easiest to evaluate. One gets,

$$-(q - \bar{q})^2 \partial_\mu G \partial_\nu G G^J (N/2)^{J+3}. \tag{B.5}$$

Contraction of first term in O_μ^{eff} with second term in \bar{O}_ν^{eff} gives,

$$-(N/2)^2 (q - \bar{q}) q (q - 1) G \partial_\mu G \sum_{l=0}^{J-1} q^l (Z^l \partial_\nu Z Z^{J-l-1} p) (p \bar{Z}^J)$$

$$\begin{aligned}
&= -(N/2)^{J+3}(q - \bar{q})q(q - 1)G\partial_\mu\partial_\nu\left(\sum_{l=0}^{J-1}q^l\right) \\
&= (q - \bar{q})^2\partial_\mu G\partial_\nu G G^J(N/2)^{J+3}.
\end{aligned} \tag{B.6}$$

$$\tag{B.7}$$

The other cross-term yields the same expression hence doubles (B.6). Contraction of first terms of O_μ^{eff} and \bar{O}_ν^{eff} is,

$$G^4\frac{1}{2}(N/2)^2(1 - q)(1 - \bar{q})\sum_{l,l'=0}^{J-1}q^l\bar{q}^{l'}(Z^l\partial_\mu Z Z^{J-l-1}\bar{Z}^{J-l'-1}\partial_\nu\bar{Z}\bar{Z}^{l'}).$$

One can break up the trace into two pieces by contracting $\partial_\mu Z$ with a \bar{Z} in the first group, with $\partial_\nu\bar{Z}$ or with a \bar{Z} in the last group. First possibility gives, (up to the factors in front of the sum)

$$\begin{aligned}
&\frac{1}{2}\partial_\mu G\sum_{p=0}^{J-l'-2}(Z^{J-l-1}\bar{Z}^p)(\bar{Z}^{J-l'-p-2}\partial_\nu\bar{Z}\bar{Z}^{l'}Z^l) \\
&= \frac{1}{4}\partial_\mu G\partial_\nu G\sum_{p=0}^{J-l'-2}\sum_{r=0}^{l-1}(Z^{J-l-1}\bar{Z}^p)(Z^r\bar{Z}^{l'})(Z^{l-r-1}\bar{Z}^{J-l'-p-2}) \\
&= (N/2)^{J-2}\frac{N^3}{4}G^{J-2}\partial_\mu G\partial_\nu G\sum_{l<l'}q^l\bar{q}^{l'}.
\end{aligned}$$

Including the factors in front, one has,

$$(1 - q)(1 - \bar{q})(N/2)^{J+3}G^J\partial_\mu G\partial_\nu G\sum_{l<l'}q^l\bar{q}^{l'}.$$

whereas the second possibility gives,

$$(1 - q)(1 - \bar{q})(N/2)^{J+3}G^{J+1}\partial_\mu\partial_\nu G.$$

A similar calculation shows that third possibility yields,

$$(1 - q)(1 - \bar{q})(N/2)^{J+3}G^J\partial_\mu G\partial_\nu G\sum_{l>l'}q^l\bar{q}^{l'},$$

giving all in all,

$$(N/2)^{J+3} G^{J+2} \left\{ J \frac{2J_{\mu\nu}}{(x-y)^2} + (1+q)(1+\bar{q}) \partial_\mu G \partial_\nu G \right\}. \quad (\text{B.8})$$

Combining the various pieces we have computed, we see that (B.5), (B.6) and the second term in (B.8) cancels out, leaving us with,

$$(N/2)^{J+3} G^{J+2} J \frac{2J_{\mu\nu}}{(x-y)^2}. \quad (\text{B.9})$$

Taking into account the integral over the interaction vertex, (3.37), one arrives at the final contribution of the F-terms,

$$\langle O_\mu^n(x) \bar{O}_\nu^m(y) \rangle_F = -\lambda' n^2 \ln \left((x-y)^2 \Lambda^2 \right) \frac{J_{\mu\nu}(x,y)}{(x-y)^2} G(x,y)^{J+2} \quad (\text{B.10})$$

which exactly equals the sum of the contributions from D-terms, self-energy and external gluons. Therefore total anomalous dimension is twice the dimension in B.10).

One can use the effective operator method also to calculate the F-term contribution to torus anomalous dimension. For that purpose one should keep the second order terms in the expansion of (B.4). This calculation was computed in Appendix D of [24] and one gets the same expression as (3.38).

Appendix C

Disconnectedness of GT correlators

In this appendix we will derive eq. (4.28). A study of the corresponding Feynman diagrams suffice to obtain the leading order scaling of a generic correlator with g_2 and J . Dependence on g_2 of a correlator is fixed by power of N in a Feynman diagram. This can be determined either by direct evaluation of the traces over the color structure (all fields are in adjoint rep. in $\mathcal{N} = 4$ SYM) or by loop-counting. Since we are interested in the leading order g_2 dependence, the latter is easier. Explicit J dependence is determined by working out the symmetry factors in a Feynman diagram. As a warm-up consider the *free* extremal correlation function,

$$C^{i,1} = \langle \bar{O}_n^J : O_m^{J_1} O^{J_2} \dots O^{J_i} : \rangle.$$

Leading order diagram drawn on a plane is shown in Fig C-1. Taking the normalization factor $\sim 1/N^{J+2}$ into account, trivial loop counting teaches us that,

$$C^{i,1} \propto \frac{1}{N^{i-1}} = \frac{g_2^{i-1}}{J^{2i-2}}. \quad (\text{C.1})$$

Now, consider the combinatorics in Fig. C-1 to determine the power of J . Planarity requires Wick contraction of O^{J_i} 's into \bar{O}_n^J as a whole. Fix the position of, say O^{J_2} in \bar{O}_n^J . Then one has to sum over positions of other O^{J_i} operators for $i > 2$ within \bar{O}_n^J obtaining a factor of J^{i-2} . There is a phase summation over positions of ϕ and ψ impurities in \bar{O}_n^J , giving a factor of J^2 . Cyclicity of O^{J_i} , $i > 1$, provides a factor

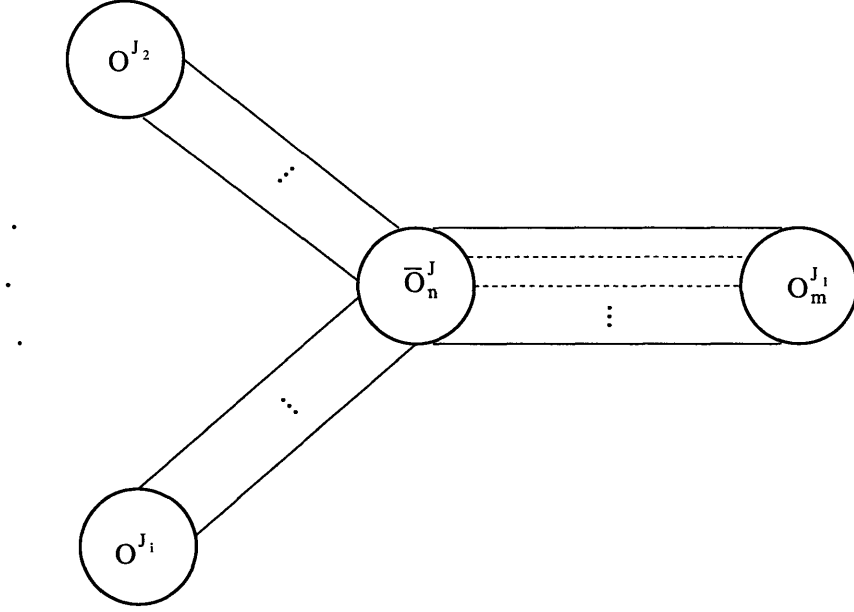


Figure C-1: A typical planar contribution to $C^{1,i}$. Circles represent single-trace operators. Dashed lines denote impurity fields. Z lines are not shown explicitly and represented by “...”.

of J^{i-1} . Taking into account the $J^{-(i+1)/2}$ suppression from the normalization and $\mathcal{O}(J^{-2i+2})$ suppression in (C.1), we learn that,

$$C^{i,1} \sim \frac{g_2^{i-1}}{J^{(i-1)/2}}. \quad (\text{C.2})$$

Next task is to obtain similar information for a general, non-extremal *free* correlator in (4.27). Without loss of generality, one can assume $j \leq i$. There are various connected and disconnected diagrams with different topology. Since the results for disconnected contributions will recursively be included in the fully connected pieces for smaller i and j , it suffices to consider the fully-connected contribution to (4.27). We first ask for the dependence on g_2 for the leading order (planar) fully connected diagram. As an example, a list of all distinct topologies for fully connected $i = 3$, $j = 2$ correlator is shown in Fig. C-2. It is immediate to see that conservation of number of legs for each operator in the correlator (for each node in Fig. C-2) requires that *all planar fully-connected diagrams have same g_2 power* irrespective of the topology (here, by topology we refer to different type of diagrams that are exemplified in

Fig. C-2, not the order in g_2). Then, it is sufficient to count the loops in a connected diagram that is the simplest for loop counting purposes. This simplest diagram is shown in Fig. C-3. Each outer leg in Fig. C-3 represent a bunch of J_s propagators (inner line has $J_1 - J_{i+2} - \dots - J_{i+j} + 2$ propagators). Drawn on a plane, this means that there are a total of $(J + 2) - (i + j - 1) + 1$ loops in Fig. C-3, including the circumference loop. Finally, a factor of N^{J+2} from normalizations and we obtain that,

$$C^{i,j} \propto \frac{1}{N^{i+j-2}} = \frac{g_2^{i+j-2}}{J^{2(i+j-2)}}. \quad (\text{C.3})$$

Apart from the dependence on J coming from singling out the g_2 dependence as above, there are additional contributions from the combinatorics and normalizations. Determination of the power of J from the combinatorics works much as in the case of $C^{1,i}$. Fixing position of one O^{J_i} inside another operator that it connects to, we are left with sum over position of $i + j - 3$ operators. This reasoning holds only for tree-type diagrams like in the first diagrams shown in Fig. C-2.a and Fig. C-2.b.

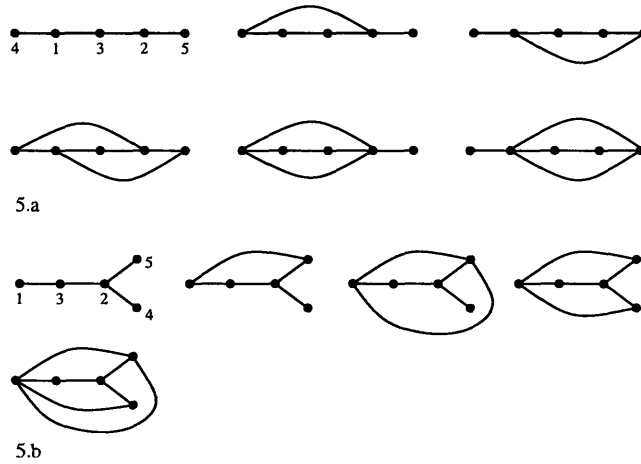


Figure C-2: All distinct topologies of planar Feynman diagrams that contribute to $\langle : \bar{O}_n^{J_1} \bar{O}_m^{J_2} :: O_m^{J_3} O^{J_4} O^{J_5} : \rangle$. Nodes represent the operators while solid lines represent a bunch of Z propagators. Line between the nodes 1 and 3 also include two scalar impurities ϕ and ψ . All other topologies are obtained from these two classes by permutations among 3,4,5 and 1,2 separately. Other planar graphs are obtained from these by moving the nodes within the solid lines without disconnecting the diagram. For example 4 in the first diagram can be moved within the solid line 1-3.

But it is not hard to see that the combinatorial factor for diagrams involving loops

e.g. second diagram in Fig. C-2. is also equal to $i + j - 3$. This is because for each factor that one loses from the sum over positions of O_{J_i} because of the appearance of a loop, one gains a compensating factor of J for the loop summation. Also, cyclicity of BPS type operators within (4.27) provides a factor of J^{i+j-2} . Finally, including the powers of J coming from the normalizations and (C.3) we arrive at the general result,

$$C^{i,j} \sim \frac{g_2^{i+j-2}}{J^{(i+j)/2-1}}. \quad (\text{C.4})$$

Note that this is for the connected contribution to (4.27). To obtain the g_2 and J dependence of disconnected contributions, one simply uses (C.4) for smaller i and/or j which shows that disconnected diagrams have lower powers in g_2 and they are less suppressed by a power of J . For example a disconnected contribution to C^{ij} where the process $i \rightarrow j$ is separated into two disconnected processes, the scaling would be,

$$C^{i,j} \sim \frac{g_2^{i+j-2}}{J^{(i+j)/2-2}}.$$

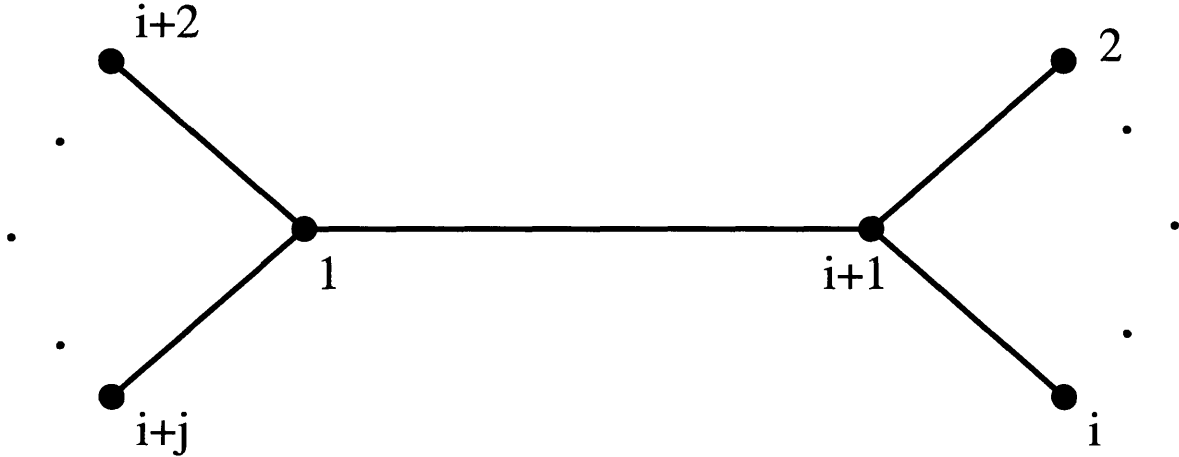


Figure C-3: Simplest connected tree diagram for the loop counting purposes. The solid line between 1 and $i + 1$ includes ϕ and ψ .

With a little more effort one can show that,

theorem 1 *For scalar impurity BMN operators $\mathcal{O}(g_{YM}^2)$ interactions will not change the scaling law of (C.4) at all.*

Let us outline the proof shortly. As a first step, one can show that the only interactions involved in *scalar impurity* BMN operators are coming from F-terms in $\mathcal{N} = 4$ SYM lagrangian. F and D type interaction terms written in $\mathcal{N} = 1$ component notation reads,

$$F \propto (f^{abc} \bar{Z}_b^i Z_c^i)^2, \quad D \propto f^{abc} f^{ade} \epsilon_{ijk} \epsilon_{ilm} Z_b^j Z_c^k \bar{Z}_d^l \bar{Z}_e^m. \quad (\text{C.5})$$

Here, a, \dots are the color indices while i, \dots denote flavor. Note that when one specifies the orientation in a scalar propagator $Z^i \bar{Z}^i$ as from Z to \bar{Z} , these quartic vertices can be represented as in Fig C-5. In [53] it was shown that, correlation functions of BPS type multi-trace operators,

$$\text{Tr}(Z_1^J) \cdots \text{Tr}(Z_r^J) \quad (\text{C.6})$$

do not receive any radiative corrections. To see this one first notes that F-type quartic vertex vanishes when fields are all have the same flavor. Secondly one discovers that contribution of D-type quartic vertex exactly cancels out the contributions from self energies and gluon exchange [53].

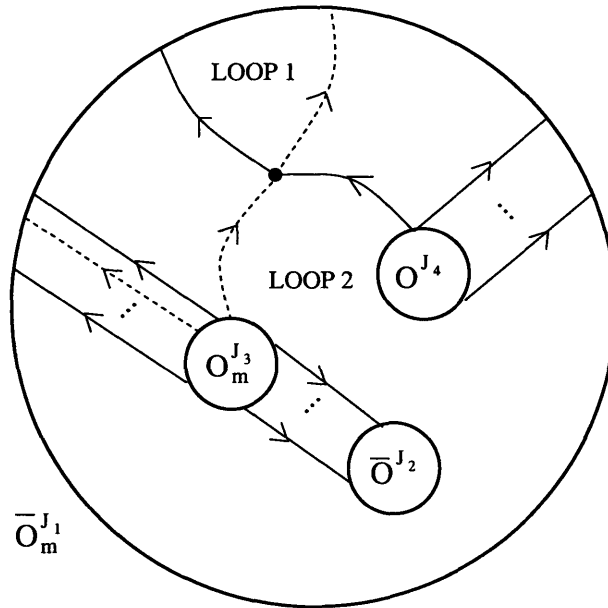


Figure C-4: A quartic interaction in a typical diagram introduce two interaction loops. Here, loop 1 is contractible while loop 2 is non-contractible, therefore this diagram represents a semi-contractible interaction.

Now consider replacing some of the BPS operators in (C.6) with BMN operators,

(2.37). Since the scalar impurities in BMN operators are distinguished from Z fields by their flavor, F-terms are now allowed. However, unlike F-type interactions D-term quartic vertex, gluon exchange and self energies are all flavor blind, therefore one can replace the ϕ and ψ impurities with Z fields for the sake of studying possible contributions from these interactions. After this replacement the phase sum over the position of impurities in O_n^J becomes trivial and factors out of the operator, hence BMN operators reduce to BPS type operators times an overall phase factor. Therefore the theorem of [53] for BMN type multi-trace operators becomes,

theorem 2 *The only radiative corrections to n -point functions of multi-trace BMN operators come from F-type interactions.*

Second step in the proof of theorem 1 is the classification of topologies of Feynman diagrams with one F-term interaction. Any $\mathcal{O}(\lambda')$ interaction that one inserts in (4.27) introduces two “interaction loops” on the plane diagrams. A generic example is shown in Fig. C-4. According to the contractibility of these interaction loops one can classify planar F-term interactions as,

1. *Contractible*: Both interaction loops are contractible,
2. *Semi-Contractible*: Only one of the loops is contractible,
3. *Non-Contractible*: None of the loops are contractible.

Requirement of contractibility means that two incoming lines and two outgoing lines in the F-term vertex of Fig. C-4 i) belong to the same operator and ii) adjacent to each other when drawn on a plane. Now, we note that this classification of interactions would hardly make any difference if we were not dealing with BMN type operators which involve a non-trivial phase summation over the position of the impurity. Structure of the F-term interactions in (C.5) makes it clear that interactions of adjacent lines yield a phase factor

$$1 - e^{\frac{2i\pi n}{J_1}} \sim \frac{1}{J}.$$

Therefore we learn that the phases in BMN operators provide a factor of $1/J^2$ for “contractible” interactions, $1/J$ for “semi-contractible” interactions, $1/J^0$ for “non-contractible” interactions.

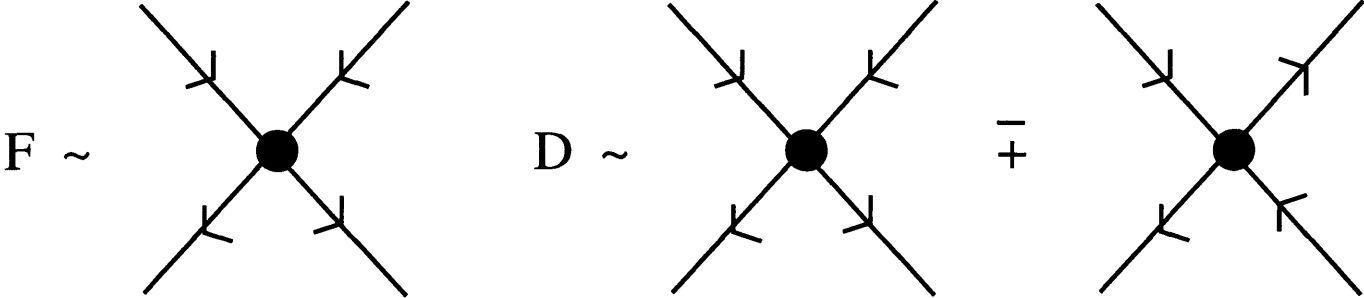


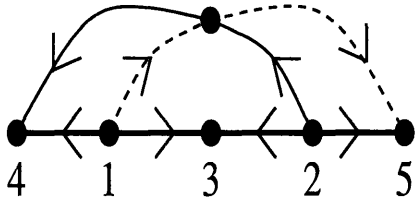
Figure C-5: Orientations of F-term and D-term quartic vertices.

As the last step in our proof of theorem 1, let us show that non-contractibility of each interaction loop supplies another factor of $1/J$. It should be clear from above requirements for contractibility that there are two distinct situations that non-contractibility of an interaction loop can arise:

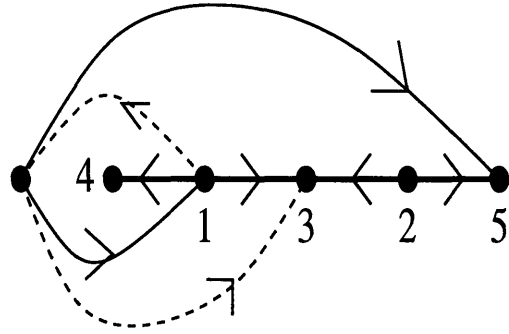
1. the incoming (or outgoing) lines in Fig. C-5 belong to different operators within a multi-trace operator *or*
2. belong to the same operator but are not adjacent to each other.

Let us now recall that among various contributions to the power of J in free correlators, there is a combinatorial factor of J^{i+j-3} coming from summing over positions of the insertions of O^{J_i} operators inside \bar{O}^{J_i} 's. In case 1 above, clearly, one of these position sums will be missing, hence a suppression by $1/J$. On the other hand case 2 can only arise in a situation where there is at least one operator inserted in between the incoming or (outgoing) lines which take place in the interaction. Since the position of this inserted operator is required to have a fixed position in between the interacting legs one also arrives at a suppression by $1/J$. These two situations are illustrated in an example of $G^{3,2}$ in Fig. C-6.

When combined with the powers of J coming from the phase factors that we described above, we see that they compensate each other and one gets a universal factor



9.a



9.b

Figure C-6: In **a** both of the interactions loops are non-contractible due to case 1: incoming and outgoing line pairs of the quartic vertex connect to different operators. In **b** one interaction loop is non-contractible due to case 1 the other due to case 2.

$1/J^2$ for all of the different topologies in an F-term interaction, namely contractible, semi-contractible and non-contractible. Finally note that all interactions come with a factor of $g_{YM}^2 N$. Combined with $1/J^2$ this yields λ' and therefore we concluded the proof of theorem 1: One-loop radiative corrections to (4.27) is of the form,

$$C^{i,j} \sim \frac{g_2^{i+j-2}}{J^{(i+j)/2-1}} \lambda'.$$

The reason that this theorem might fail in case of BMN operators with non-scalar impurities is that D-term interactions might give non-vanishing contributions (see [12]).

Appendix D

Field theory basis change at finite

g_2

Apart from the purely field theoretical task of determining the eigenvalues and eigenoperators of $\Delta - J$, one can ask for the identification of the string basis in field theory for non-zero g_2 [26][27]. For non-zero g_2 , the inner product in field theory becomes non-diagonal in the original basis of BMN where there is an explicit identification of n -string states with n -trace operators. On the other hand, to identify the “string theory basis” in field theory one should require the field theory inner product to be diagonal for all g_2 . However, this requirement alone *does not* uniquely specify the necessary basis change from BMN basis to string theory basis for finite g_2 . One always has the freedom of performing an arbitrary unitary transformation.

In the recent literature, two independent but compatible approaches for the identification of string basis were presented. In the string bit formalism (SBF), it is possible to capture the kinematics and dynamics of gauge theory amplitudes by the discretized theory of bit strings.¹ According to the conjecture of [26], in the string bit language, the basis transformation which takes from BMN basis to string basis for all g_2 reads,

$$|\tilde{\psi}_i\rangle = \left(e^{-\frac{g_2}{2}\Sigma}\right)_{ij} |\psi_j\rangle \equiv (U_\Sigma)_{ij} |\psi_j\rangle \quad (\text{D.1})$$

¹Strictly speaking this has been shown only at $\mathcal{O}(g_2^2\lambda')$ and only for scalar impurities[45].

where ψ_n denotes an n -string state. Here Σ is the sum over all distinct transpositions of two string bits,

$$\Sigma = \frac{1}{J^2} \sum_{mn} \Sigma_{(mn)}.$$

Σ has the effect of a single string splitting or joining, *i.e.* it can map an i string state into an $i \pm 1$ -string state. Note that the transformation matrix $e^{-\frac{g_2}{2}\Sigma}$ is real and symmetric.

Another method [27] which leads an identification of the string basis is simply to find the transformation U which diagonalizes the matrix of inner products between BMN operators, order by order in g_2 . In the *free* theory, we define the following matrix,

$$G_{ij} = \langle \bar{O}_i O_j \rangle.$$

Here n is a collective index for a generic n -trace BMN operator. One identifies the basis transformation, U by requiring that G is diagonal in the new, “string basis”:

$$U_{ik} G_{kl} U_{lj}^\dagger = d_{ij}, \quad \tilde{O}_i \equiv U_{ij} O_j.$$

As in the SBF basis change U is specified up to an arbitrary unitary transformation. One can fix this freedom by requiring that U is real and symmetric. Call this transformation, U_G . Then the solution of the above equation up to $\mathcal{O}(g_2^2)$ reads,

$$U_G = \mathbf{1} + g_2 \left(\frac{1}{2} G^{(1)} \right) + g_2^2 \left(-\frac{1}{2} G^{(2)} + \frac{3}{8} (G^{(1)})^2 \right) + \dots \quad (\text{D.2})$$

where $G^{(i)}$ denotes $\mathcal{O}(g_2^i)$ piece of the metric.

The requirement of reality and symmetry completely fixes the freedom in the choice of the transformation. It was independently shown in [26] and [27] that this simple choice leads to an agreement with string theory calculations. In particular the inner product of a single and double trace operator in the *interacting* theory in this basis, agrees with the cubic string vertex. Recently, [28] also gives evidence for an agreement between the $\mathcal{O}(g_2^2 \lambda')$ eigenvalue of $\Delta - J$ and the matrix element of light cone Hamiltonian in single string sector. Despite the agreement at this order, there

is no reason to believe that this simple choice should hold at higher orders in g_2 or for higher trace multi-trace operators.

Here, we will confine ourselves to checking the compatibility of this basis transformation with free field theory correlators at g_2^2 , including the effects of triple-trace operators. As a bonus we obtain new deconstruction identities decomposing some multi-trace inner products in terms of smaller multi-trace inner products. Since the requirement of reality and symmetry of the basis transformation matrix completely fixes the definition of the new basis, the two prescriptions described above should be equivalent. Equating various matrix elements of U_G and U_Σ we will obtain identities involving free field theory correlators which are subject to should be check in field theory.

The first non-trivial requirement is coming from the single-trace operators at $\mathcal{O}(g_2^2)$,

$$\langle \psi_1 | \tilde{\psi}_1 \rangle_G = \langle \psi_1 | \tilde{\psi}_1 \rangle_\Sigma.$$

LHS is, (we suppress indices labeling a multi trace operator),

$$\langle \psi_1 | U_G | \psi_1 \rangle = 1 + g_2^2 \left(-\frac{1}{2} G^{11} + \frac{3}{8} G^{12} G^{21} \right).$$

G^{11} is the torus level, free single-single correlator with the space-time dependence removed. Similarly G^{12} is $\mathcal{O}(g_2)$ level single-double correlator which is presented in eq. (4.14). RHS reads,

$$\langle \psi_1 | 1 + \frac{1}{2} \left(-\frac{g_2^2}{2} \right)^2 \Sigma^2 | \psi_1 \rangle = \frac{g_2^2}{8} G^{12} G^{21},$$

where we used the fact that Σ changes the string number by ± 1 . Hence we obtain,

$$G_{nm}^{11} = \frac{1}{2} \sum_i G_{n;i}^{12} G_{i;m}^{12}. \quad (\text{D.3})$$

Here i is a collective index labeling either of the two types of double-trace operators which can appear in the intermediate process *i.e.* $i = \{ny\}$ for BMN double-trace

and $i = y$ for BPS double-trace.

This identity indeed holds in the gauge theory as first shown in [54]. With the inverse reasoning we can view this simple calculation as the *derivation* of this non-trivial sum formula. As a next application let us derive identities involving triple trace operators. We require,

$$\langle \psi_3 | \tilde{\psi}_1 \rangle_G = \langle \psi_3 | \tilde{\psi}_1 \rangle_\Sigma.$$

Much as above, $O(g_2^2)$ term in LHS is,

$$-\frac{1}{2}G^{13} + \frac{3}{8}G^{12}G^{23}$$

and the RHS is,

$$\frac{g_2^2}{8} \langle \psi_3 | \Sigma^2 | \psi_1 \rangle = \frac{g_2^2}{8} G^{12} G^{23}.$$

We learn that

$$G^{13} = \frac{1}{2} G^{12} G^{23}.$$

Notice that “2” in the intermediate step can not be a BPS double-trace operator, because the lowest order G^{23} between a BPS double-trace and a BMN triple trace is at $\mathcal{O}(g_2^3)$.² Therefore we arrive at the formula,

$$G_{m;nyz}^{13} = \frac{1}{2} \sum_{py'} G_{m;py'}^{12} G_{py';nyz}^{23}. \quad (\text{D.4})$$

The single-triple correlation function G^{13} is computed in Appendix F. Again this identity is subject to check by a direct field theory computation. This is done in Appendix E and (D.4) passes the test. A similar calculation with the requirement

²It is easy to see (either by using trace algebra or by counting the loops in Feynman diagrams) that there exists only *disconnected* $\mathcal{O}(g_2)$ contributions to any double-triple correlator where the 2-3 correlator separates as 1-2, and 1-1. This obviously cannot happen for a correlation function of a BPS double-trace operator and a BMN triple-trace operator.

$\langle \psi_2 | \tilde{\psi}_2 \rangle_G = \langle \psi_2 | \tilde{\psi}_2 \rangle_\Sigma$, one reaches at another useful identity,

$$G_{my;m'y'}^{22} = \frac{1}{2} \left(\sum_n G_{my;n}^{12} G_{n;m'y'}^{12} + \sum_i G_{my;i}^{23} G_{i;m'y'}^{23} \right). \quad (\text{D.5})$$

Here $i = \{ny''z''\}$ or $i = \{y''z''\}$ for BMN and BPS triple-trace operators. An expression for the free $\mathcal{O}(g_2^2)$ double-double correlator, G^{22} , is given in eq. (4.43) We also checked this by direct computation in Appendix E. We emphasize that these are highly non-trivial identities viewed as representation of a trigonometric function, say G^{13} in (4.17) as an infinite series of products of simpler functions. In comparison to (D.3) the non-triviality comes from the fact that summands are trigonometric functions rather than rational functions as in the RHS of (D.3). These identities will prove extremely useful for the computations of the next sections. Finally we note immediate generalizations,

$$\begin{aligned} G^{m,m+2} &= \frac{1}{2} G^{m,m+1} G^{m+1,m+2} \\ G^{mm} &= \frac{1}{2} \left(G^{m,m-1} G^{m-1,m} + G^{m,m+1} G^{m+1,m} \right). \end{aligned}$$

Appendix E

Sum formulas

Let us first reproduce the matrices $A_{mm'}$ and $B_{mm'}$ that appear in the $\mathcal{O}(g_2^2)$ and $\mathcal{O}(g_2^2\lambda')$ pieces of the single-trace two-point function. These were defined in [24]:

$$A_{m,n} = \begin{cases} \frac{1}{24}, & m = n = 0; \\ 0, & m = 0, n \neq 0 \text{ or } n = 0, m \neq 0; \\ \frac{1}{60} - \frac{1}{6u^2} + \frac{7}{u^4}, & m = n \neq 0; \\ \frac{1}{4u^2} \left(\frac{1}{3} + \frac{35}{2u^2} \right), & m = -n \neq 0; \\ \frac{1}{(u-v)^2} \left(\frac{1}{3} + \frac{4}{v^2} + \frac{4}{u^2} - \frac{6}{uv} - \frac{2}{(u-v)^2} \right), & \text{all other cases} \end{cases} \quad (\text{E.1})$$

and

$$4\pi^2 B_{m,n} = \begin{cases} 0, & m = n = 0; \\ \frac{1}{3} + \frac{10}{u^2}, & m = n \neq 0; \\ -\frac{15}{2u^2}, & m = -n \neq 0; \\ \frac{6}{uv} + \frac{2}{(u-v)^2}, & \text{all other cases} \end{cases} \quad (\text{E.2})$$

where $u = 2\pi m, v = 2\pi n$.

The rest of this appendix outlines the computation of non-trivial summations that appear along the computations in sections 4-2, 4-3, 4-5 and the previous appendix. We will first prove that (D.4) and (D.5) indeed hold in GT. These were obtained in the previous appendix simply by equating the basis transformations U_Σ and U_G . A second task is to derive (4.26) of section 4. Finally we will define and evaluate the

last term in (4.51) of section 5.

We reproduce (D.4) here for completeness:

$$G_{m;nyz}^{13} = \frac{1}{2} \sum_{py'} G_{m;py'}^{12} G_{py';nyz}^{23}. \quad (\text{E.3})$$

LHS of (E.3) is computed in Appendix F and presented in eq. (4.16). G^{23} that appear on the RHS gets $\mathcal{O}(g_2)$ contributions only from disconnected diagrams as $2 \rightarrow 3$ decouples as, $1 \rightarrow 2$ and $1 \rightarrow 1$. This quantity is also computed in Appendix F, result is given in (4.19). One gets two contributions to RHS of (E.3) from first and second pieces in (4.19). Second contribution gives,

$$\frac{1}{2} \int_0^1 dy' \sum_{p=-\infty}^{\infty} G_{m,py'}^{12} \frac{g_2}{\sqrt{J}} d_{np} d_{yy'} \sqrt{(1-y)z\bar{z}} = \frac{1}{2} \frac{g_2}{\sqrt{J}} \sqrt{(1-y)z\bar{z}} G_{m,ny}^{12}. \quad (\text{E.4})$$

First piece in G^{23} gives,

$$\frac{1}{2} \sqrt{\frac{z\bar{z}}{y}} \int_0^1 dy' y'^3 (d_{y',y+z} + d_{y',y+\bar{z}}) \frac{\sin^2(m\pi y')}{\pi^4} \left\{ \sum_{p=-\infty}^{\infty} \frac{\sin^2(p\pi y/y')}{(p-my')^2 (p-ny'/y)^2} \right\}. \quad (\text{E.5})$$

We will now describe the evaluation of the sum in this expression. Let us separate the sum into two pieces as,

$$S = S_1 + S_2 \equiv \sum_{p=-\infty}^{\infty} \frac{1}{(p-a)^2 (p-b)^2} - \sum_{p=-\infty}^{\infty} \frac{\cos^2(px)}{(p-a)^2 (p-b)^2}, \quad (\text{E.6})$$

where we defined,

$$x \equiv \pi y/y', \quad a \equiv my', \quad b \equiv ny'/y.$$

S_1 is easy to evaluate (can be done with a computer code) and the result is,

$$S_1 = \frac{1}{(a-b)^3} \left(2\pi \cot(\pi a) - 2\pi \cot(\pi b) + \frac{(a-b)\pi^2}{\sin^2(\pi a)} + \frac{(a-b)\pi^2}{\sin^2(\pi b)} \right). \quad (\text{E.7})$$

It is not possible to evaluate S_2 neither with a well-known computer program nor it can be found in standard tables of infinite series (like Gradhsteyn-Rhyzik or Prudnikov).

To tackle with it we reduce it into a product of two sums as,

$$\begin{aligned} S_2 &= \frac{d^2}{dad b} \left(\sum_{p=-\infty}^{\infty} \frac{\cos(px)}{(p-a)} \right) \left(\sum_{r=-\infty}^{\infty} \frac{\cos(rx)}{(r-b)} d_{pr} \right) \\ &= \frac{d^2}{dad b} \frac{1}{2\pi} \int_0^{2\pi} dt \left(\sum_{p=-\infty}^{\infty} \frac{\cos(px)e^{ipt}}{(p-a)} \right) \left(\sum_{r=-\infty}^{\infty} \frac{\cos(rx)e^{-irt}}{(r-b)} \right), \end{aligned}$$

where in the second step we used the integral representation of d_{pr} . Expanding the exponentials in terms of cos and sin we now reduced the sum into sums of the following form,

$$\sum_{p=-\infty}^{\infty} \frac{\cos(p(x \pm t))}{p-a} = -\frac{1}{a} + 2a \sum_{p=1}^{\infty} \frac{\cos(p(x \pm t))}{p^2 - a^2} = -\frac{1}{a} + 2af_m(x \pm t, a). \quad (\text{E.8})$$

We can read off the function $f_m(z, a)$ from *e.g.* [55],

$$f_m(z, a) = \frac{1}{2a^2} - \frac{\pi \cos(a(z - (2m+1)\pi))}{2a \sin(\pi a)}, \quad (\text{E.9})$$

where m is an integer defined as, $2\pi m \leq z \leq 2\pi(m+1)$. With the given information it is straightforward to evaluate these sums. Integrating over t and combining with S_1 in (E.7), one gets,

$$\begin{aligned} \sin^2(\pi a)S &= \frac{\pi}{2(a-b)^3} [\sin(2\pi a) - \sin(2ax) - \sin(2a(\pi-x))] \\ &+ \frac{\pi}{(a-b)^2} [x \sin^2(\pi a) + x \sin^2(a(\pi-x)) + (\pi-x) \sin^2(ax)]. \end{aligned}$$

We insert this expression into (E.5), carry out the trivial integration over y' . Using the definitions of x , a and b given above one gets,

$$\begin{aligned} &-\frac{\pi}{2(m-k)^3} \{\sin(2\pi mz) + \sin(2\pi m\bar{z}) + \sin(2\pi my)\} + \frac{\pi^2}{(m-k)^2} y(\sin^2(\pi mz) + \sin^2(\pi m\bar{z})) \\ &+ \frac{\pi^2}{2(m-k)^2} (1-y) \sin^2(\pi my), \end{aligned}$$

where $k = n/y$. Comparison of this expression with (4.16) shows that this expression

equals,

$$G_{m;nyz}^{13} - \frac{g_2}{2} \sqrt{\frac{z\bar{z}(1-y)}{J}} G_{m,ny}^{12}$$

Adding up to this the first contribution in (E.4) we proved (E.3).

Now, let us move on the proof of the second decomposition identity, (D.5) that we reproduce here,

$$G_{m,y;m',y'}^{22} = \frac{1}{2} \left(\sum_n G_{m,y;n}^{12} G_{n;m'y'}^{12} + \sum_i G_{m,y;i}^{23} G_{i;m'y'}^{23} \right). \quad (\text{E.10})$$

As mentioned before, there are disconnected and connected contributions to both LHS and RHS of this equation. Since connected contributions differ from the disconnected ones by a factor of $1/J$, one should match $\mathcal{O}(1)$ and $\mathcal{O}(1/J)$ pieces on both sides separately. Here we will present the equality of $\mathcal{O}(1)$ parts of LHS and RHS and leave the question of $\mathcal{O}(1/J)$ pieces for future. We did not need $\mathcal{O}(1/J)$ terms anywhere in our computations. $\mathcal{O}(g_2^2)$ disconnected contribution to G^{22} is just

$$\langle \bar{O}_n^{J_1} O_m^{J_3} \rangle_{g_2^0} \langle \bar{O}^{J_2} O^{J_4} \rangle_{g_2^0}$$

plus

$$\langle \bar{O}_n^{J_1} O_m^{J_3} \rangle_{g_2^0} \langle \bar{O}^{J_2} O^{J_4} \rangle_{g_2^0}.$$

All required terms here were already computed in the literature (see [22][24]) and the total result is,

$$g_2^2 \left(y^4 A_{mm'} + \frac{d_{mm'}}{24} (1-y)^4 \right).$$

Turning to the RHS of (E.10) now, we first note that $2 \rightarrow 1 \rightarrow 2$ process can not be disconnected hence does not contribute at this order. Evaluation of the second term in RHS is straightforward by using (4.19) that is derived in the next appendix. The triple-vertex that appears in the intermediate step can either be a BMN or a BPS operator. Let us first consider the former case. We need to compute,

$$G_{m_y;pst}^{23} G_{p'st,m'y'}^{23} = \left(y^{3/2} G_{m;ps/y}^{12} (d_{y,s+t} + d_{y,1-t}) + \frac{g_2}{\sqrt{J}} d_{mp} d_{ys} \sqrt{(1-y)t\bar{t}} \right)$$

$$\times \left(y'^{3/2} G_{m',ps/y'}^{12} (d_{y',s+t} + d_{y',1-t}) + \frac{g_2}{\sqrt{J}} d_{m'p} d_{y's} \sqrt{(1-y')t\tilde{t}} \right),$$

where one sums over pst . When last term in the first parenthesis goes with the last term of the second we have the expression,

$$\frac{g_2^2}{J} \sum_{p=-\infty}^{\infty} d_{pm} d_{pm'} (J \int_0^1 ds) \left(\frac{J}{2} \int_0^{1-y} dt \right) d_{sy} d_{sy'} \sqrt{(1-y)(1-y')t(1-y-t)} = d_{yy'} d_{mm'} \frac{(1-y)^4}{24}, \quad (\text{E.11})$$

where in the integral over t we divided by a factor of 2 to reconcile with the double-counting (note that $t \rightarrow 1-t$ is not distinguishable at the level of Feynman diagrams when triple trace is BPS, and one should divide out the symmetry factor). When first term in the first parenthesis goes with second or third terms of the second, both of the integrals over s and t are constraint by the delta-functions and one gets a $1/J$ suppression. A similar remark apply the case when second goes with third. Therefore we see that all cross terms are suppressed and only other non-vanishing contribution comes by matching second with second and third with third. This is,

$$\frac{1}{2} 2 (yy')^{3/2} d_{yy'} \sum_{p=-\infty}^{\infty} \int_0^y ds G_{m,ps/y}^{12} G_{m',ps/y'}^{12} = y^4 \sum_{p=-\infty}^{\infty} \int_0^1 dx G_{m,px}^{12} G_{m',px}^{12}$$

where we again divided out a similar symmetry factor. It is easy to see that when the intermediate triple-trace operators are BPS type one gets the expression,

$$y^4 \sum_{p=-\infty}^{\infty} \int_0^1 dx G_{m,x}^{12} G_{m',x}^{12}$$

instead of the above expression. Adding these two up and using (D.3), one gets $2y^4 G_{mm'}^{11}$. Combining it with the contribution from (E.11) and comparing with (4.43) for the case of $i = 2$ we proved (D.5) at the leading order.

Next, we shall present two new ‘‘interacting level’’ decomposition identities which are essentially the analogs of the identities given in Appendix F of [29]:

$$\sum_{p,y'} \frac{p}{y'} G_{n,py'} G_{py',myz} = \left(n + \frac{m}{y} \right) G_{n,myz}, \quad (\text{E.12})$$

$$\sum_{p,y'} \frac{p^2}{y'^2} G_{n,py'} G_{py',myz} = (n^2 + (\frac{m}{y})^2) G_{n,myz} + B_{n,myz}^{13} \quad (\text{E.13})$$

where B^{13} is given in (4.18). These identities can easily be proven by the methods described above.

As an application of these decomposition identities let us prove (4.22). For notational simplicity we will not show the indices fully in the following *e.g.* we denote Γ_n^{myz} as Γ_1^3 , etc. Eq. (4.23) gives,

$$\begin{aligned} \Gamma_1^3 &= G^{33}\Gamma_{31} + G^{32}\Gamma_{21} + G^{31}\Gamma_{11} \\ &= \frac{1}{2} \frac{m}{y} (\frac{m}{y} - n) G^{13} + \frac{1}{2} B^{13} - \frac{1}{2} \sum_{p,y'} \frac{p}{y'} (\frac{p}{y'} - n) G^{12} G^{23}. \end{aligned}$$

where the second line follows after trivial algebra. Now, using (D.4), (E.12) and (E.13) it is immediate to see that

$$\Gamma_1^3 = 0.$$

Let us now describe the evaluation of (4.26) in section 2. We separate the LHS of (4.26) into two parts as,

$$\sum_p (-nA(p) + B(p)) \equiv \sum_p \left(-n \frac{\sin^2(\pi py/y')}{(n - p/y')^2 (n^2 - (p/y')^2)} + \frac{\sin^2(\pi py/y')}{(n - p/y')^3} \right). \quad (\text{E.14})$$

Evaluation of $\sum_p B(p)$ is easier. It can be written as,

$$\sum_p B(p) = \frac{y'^3}{2} \left(- \sum_{p=-\infty}^{\infty} \frac{1}{(p-a)^3} + \frac{1}{2} \frac{d^2}{da^2} \left\{ 2a \sum_{p=1}^{\infty} \frac{\cos(px)}{p^2 - a^2} - \frac{1}{a} \right\} \right).$$

Each of the sums can be found in standard tables such as [55] and the result is,

$$\sum_p B(p) = \pi^3 y^2 y' \cot(\pi n y'). \quad (\text{E.15})$$

To compute $\sum_p A(p)$ we write it as,

$$A(p) = \frac{y'^4}{2} \left(\frac{\cos(px)}{(p-a)^2 (p^2 - a^2)} - \frac{1}{(p-a)^2 (p^2 - a^2)} \right).$$

Second can be done by a standard computer code. First can be written as,

$$\sum_p \frac{\cos(px)}{(p-a)^2(p^2-a^2)} = -\frac{1}{a^4} + \left(\frac{d^2}{dx^2} + a^2\right) \frac{d^2}{db^2} \sum_{p=1}^{\infty} \frac{\cos(px)}{(p^2-b)}$$

where $b = \sqrt{a}$. This can be looked up in [55]. Combining the result with (E.15) one obtains (4.26).

Appendix F

Computation of G^{13} , G^{23} , Γ^{13} and Γ^{23}

We will first describe the evaluation of free planar single-triple correlator at the planar level, $\langle \bar{O}_n^J : O_m^{J_1} O^{J_2} O^{J_3} \rangle$. We will refer to the operators that appear in this expression as “big operator”, “operator 1”, “operator 2” and “operator 3”, respectively. Let us also denote the ratios of the “sizes” of these operators by

$$y = \frac{J_1}{J}, \quad z = \frac{J_2}{J}, \quad \tilde{z} = \frac{J_3}{J}. \quad (\text{F.1})$$

Since the space-time dependence of two-point functions of scalar operators is trivial we will only be interested in the coefficient that multiplies the space-time factors, *i.e.* G^{13} and Γ^{13} . Nevertheless, let us show the space-time factors here, for completeness. For the free case it is just product of $J + 2$ scalar propagators,

$$\frac{1}{(4\pi^2 x^2)^{J+2}}.$$

In case of one-loop interactions, one needs to perform the following interaction over the position of the vertex,

$$\frac{1}{16\pi^4} \int \frac{d^4 y}{y^4 (y-x)^4} = \frac{\ln(\Lambda^2 x^2)}{8\pi^2 x^4}.$$

Therefore the space-time dependence at $\mathcal{O}(\lambda')$ is,

$$\frac{1}{8\pi^2(4\pi^2x^2)^{J+2}} \ln(\Lambda^2x^2).$$

Let us now describe the evaluation of the coefficients that multiply these space-time factors.

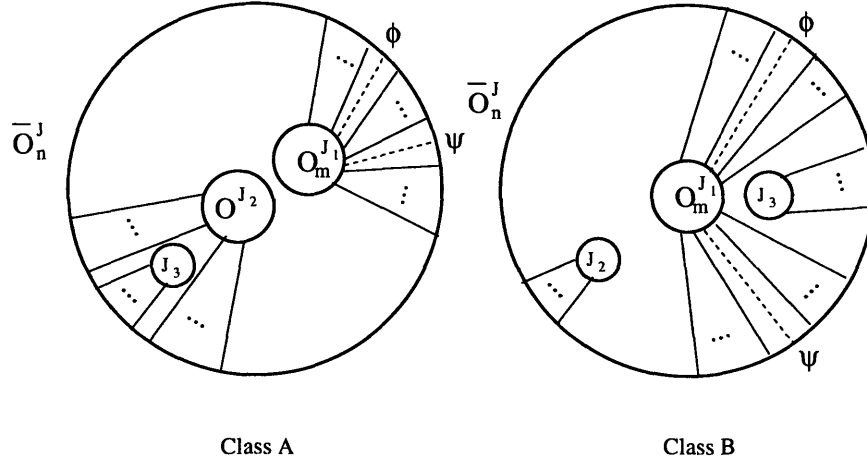


Figure F-1: Two different classes of free diagrams. Dashed lines denote propagators of impurity fields.

General strategy is first to fix the position of one operator, say 2 inside the big operator. Then we are left with phase sums over positions of both of the impurities and the position of operator 3 inside the big operator. Of course one still has to take into account the cyclicity of 2 and 3 which yield a multiplicative factor of J_2J_3 . After fixing the position of 2, we can divide the planar diagrams into two classes.

In **class A** (see Fig. F-1.) operator 2 is “outside” the bunch of lines connecting operator 1 to operator the big operator, hence the phase sum over ϕ and ψ is trivial:

$$J_1^2 \int_0^1 da \int_0^1 db e^{2i\pi(m-ny)a} e^{-2i\pi(m-ny)b} = \frac{\sin^2(2\pi ny)}{\pi^2(ny - m)^2}.$$

One also has to sum over the position of operator 3 “under” 2 and position of operator 2 “under” 3. This gives a combinatorial factor of $J_2 + J_3$. As apparent from Fig. A-. class A is equivalent to single-double correlator up to the aforementioned overall

combinatorial factor. Therefore the left diagram in Fig. A-1. equals,

$$G_A^{13} = \frac{g_2^2}{J} (1-y) \sqrt{\frac{z\bar{z}}{y}} \frac{\sin^2(2\pi ny)}{\pi^2(n-k)^2} \quad (\text{F.2})$$

where we took into account the normalization of operators and defined $k \equiv m/y$.

In **class B** (see Fig. A-1), operator 3 is inserted inside the bunch of lines connecting 1 to the big operator, hence the phase summations become non-trivial. One fixes the position of 2 inside the bunch, then sums over the positions of ϕ and ψ . As one impurity jumps over operator 3 one gets an enhancement in the phase of the big operator by a factor of $-2\pi in\bar{z}$. One evaluates the sums taking this point into account, than one sums over the position of operator 2. This procedure gives,

$$G_B^{13} = \frac{g_2^2}{\pi^2 J} \sqrt{\frac{z\bar{z}}{y}} \frac{1}{(n-k)^2} \left(y(\sin^2(\pi nz) + \sin^2(\pi n\bar{z})) - \frac{1}{2\pi(n-k)} (\sin(2\pi ny) + \sin(2\pi nz) + \sin(2\pi n\bar{z})) \right). \quad (\text{F.3})$$

Adding up (F.2) and (F.3) gives eq. (4.16)¹

There are two consistency checks that one can perform. First of all -as apparent from the diagrams- the final expression should be symmetric in $J_2 \leftrightarrow J_3$.(4.16) nicely passes this test. A more non-trivial test is to check whether G^{13} reduces to G^{12} as one takes $J_3 \rightarrow 0$. Straightforward algebra shows that,

$$G_{n,myz}^{13} \rightarrow \sqrt{\frac{\bar{z}}{J}} G_{n,my}^{12}$$

and confirms our expectation.

Now let us discuss how to add interactions to Figs. A-1, by preserving *planarity*. As already mentioned for the evaluation of general correlators in Appendix C, there are three distinct classes of planar interactions: *contractible*, *semi-contractible* and *non-contractible*. Above we noted that evaluation of class A diagrams are completely

¹We thank Neil Constable who computed this quantity by a completely different method (direct evaluation of the traces over the color structure and extracting out the $\mathcal{O}(g_2^2)$ piece) and who obtained the same result.

equivalent to single-double correlator. This continues to be the case when one introduces planar interactions. There are only contractible and semi-contractible contributions in this case and since $\mathcal{O}(\lambda')$ corrections to this correlator was already computed in [29] (that we reproduced in eq. (4.15)), we will only show the final result,

$$\text{Class A interactions} \Rightarrow \frac{g_2^2 \lambda'}{J \pi^2} (1-y) \sqrt{\frac{z \bar{z}}{y}} \frac{\sin^2(2\pi n y)}{\pi^2 (n-k)^2} (k^2 - nk + n^2). \quad (\text{F.4})$$

Let us explain the evaluation of interactions in class B in some detail. Contractible interactions are coming from the situation where an impurity interacts with its nearest-neighbor in such a way that both interaction loops are contractible. As described in Appendix C this gives a phase factor of

$$(1 - e^{-\frac{2i\pi n}{J}})(1 - e^{\frac{2i\pi m}{J_1}}) \approx \frac{4\pi^2}{J^2} nk \quad (\text{F.5})$$

for each possible nearest-neighbour interaction. One should sum over the insertions of this interaction between all adjacent line pairs between operator 1 and the big operator in Fig. A-1.b, *except* the particular position when this line pair coincides with the position of operator 3. In this particular case one gets a semi-contractible diagram (see Fig. A-2.a). This sum procedure obviously gives the phase factor in (F.5) times (F.3).

Semi-nearest interactions in class B arise in two possible ways. First possibility is already mentioned above and shown in Fig. A-2.a. Another possibility arise when one of the interaction loops is non-contractible for another reason: the line pair that is incoming to the vertex connect to different operators. This is illustrated in Fig. A-2.b. Evaluation of the phase factors in both of these cases is simple:

In case 1, when one takes all possible orderings of the interacting pairs of lines, one gets a factor of

$$(1 - e^{2i\pi n \bar{z}})(1 - e^{-\frac{2i\pi m}{J_1}})$$

in place of (F.5). Next, one has to sum over all possible positions of operator 3 in Fig. A-2.a. Finally one evaluates the phase sum over ψ . There is an analogous

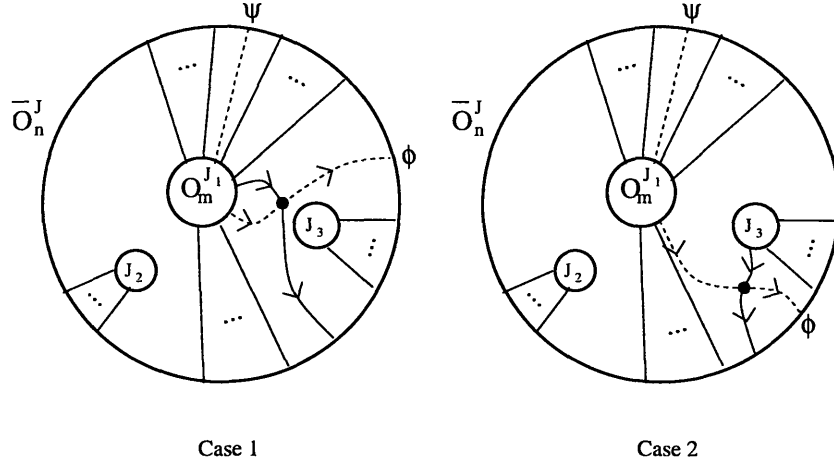


Figure F-2: Two different types of semi-contractible diagrams. One should also consider the cases when two incoming and outgoing lines are interchanged. Also analogous contributions come from exchanging operator 2 with operator 3.

contribution where ψ impurity takes place in the interaction instead of ϕ . But that is obviously obtained from the former just by taking the complex conjugate.

In case 2, Fig. A-2, one has to sum over the possibilities where ϕ interacts with the leftmost and the rightmost Z line in operator 3. Considering also the two different orderings of the ϕ and Z that are outgoing from the vertex, one obtains an overall phase factor of,

$$(1 - e^{-\frac{2i\pi n}{J}})(1 - e^{2i\pi n \bar{z}}).$$

Next, just as in the case 1 above, one sums over all possible insertions of operator 3 and positions of ψ impurity. Similarly one considers the conjugate case where ψ takes place in the interaction instead of ϕ . Finally one gets similar expressions to the ones obtained in case 1 and case 2 by exchanging the roles played by operator 3 and operator 2.

Combining all of the results above, namely both contractible and semi-contractible contributions in class A given in (F.4), contractible contributions in class B and all semi-nearest contributions in class B, one obtains a surprisingly simple expression. All of the factors conspire to give,

$$\Gamma_A^{13} + \Gamma_{B,cont.}^{13} + \Gamma_{B,semi-cont.}^{13} = \lambda'(n^2 - nk + k^2)G^{13}. \quad (\text{F.6})$$

A few observations are in order. Notice that one obtains the same form for the interacting single-double correlator as shown in [29], see eq. (4.15). The proportionality to G^{12} (or G^{13} in our case) is obvious from the beginning. Because eventually, the effect of interactions is to dress the free expression with an overall phase factor. The surprise is that this phase factor,

$$n^2 - nk + k^2,$$

is the same in the cases of single-double and single-triple correlators! One appreciates the non-triviality of this after seeing the delicate conspiring of many different terms in our case. We also see the same phase dependence, in case of double-triple correlator, eq. (4.21). It is tempting to believe that this remains to be true in case of general i -trace j -trace correlator. Namely we believe that the result of contractible and semi-contractible interactions at $\mathcal{O}(\lambda')$ for more general extremal correlators can be summarized as,

$$\Gamma_{cont.+semi-cont.}^{i,j} = \lambda'(n^2 - nk + k^2)G^{i,j}.$$

Actually it suffices to see this behaviour in case of extremal correlators of the type $\Gamma^{1,i}$ since $\Gamma^{i,j}$ can be related to this by the disconnectedness argument.

However, this is not the whole story. There is a very important new class of planar diagrams which contributes to G^{13} : *non-contractible* diagrams. This was absent in the case of Γ^{12} because there was not enough number of operators to create this new interaction topology. This will become clear in the following.

We show all possible non-contractible diagrams in Fig. A-3. Note that both of the interaction loops are non-contractible in this case. The loop formed by incoming lines is non-contractible because they belong to different operators. The loop formed by the outgoing lines is non-contractible because there is an operator inserted between them. This exemplifies our schematic discussion about the non-contractibility of planar diagrams in Appendix C where we referred to these possibilities as case 1 and 2. At first sight one expects that these diagrams be suppressed by a factor of $1/J^2$ when compared with the contractible diagrams or by a factor of $1/J$ when

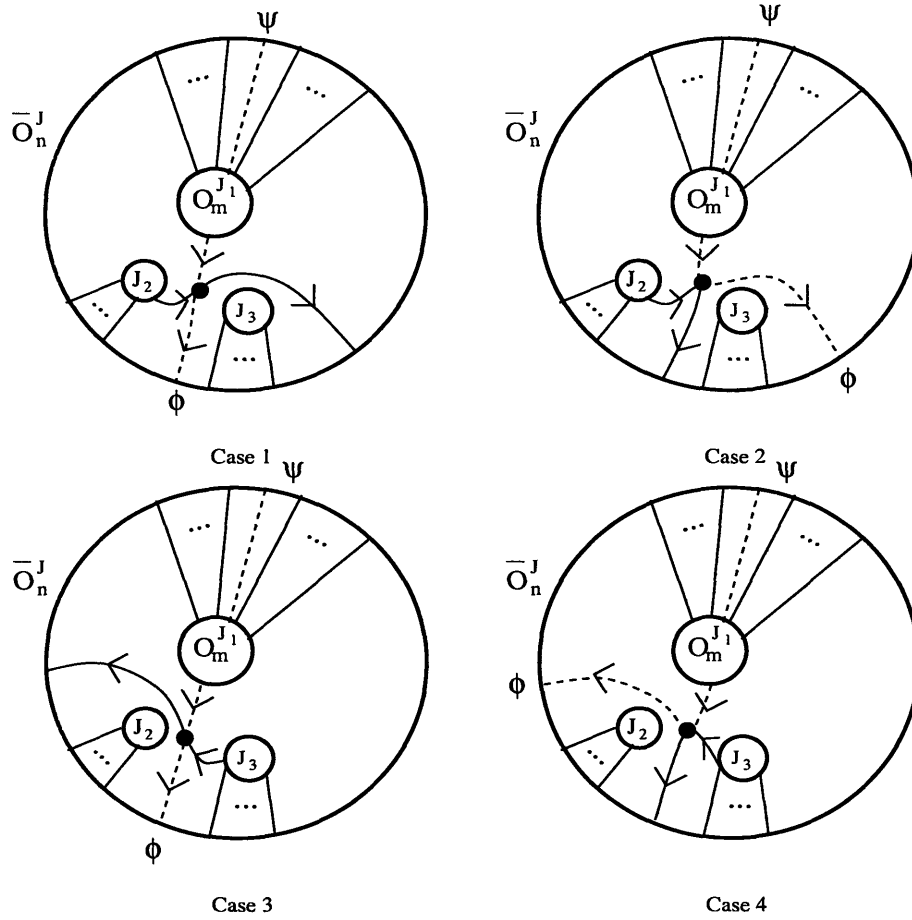


Figure F-3: Contributions from non-contractible planar interactions. There are four more diagrams which are obtained by exchanging operator 2 with operator 3.

compared with the semi-contractible diagrams, because the sums over the position of the operator 3 and the position of ϕ impurity are missing. However as noted in the general discussion of Appendix C, there is a compensating enhancement coming from the overall phase factors associated with these diagrams, namely the $O(1/J^2)$ phase suppression given by (F.5) is absent. Therefore these diagrams are on the equal footing with the rest *i.e.* (F.6).

The evaluation of non-contractible diagrams is the simplest. One adds up all possible contributions that are displayed in Fig. A-3, and include the analogous cases where one interchanges operator 2 with operator 3. Finally one performs the phase summation over ψ . Adding this result with the conjugate one which is obtained by interchanging the roles of ϕ and ψ , one gets (4.18).

Adding up (4.18) with (F.6), one obtains the total $\mathcal{O}(g_2^2 \lambda')$ single-triple correlator, (4.17). Again, there are two consistency checks that one can perform. Firstly it is easy to see that, (4.17) is symmetric in $J_2 \leftrightarrow J_3$. Secondly when one takes the limit $J_3 \rightarrow 0$, B^{13} vanishes (as it should) and the rest of the expression boils down to the single-double result,

$$\Gamma^{13} \rightarrow \sqrt{\frac{z}{J}} \Gamma^{12}.$$

Let us now explain the computations that lead to the expressions in (4.19) and (4.21). When compared with the evaluation of single-triple correlators, evaluation of lowest order G^{23} and Γ^{23} is almost trivial. This is because only the disconnected diagrams contribute to these correlators at $\mathcal{O}(g_2)$. We now describe the evaluation of G^{23} . It will suffice to describe possible ways that $2 \rightarrow 3$ correlator can be separated into $1 \rightarrow 1$ and $1 \rightarrow 2$. Consider the correlator $\langle : \bar{O}_n^{J_1} \bar{O}^{J_2} :: O_m^{J_3} O^{J_4} O^{J_5} : \rangle$ define the ratios of lengths of the operators,

$$y = \frac{J_1}{J}, \quad y' = \frac{J_3}{J}, \quad z' = \frac{J_4}{J}, \quad \tilde{z}' = \frac{J_5}{J}. \quad (\text{F.7})$$

Since the impurity fields in operator 1 and operator 3 should be Wick contracted with each other, the only disconnected contributions arise when,

1. 1 connects to 3, 2 connects to 4 and 5,
2. 1 connects to 3 and 4, 2 connects to 5,
3. 1 connects to 3 and 5, 2 connects to 4.

A simple loop counting shows that all other contractions will result in higher orders in g_2 . Cases 2 and 3 are easily expressible in terms of the results already reported in the literature, (see [24]). Therefore we only show case 1 which turns out to be the simplest,

$$\langle : \bar{O}_n^{J_1} \bar{O}^{J_2} :: O_m^{J_3} O^{J_4} O^{J_5} : \rangle_1 = \langle \bar{O}_n^{J_1} O_m^{J_3} \rangle \langle \bar{O}^{J_2} : O^{J_4} O^{J_5} : \rangle,$$

where one needs the lowest order contributions to the correlators on RHS. First one is just d_{nm} . One evaluates the BPS correlator above by noting that the cyclicity factor

of $J_2 J_4 J_5$ and the normalizations; hence one gets,

$$\frac{g_2}{\sqrt{J}} \sqrt{(1-y)z'\bar{z}'}$$

Combining this contribution with cases 2 and 3, one easily obtains, (4.19).

Computation of Γ^{23} at the lowest order, $\mathcal{O}(g_2 \lambda')$, goes by inserting planar interactions into the cases 1,2, and 3 that we listed above in all possible ways. In case 1, interactions can only be inserted in the correlator 1-3 since 2-4+5 -being a BPS correlator- does not receive radiative corrections. For the same reason interactions can be inserted only in the first correlators in cases 2 and 3. Necessary computations were already done in the literature (see *e.g.* [24], [29]) and one immediately gets, (4.21).

Bibliography

- [1] Gerard 't Hooft. A planar diagram theory for strong interactions. *Nucl. Phys.*, B72:461, 1974.
- [2] Alexander M. Polyakov. Quantum geometry of bosonic strings. *Phys. Lett.*, B103:207–210, 1981.
- [3] Juan M. Maldacena. The large n limit of superconformal field theories and supergravity. *Adv. Theor. Math. Phys.*, 2:231–252, 1998.
- [4] Ofer Aharony, Steven S. Gubser, Juan M. Maldacena, Hirosi Ooguri, and Yaron Oz. Large n field theories, string theory and gravity. *Phys. Rept.*, 323:183–386, 2000.
- [5] Gary T. Horowitz and Andrew Strominger. Black strings and p-branes. *Nucl. Phys.*, B360:197–209, 1991.
- [6] Igor R. Klebanov. Tasi lectures: Introduction to the ads/cft correspondence. 2000.
- [7] Joseph Polchinski. Dirichlet-branes and ramond-ramond charges. *Phys. Rev. Lett.*, 75:4724–4727, 1995.
- [8] S. S. Gubser, Igor R. Klebanov, and Alexander M. Polyakov. Gauge theory correlators from non-critical string theory. *Phys. Lett.*, B428:105–114, 1998.
- [9] Edward Witten. Anti-de sitter space and holography. *Adv. Theor. Math. Phys.*, 2:253–291, 1998.

- [10] Daniel Z. Freedman, Samir D. Mathur, Alec Matusis, and Leonardo Rastelli. Correlation functions in the $\text{cft}(d)/\text{ads}(d+1)$ correspondence. *Nucl. Phys.*, B546:96–118, 1999.
- [11] David Berenstein, Juan M. Maldacena, and Horatiu Nastase. Strings in flat space and pp waves from $n = 4$ super yang mills. *JHEP*, 04:013, 2002.
- [12] Umut Gursoy. Vector operators in the bmn correspondence. *JHEP*, 07:048, 2003.
- [13] Umut Gursoy. Predictions for pp-wave string amplitudes from perturbative sym. *JHEP*, 10:027, 2003.
- [14] David J. Gross, Andrei Mikhailov, and Radu Roiban. A calculation of the plane wave string hamiltonian from $n = 4$ super-yang-mills theory. *JHEP*, 05:025, 2003.
- [15] Daniel Z. Freedman and Umut Gursoy. Instability and degeneracy in the bmn correspondence. *JHEP*, 08:027, 2003.
- [16] Kazumi Okuyama. $N = 4$ sym on $r \times s(3)$ and pp-wave. *JHEP*, 11:043, 2002.
- [17] Matthias Blau, Jose Figueroa-O’Farrill, Christopher Hull, and George Papadopoulos. A new maximally supersymmetric background of iib superstring theory. *JHEP*, 01:047, 2002.
- [18] Matthias Blau, Jose Figueroa-O’Farrill, Christopher Hull, and George Papadopoulos. Penrose limits and maximal supersymmetry. *Class. Quant. Grav.*, 19:L87–L95, 2002.
- [19] R. Gueven. Plane wave limits and t-duality. *Phys. Lett.*, B482:255–263, 2000.
- [20] Darius Sadri and Mohammad M. Sheikh-Jabbari. The plane-wave / super yang-mills duality. *Rev. Mod. Phys.*, 76:853, 2004.
- [21] R. R. Metsaev. Type iib green-schwarz superstring in plane wave ramond-ramond background. *Nucl. Phys.*, B625:70–96, 2002.

- [22] N. Beisert, C. Kristjansen, J. Plefka, G. W. Semenoff, and M. Staudacher. Bmn correlators and operator mixing in $n = 4$ super yang- mills theory. *Nucl. Phys.*, B650:125–161, 2003.
- [23] David J. Gross, Andrei Mikhailov, and Radu Roiban. Operators with large r charge in $n = 4$ yang-mills theory. *Annals Phys.*, 301:31–52, 2002.
- [24] Neil R. Constable, Daniel Z. Freedman, Matthew Headrick, and Shiraz Minwalla. Operator mixing and the bmn correspondence. *JHEP*, 10:068, 2002.
- [25] Rajesh Gopakumar. String interactions in pp-waves. *Phys. Rev. Lett.*, 89:171601, 2002.
- [26] John Pearson, Marcus Spradlin, Diana Vaman, Herman Verlinde, and Anastasia Volovich. Tracing the string: Bmn correspondence at finite j^{**2}/n . *JHEP*, 05:022, 2003.
- [27] Jaume Gomis, Sanefumi Moriyama, and Jong-won Park. Sym description of sft hamiltonian in a pp-wave background. *Nucl. Phys.*, B659:179–192, 2003.
- [28] Radu Roiban, Marcus Spradlin, and Anastasia Volovich. On light-cone sft contact terms in a plane wave. *JHEP*, 10:055, 2003.
- [29] Neil R. Constable, Daniel Z. Freedman, Matthew Headrick, and Shiraz Minwalla. Operator mixing and the bmn correspondence. *JHEP*, 10:068, 2002.
- [30] N. Beisert, C. Kristjansen, J. Plefka, G. W. Semenoff, and M. Staudacher. Bmn correlators and operator mixing in $n = 4$ super yang- mills theory. *Nucl. Phys.*, B650:125–161, 2003.
- [31] Herman Verlinde. Bits, matrices and $1/n$. *JHEP*, 12:052, 2003.
- [32] Marcus Spradlin and Anastasia Volovich. Superstring interactions in a pp-wave background. *Phys. Rev.*, D66:086004, 2002.
- [33] Eric D’Hoker, Daniel Z. Freedman, and Witold Skiba. Field theory tests for correlators in the ads/cft correspondence. *Phys. Rev.*, D59:045008, 1999.

- [34] Daniel Z. Freedman, Kenneth Johnson, and Jose I. Latorre. Differential regularization and renormalization: A new method of calculation in quantum field theory. *Nucl. Phys.*, B371:353–414, 1992.
- [35] Sang-Min Lee, Shiraz Minwalla, Mukund Rangamani, and Nathan Seiberg. Three-point functions of chiral operators in $d = 4$, $n = 4$ sym at large n . *Adv. Theor. Math. Phys.*, 2:697–718, 1998.
- [36] Marcus Spradlin and Anastasia Volovich. Superstring interactions in a pp-wave background. ii. *JHEP*, 01:036, 2003.
- [37] Michael B. Green, J. H. Schwarz, and Edward Witten. Superstring theory. vol. 2: Loop amplitudes, anomalies and phenomenology. Cambridge, Uk: Univ. Pr. (1987) 596 P. (Cambridge Monographs On Mathematical Physics).
- [38] David Berenstein and Horatiu Nastase. On lightcone string field theory from super yang-mills and holography. 2002.
- [39] J. Greensite and F. R. Klinkhamer. New interactions for superstrings. *Nucl. Phys.*, B281:269, 1987.
- [40] Michael B. Green and Nathan Seiberg. Contact interactions in superstring theory. *Nucl. Phys.*, B299:559, 1988.
- [41] N. Beisert, C. Kristjansen, J. Plefka, and M. Staudacher. Bmn gauge theory as a quantum mechanical system. *Phys. Lett.*, B558:229–237, 2003.
- [42] Alberto Santambrogio and Daniela Zanon. Exact anomalous dimensions of $n = 4$ yang-mills operators with large r charge. *Phys. Lett.*, B545:425–429, 2002.
- [43] Niklas Beisert. Bmn operators and superconformal symmetry. *Nucl. Phys.*, B659:79–118, 2003.
- [44] Massimo Bianchi, Burkhard Eden, Giancarlo Rossi, and Yassen S. Stanev. On operator mixing in $n = 4$ sym. *Nucl. Phys.*, B646:69–101, 2002.

- [45] Diana Vaman and Herman Verlinde. Bit strings from $n = 4$ gauge theory. *JHEP*, 11:041, 2003.
- [46] Parsa Bonderson. Decay modes of unstable strings in plane-wave string field theory. *JHEP*, 06:025, 2004.
- [47] B. Diu C. Cohen-Tannoudji and F. Laloe. Quantum mechanics. Vol. II, Ch.XIII, Wiley and Sons, New York, 1977.
- [48] Marcus Spradlin and Anastasia Volovich. Note on plane wave quantum mechanics. *Phys. Lett.*, B565:253–265, 2003.
- [49] N. Beisert, C. Kristjansen, and M. Staudacher. The dilatation operator of $n = 4$ super yang-mills theory. *Nucl. Phys.*, B664:131–184, 2003.
- [50] J. A. Minahan and K. Zarembo. The bethe-ansatz for $n = 4$ super yang-mills. *JHEP*, 03:013, 2003.
- [51] Dong-su Bak and Mohammad M. Sheikh-Jabbari. Strong evidence in favor of the existence of s-matrix for strings in plane waves. *JHEP*, 02:019, 2003.
- [52] Predrag Cvitanovic. Group theory for feynman diagrams in nonabelian gauge theories: Exceptional groups. *Phys. Rev.*, D14:1536–1553, 1976.
- [53] Witold Skiba. Correlators of short multi-trace operators in $n = 4$ supersymmetric yang-mills. *Phys. Rev.*, D60:105038, 1999.
- [54] Min-xin Huang. Three point functions of $n = 4$ super yang mills from light cone string field theory in pp-wave. *Phys. Lett.*, B542:255–260, 2002.
- [55] Gradshteyn and Ryzhik. Table of integrals, series and products. Fifth edition. Alan Jeffrey Ed.